

**Role of epithelial cells in gastrointestinal diseases of the  
oesophagus and the pancreas**

**Eszter Becskeházi M.D.**

**Ph.D. thesis**

**Szeged**

**2023**

University of Szeged

Albert Szent-Györgyi Medical School

Doctoral School of Theoretical Medicine

**Role of epithelial cells in gastrointestinal diseases of the  
oesophagus and the pancreas**

Ph.D. thesis

Eszter Becskeházi M.D.

Supervisor:

Viktória Venglovecz Ph.D., D.Sc.



Szeged

2023

## Publications

### List of publications included in the thesis

- I. **Becskeházi, E.**, Korsós, M. M., Gál, E., Tiszlavicz, L., Hoyk, Z., Deli, M. A., Köhler, Z. M., Keller-Pintér, A., Horváth, A., Csekő, K., Helyes, Z., Hegyi, P., & Venglovecz, V. (2021). Inhibition of NHE-1 Increases Smoke-Induced Proliferative Activity of Barrett's Esophageal Cell Line. *International journal of molecular sciences*, 22(19), 10581. <https://doi.org/10.3390/ijms221910581>  
IF: 5.924 (Q2)
- II. Gál, E., Veréb, Z., Kemény, L., Rakk, D., Szekeres, A., **Becskeházi, E.**, Tiszlavicz, L., Takács, T., Czakó, L., Hegyi, P., & Venglovecz, V. (2020). Bile accelerates carcinogenic processes in pancreatic ductal adenocarcinoma cells through the overexpression of MUC4. *Scientific reports*, 10(1), 22088. <https://doi.org/10.1038/s41598-020-79181-6>  
IF: 4.38 (D1)

### List of publications related to the subject of the thesis

- III. Korsós, M. M., Bellák, T., **Becskeházi, E.**, Gál, E., Veréb, Z., Hegyi, P., & Venglovecz, V. (2021). Mouse organoid culture is a suitable model to study esophageal ion transport mechanisms. *American journal of physiology. Cell physiology*, 321(5), C798–C811. <https://doi.org/10.1152/ajpcell.00295.2021>  
IF: 4.249 (Q1)
- IV. **Becskeházi, E.\***, Korsós, M. M.\*, Eröss, B., Hegyi, P., & Venglovecz, V. (2020). OEsophageal Ion Transport Mechanisms and Significance Under Pathological Conditions. *Frontiers in physiology*, 11, 855. <https://doi.org/10.3389/fphys.2020.00855>  
\*: contributed equally  
IF: 4.566 (Q2)

Summarized impact factor of publications I-IV.: 19.119

### List of other publications

- V. Venglovecz, V., Pallagi, P., Kemény, L. V., Balázs, A., Balla, Z., **Becskeházi, E.**, Gál, E., Tóth, E., Zvara, Á., Puskás, L. G., Borka, K., Sandler, M., Lerch, M. M., Mayerle, J., Kühn, J. P., Rakonczay, Z., Jr, & Hegyi, P. (2018). The Importance of Aquaporin 1 in Pancreatitis and Its Relation to the CFTR Cl<sup>-</sup> Channel. *Frontiers in physiology*, 9, 854. <https://doi.org/10.3389/fphys.2018.00854>  
IF: 3.201 (Q2)

Impact factor of all publications: 22.32

# Table of contents

Publications .....	3
Abbreviations .....	6
Summary .....	9
1. Introduction.....	11
1.1 Epithelial cells in the gastrointestinal tract.....	11
1.2 The oesophagus .....	11
1.2.1 Anatomical and histological overview of the oesophagus .....	11
1.2.2 Oesophageal defence mechanisms .....	13
1.2.3 Ion transporters of oesophageal epithelial cells .....	14
1.2.4 Physiological function of Na <sup>+</sup> /H <sup>+</sup> -exchanger-1 in oesophageal epithelial cells.	18
1.2.5 Pathophysiological relevance of Na <sup>+</sup> /H <sup>+</sup> -exchanger-1 in the oesophagus .....	20
1.2.6 The effect of smoking on the oesophagus .....	23
1.3 The pancreas .....	24
1.3.1 Anatomy and function of the pancreas.....	24
1.3.2 Role of epithelial cells in the pancreas .....	24
1.3.3 Duct-related pancreatic diseases .....	25
1.3.4 Bile acids as etiological factor in pancreatic cancer.....	25
2. Aims of the study .....	27
3. Materials and Methods.....	28
3.1 Human samples.....	28
3.2 Animals.....	28
3.3 Cell lines .....	28
3.4 Chemicals and Solutions .....	29
3.5 Cigarette smoke exposure.....	29
3.6 Cigarette smoke extract and treatment .....	30
3.7 Isolation of guinea pig oesophageal epithelial cells .....	30
3.8 Immunohistochemistry .....	31
3.9 Western blot.....	31
3.10 Measurement of intracellular pH.....	32
3.11 Determination of buffering capacity.....	32
3.12 Measurement of Na <sup>+</sup> /H <sup>+</sup> -exchanger-1 activity .....	32



3.13	RT-qPCR .....	33
3.14	<i>SLC9A1</i> gene silencing .....	33
3.15	Evaluation of cytotoxicity .....	33
3.16	Proliferation .....	34
3.17	Statistical analysis.....	34
4.	Results.....	35
4.1	Effect of smoking on the proliferation and viability of oesophageal cells.....	35
4.2	Na <sup>+</sup> /H <sup>+</sup> -exchanger-1 activity and expression in metaplastic and dysplastic Barrett cell lines .....	36
4.3	Effect of cigarette smoke extract on Na <sup>+</sup> /H <sup>+</sup> -exchanger-1 activity and expression in metaplastic and dysplastic Barrett cell lines.....	38
4.4	Effect of smoking on Na <sup>+</sup> /H <sup>+</sup> -exchanger-1 activity in normal oesophageal cells .....	40
4.5	Effect of long-term smoking on Na <sup>+</sup> /H <sup>+</sup> -exchanger-1 expression in human oesophageal samples.....	41
4.6	Effect of knockdown of <i>SLC9A1</i> gene on the proliferation of metaplastic and dysplastic oesophageal epithelial cell lines .....	43
4.7	Effect of bile acids on the proliferation of Capan-1 cells.....	44
5.	Discussion.....	45
6.	Conclusion .....	51
7.	Acknowledgements.....	52
8.	References.....	53
9.	Annex .....	62

## Abbreviations

ATP: adenosine triphosphate

BA: bile acid

BCECF-AM: 2,7-bis-(2-carboxyethyl)-5(6)-carboxyfluorescein acetoxymethyl ester

BO: Barrett's oesophagus

CA: cholic acid

CaMKII: Ca<sup>2+</sup>/calmodulin-dependent kinase II

CDCA: chenodeoxycholic acid

cDNA: complementary deoxyribonucleic acid

Cdx2: caudal-type homeobox 2

CFTR: cystic fibrosis transmembrane conductance regulator

Cl<sup>-</sup>: chloride ion

CSE: cigarette smoke extract

DCA: deoxycholic acid

DGOR: duodeno-gastro-oesophageal reflux

DIDS: 4,4'-Diisothiocyano-2,2'-stilbenedisulfonic acid

DMA: dimethylamiloride

DNA: deoxyribonucleic acid

ECM: extracellular matrix

EIPA: ethylisopropylamiloride

ERK1/2: extracellular signal-regulated kinase 1/2

FAK: focal adhesion kinase

FXR: farnesoid X receptor

GCA: glycocholic acid

GCDCA: glycochenodeoxycholic acid

GDCA: glycodeoxycholic acid

GI: gastrointestinal

GORD: gastro-oesophageal reflux disease

H<sup>+</sup>: hydrogen ion

HBSS: Hank's Balanced Salt Solution

HCO<sub>3</sub><sup>-</sup>: bicarbonate ion

hEGF: human epidermal growth factor

HMA: 5-N-(methylpropyl)amiloride

HOE642: cariporide, *N*-(Aminoiminomethyl)-4-(1-methylethyl)-3-(methylsulfonyl)benzamide

HOE694: 3-methylsulphonyl-4-piperidinobenzoyl, guanidine hydrochloride

IPMN: intraductal papillary mucinous neoplasm

KSFM: keratinocyte serum free media

LDH: lactate dehydrogenase

LOS: lower oesophageal sphincter

mRNA: messenger ribonucleic acid

NaCl: sodium chloride

NF- $\kappa$ B: nuclear factor -  $\kappa$ B

NH<sub>4</sub>Cl: ammonium chloride

NHE-1: Na<sup>+</sup>/H<sup>+</sup> exchanger-1

NIK: Nck-interacting kinase

NO: nitric oxide

NOS: nitric oxide synthase

OAC: oesophageal adenocarcinoma

OECs: oesophageal epithelial cells

OJ: obstructive jaundice

OSCC: oesophageal squamous cell carcinoma

p90<sup>rsk</sup>: p90 ribosomal S6 kinase

PanIN: pancreatic intraepithelial neoplasia

PC: pancreatic cancer

PDAC: pancreatic ductal adenocarcinoma

pH<sub>e</sub>: extracellular pH

pH<sub>i</sub>: intracellular pH

PIP<sub>2</sub>: phosphatidylinositol-4,5-bisphosphate

PKC: protein kinase C

PPI: proton pump inhibitor

ROI: region of interest

RT-qPCR: quantitative reverse transcription polymerase chain reaction

SEC: squamous epithelial cell

SEM: standard error of the mean

siRNA: short interfering ribonucleic acid

SLC: solute carrier family

SMG: submucosal gland

TCA: taurocholic acid

TCDCA: taurochenodeoxycholic acid

TDCA: taurodeoxycholic acid

TRPP3: transient receptor potential polycystin-3

UOS: upper oesophageal sphincter

## Summary

**Introduction:** Gastrointestinal epithelial cells fulfil diverse roles in the body and it has been shown, that disturbances in their function such as intracellular pH ( $\text{pH}_i$ ) alterations can lead to malignant diseases. Smoking is considered a main risk factor of oesophageal inflammatory and malignant diseases, but the cellular background is not completely understood yet. As a part of the oesophageal defence, ion transporters of oesophageal epithelial cells (OECs) maintain pH homeostasis, and prevent potentially damaging effect of acidic luminal content and toxic agents. In the first part of this thesis, we tried to find the answer for our question whether smoking influences oesophageal epithelial ion transport mechanisms, especially the activity of  $\text{Na}^+/\text{H}^+$  exchanger-1 (NHE-1), which has a great impact on  $\text{pH}_i$  homeostasis of the cells. In the second part of the thesis we investigated a carcinogenic feature, such as proliferation of pancreatic ductal adenocarcinoma (PDAC) cells after bile acid (BA) treatment. The tumorigenic potential of BAs is well-known when PDAC located in the head of the pancreas. In this case, the growing tumour can cause obstruction of the main pancreatic and bile ducts, which results in obstructive jaundice as well as increased concentration of BAs in the blood. We hypothesised that BAs increase the rate of proliferation of cancer cells, therefore worsen the outcome of PDAC.

**Methods:** The effect of cigarette smoke extract (CSE) (1, 10, 100  $\mu\text{g/ml}$ ) on NHE-1 activity was estimated by the  $\text{NH}_4\text{Cl}$  pre-pulse technique and changes in  $\text{pH}_i$  were measured using a fluorescent dye, BCECF-AM. Guinea pigs were exposed to tobacco smoke for 1, 2 and 4 months, OECs were isolated after an enzymatic digestion, then NHE-1 activity was measured. CP-A (metaplastic) and CP-D (dysplastic) Barrett's oesophageal (BO) cell lines were treated with the above mentioned concentrations of CSE for 6, 24 and 72 hours and the mRNA and protein expression of NHE-1 was investigated by qPCR and Western blotting, respectively. Viability and proliferation of CP-A and CP-D cells were estimated using LDH and CCK8 kit, respectively. Immunohistochemical analysis of NHE-1 expression was performed in human samples. *SLC9A1* knockdown was performed by using specific siRNA. For investigation the effect of BAs, Capan-1 cells were treated with various BAs (100 and 500  $\mu\text{M}$ ), then the rate of proliferation was measured by CCK8 assay.

**Results:** CSE decreased the activity of NHE-1 in normal, guinea pig OECs and CP-D cells, and high concentrations of CSE caused an elevated activity in CP-A cells. Chronic CSE treatment also elevated NHE-1 protein expression in CP-A cells. In contrast, there were no significant changes in mRNA nor protein expression in CP-D cells. Elevated CSE-induced proliferative

activity was detected in *SLC9A1*-silenced metaplastic cells. In smokers and patients with BO NHE-1 protein expression was increased. BAs significantly elevated the rate of proliferation in Capan-1 cells, almost in all treated groups.

**Conclusion:** Based on our results on OECs we propose that NHE-1 plays a protective role in metaplastic cells in order to avoid malignant transformation. Based on our results on PDAC cells we found that almost all of the tested BAs increased the proliferative potential of PDAC cells, which on the one hand strengthens literature data, and on the other hand indicates that there is no difference in the effect of individual BAs on PDAC cells.

# **1. Introduction**

## **1.1 Epithelial cells in the gastrointestinal tract**

The epithelium is comprised of closely related epithelial cells, which are connected with each other via special structures. Important transport processes are proceeded through them, which are essential for the proper functioning of the human body.

Polarization is the most characteristic feature of the epithelial cells, which means, that basal and apical surfaces are differentiated on these cells that vary in functional and biochemical properties, thereby ensuring unidirectional flow of substances. In addition, epithelial cells possess regeneration and absorption capability, and in certain cases, they can contain nerve endings. During my research, my investigations focused at the function of gastrointestinal (GI) epithelial cells.

GI epithelial cells perform diverse functions in the body. On the one hand, GI epithelial cells play highlighted role in protecting the lower layers, as it can be observed in the multi-layered non-keratinized squamous epithelium in the oral cavity, pharynx or oesophagus. Furthermore, they can help in the absorption of nutrients and water, like the epithelium of small and large intestine, or they can also perform secretory functions such as in case of stomach, salivary gland or pancreas. During my research, I focused on the investigation of the function of oesophageal and pancreatic epithelial cells. Although these two organs fulfil different functions in the body, notably, the oesophagus forwards food, whereas the pancreas takes part in the digestion, the common feature in them is, that epithelial cells play important role in both organs, and disturbances of the function of epithelial cells can lead to the development of different inflammatory and cancerous diseases. In this thesis, I would like to present my research of these two organs, to the greater extent the oesophagus, and to the lesser extent the pancreas.

## **1.2 The oesophagus**

### **1.2.1 Anatomical and histological overview of the oesophagus**

The oesophagus is a tube-shaped organ that connects the pharynx and the stomach. It commences at the level of cricoid cartilage (or level of C6 vertebra), continues in the thorax in the superior and posterior mediastinum, then crosses the diaphragm, where it ends in the cardia of the stomach. It has an average 25-30 cm length in adults and can be divided to three parts,

namely cervical, thoracic and abdominal part <sup>1</sup>. The oesophagus has two sphincters at its two ends. The upper oesophageal sphincter (UOS) is formed by the posterior surface of the cricoid cartilage, arytenoid and interarytenoid muscles, cricopharyngeus and thyropharyngeus muscles <sup>2</sup>. The lower oesophageal sphincter (LOS) is also known as the cardiac sphincter, prevents regurgitation from the stomach. The oesophagus gets its blood supply from a. thyroidea inferior, aorta thoracica through rami oesophagei, the left a. phrenica inferior and left a. gastrica. Venous blood eliminates via azygos and hemiazygos veins<sup>1</sup>.

The wall of the oesophagus is comprised of four layers, namely (from the inside) mucosa, submucosa, muscularis externa and adventitia. The mucosal layer is further divided to epithelial layer, lamina propria and lamina muscularis mucosae. The epithelial layer of the human oesophagus is composed of non-keratinized stratified squamous epithelium, which involves nearly 30 cell layers. The uppermost 7-8 flat cell layer, called stratum corneum, primarily protects the mucosa against potentially noxious luminal contents. In the intermediate region, stratum spinosum, there are several large cells arranged in multi-layered structure, with marked desmosomes in the superficial part. Stratum germinativum is a 2-3 cell-layer thick basal layer containing cuboid cells; this zone is responsible for proliferation <sup>3,4</sup>.

The following lamina propria is a loose connective tissue layer, which apart from connective tissue cells, contains small blood and lymphatic vessels, nerves and cardiac glands. Cardiac glands are located on the lower section of the organ and produce neutral pH fluid which is responsible for neutralizing regurgitating gastric acid <sup>5</sup>. Lamina muscularis mucosae is consists of thin, longitudinal smooth muscle layer, which is becomes thicker in the distal section of the oesophagus <sup>6</sup>. Moving outward, the flexible connective tissue layer underlying the mucosa is the submucosal layer. It is rich in collagen, elastic fibres, fibroblasts, blood and lymphatic vessels, nerves and submucosal glands (SMGs) are embedded here <sup>4,7</sup>. SMGs are also called as the own glands of the oesophagus; they have a tubuloacinar structure and secrete mucin- and  $\text{HCO}_3^-$  - rich, slightly alkaline fluid to the lumen of the oesophagus to lubricate the mucosa <sup>4,5,8</sup>. Muscularis externa consists of striated muscle at the proximal part, then in the middle third striated and smooth muscle are mixed, and the distal third consist of only smooth muscle. Adventitia, the outermost layer is composed of connective tissue and it covers and connects the oesophagus with other structures <sup>6</sup>.



### 1.2.2 Oesophageal defence mechanisms

The main function of the oesophagus is to forward bite and liquid from the oral cavity to the stomach. The quality and the content of the transmitted food or drink can show broad variety; mechanical, chemical, thermal and osmotic impulses affect the luminal surface even under physiological circumstances <sup>9</sup>. Regurgitation of gastric volume can also be a normal phenomenon, until it occurs only rarely, not causing symptoms e.g. heartburn, or oesophageal damage. Therefore, the organ has three lines of defence that prevents oesophageal damage, that are antireflux mechanisms, luminal clearance mechanisms, and the tissue of the oesophagus is also adapted for the prevention of its integrity (tissue resistance); these processes called oesophageal defence mechanisms <sup>10</sup>. Antireflux mechanisms consists of the function of LOS and diaphragm, that acts as a mechanical support of the LOS <sup>11</sup>. Luminal clearance shortens the contact time with luminal content using peristalsis of the oesophagus, the advantage of gravity and saliva, that not only washes the surface and helps the process of swallowing, but neutralizes acids <sup>12</sup>. These processes reduce the contact time with luminal contents.

Tissue resistance comprises three components, namely pre-epithelial, epithelial and post-epithelial defence mechanisms. The first line, the pre-epithelial defence includes mucus layer, unstirred water and bicarbonate ions <sup>10,13</sup>. Mucins have an obvious role in defence by neutralizing acid and protecting mucosal surface in the normal oesophagus. Mucus layer is relatively thin or can be absent, in spite of this, it can withstand to the acidic luminal content <sup>14,15</sup>. This mucus-buffer layer partially neutralizes hydrogen ions and slows their diffusion down, blocks the diffusion of bile acids (BAs), pepsin and trypsin, and also acts as a substrate of the latter two enzymes, thus it is an effective protective process <sup>16-18</sup>. Under physiological conditions, mucin-1 and -4 (MUC1, MUC4) isoforms are expressed in the oesophageal epithelium, MUC5B isoform is secreted by SMGs <sup>19,20</sup>.

Epithelial defence has structural and also functional components <sup>21</sup>. The uppermost zone of epithelium, stratum corneum creates a mechanical barrier by apical cell membranes and intercellular junction complexes. These two components together prevent the diffusion of certain ions and molecules from the luminal space to the intra- and intercellular space <sup>13,22,23</sup>. Among functional mechanisms, epithelial ion transporters, intra- and extracellular buffers have a crucial role in compensation of acidification caused by transcellular or paracellular entry of H<sup>+</sup> <sup>13</sup>. The essential function of the oesophageal ion transporters in epithelial defence is

explained in details in the following chapter. Cell restitution and proliferation are also mentioned among epithelial defence processes.

The main post-epithelial defence mechanism of the oesophageal mucosa is blood flow. It has been shown, that in presence of acidic luminal content, mucosal microcirculation dynamically increases via tissue nitric oxide (NO), histamine and calcitonin gene related peptide release <sup>24-27</sup>. Blood transfers oxygen, essential nutrients to the epithelial cells and eliminates CO<sub>2</sub> and acid. HCO<sub>3</sub><sup>-</sup> transport to the intercellular space is crucial, because it is required for the activity of buffer processes and Na<sup>+</sup>-dependent Cl<sup>-</sup>/HCO<sub>3</sub><sup>-</sup> exchanger, therefore has a great role in protection <sup>28</sup>.

### **1.2.3 Ion transporters of oesophageal epithelial cells**

Epithelial cells form a massive mechanical barrier that enhances epithelial resistance. Epithelial cells are polarised, apical and basal or basolateral surfaces are distinguished, and each pole shows individual molecular pattern. Cells are connected on the basal surface with extracellular matrix (ECM) via integrin receptors, and on lateral side with tight and adherens junctions. Tight junctions create a strong connection between cells and prevent the free diffusion of solutes, ions, proteins between poles. Cadherins and catenins form adherens junctions that participate in intercellular processes and bonds to the actin cytoskeleton <sup>29,30</sup>. Ion transporters are located on both the basolateral and the apical side of the squamous epithelial cells (SECs), and the distribution of different ion transporters develops an individual pattern that ensures unidirectional ion diffusion. August Krogh, Danish zoologist, physiologist and Nobel Laureate has found out first, that ion concentrations are different in the intra- and extracellular space, and this ionic gradient is maintained by metabolic energy, and a ‘steady state’ is obtained by the balance of the active and passive transport processes <sup>31</sup>. Hans Ussing, who worked with Krogh, has contributed to Krogh’s findings and has broaden the knowledge of active and passive transport mechanisms and epithelial polarity <sup>32</sup>. Koefoed-Johnsen and Ussing have published their two-membrane hypothesis, in which they declared the following observations: (i) that the two-surfaces of isolated frog skin acts differently in the absence of diffusible anions, the outer surfaces acts as a sodium electrode, whereas inward-facing one like a potassium electrode, (ii) according to these results, it is assumed, that active sodium transport functions on the inward-facing surface and (iii) there is a forced exchange of sodium and potassium <sup>33</sup>. Coordinated function of the ion transporters maintains not only a pH homeostasis,

which is essential for cell functions, but it is also important in cell growth, migration, differentiation, restitution and cell volume<sup>34-36</sup>.

As a part of the epithelial defence, ion transporters have a considerable function in the physiology of the GI tract. Numerous articles have identified the presence of ion transporters in the GI cells, and their role in some diseases was also described<sup>37-40</sup>. There was only a small amount of studies published, that focused on the ion transport mechanisms in the oesophagus. To date, the following ion transporters have been identified in the oesophagus (Figure 1.).

$\text{Na}^+/\text{K}^+/\text{2Cl}^-$  cotransporter (NKCC1) mediates the influx of  $\text{Na}^+$ ,  $\text{K}^+$  and two  $\text{Cl}^-$ <sup>41</sup>. NKCC1 is ubiquitously expressed, among others in epithelial cells, and immunohistochemical experiments confirmed its presence in the lower and middle layer of oesophageal squamous epithelium but not in the basal cell layers<sup>42</sup>. In SMGs, NKCC1 is located on the basolateral membrane of duct and mucous cells and contributes to fluid secretion<sup>43</sup>.  $\text{Cl}^-$  enters the cells through basolateral NKCC1, and in a secreting epithelia it leaves the cells through cystic fibrosis transmembrane conductance regulator (CFTR) to the luminal space<sup>32</sup>. The inward pointing chemical gradient of  $\text{Na}^+$  is maintained by  $\text{Na}^+/\text{K}^+$  pump, which ensures the driving force for  $\text{Cl}^-$  influx. Activation and function of NKCC1 is in a connection with the CFTR, and the  $\text{Cl}^-$  secretion basically depends on the function of NKCC1<sup>32</sup>. The activity of NKCC depends on the  $\text{Cl}^-$  concentration of the cell through a negative feedback mechanism<sup>44</sup>. It is activated in low pH levels and contributes to cell swelling<sup>45</sup>. Loop diuretics such as furosemide and bumetanide inhibits NKCC<sup>42</sup>. Abdalnour-Nakhoul et al. have demonstrated the role of NKCC1 in oesophageal fluid secretion by bumetanide, as the administration of bumetanide caused a significantly decreased  $\text{HCO}_3^-$  secretion, consequently  $\text{Cl}^-$  influx is required for  $\text{HCO}_3^-$  secretion<sup>43</sup>.

This research group has published also about  $\text{Cl}^-$  transport in rabbit OECs. They have observed  $\text{Cl}^-$  conductance on both basolateral and apical membrane, but it was more marked on the basolateral membrane. Their experiments supported a flufenamate-sensitive and  $\text{Ca}^{2+}$  dependent  $\text{Cl}^-$  conductance, suggesting the presence of  $\text{Ca}^{2+}$  sensitive  $\text{Cl}^-$  channel on the basolateral membrane of the OECs. In addition, they also described, that there is only a modest transcellular  $\text{Cl}^-$  transport through SECs and it cannot be enhanced by cAMP. Intracellular  $\text{Cl}^-$  concentration is mainly regulated by the basolateral  $\text{Cl}^-$  transport<sup>46</sup>. Abdalnour-Nakhoul et al. have studied oesophageal fluid secretion and ion transporters that are involved in this process, and they were the first who published the presence of CFTR in the oesophagus. CFTR was found in the mucous cells and mainly on the a luminal side of the SMG ducts. In SMGs, apical

CFTR not only mediates  $\text{Cl}^-$  efflux, but it becomes permeable to  $\text{HCO}_3^-$  and participates directly in  $\text{HCO}_3^-$  secretion <sup>43</sup>.

$\text{K}^+$  channels are expressed on both the basolateral and apical surface of epithelial cells, and they have different functions. Basolateral  $\text{K}^+$  channels have a baseline activity and a significant role in  $\text{Na}^+$  uptake and cell volume regulation after hyposmolar stress, whereas apical  $\text{K}^+$  channels determine the  $\text{K}^+$  concentration of the luminal fluid by  $\text{K}^+$  efflux. Basolateral  $\text{K}^+$  conductance, that has a baseline activity was described in rabbit OECs by Goldstein et al <sup>47,48</sup>. Voltage-dependent  $\text{K}^+$  channel is located on the basolateral membrane, and its main function is to determine cell membrane potential and to ensure an electrochemical driving force for other ions such as  $\text{Na}^+$ ,  $\text{Cl}^-$  and also has a role in regulating cell volume <sup>49</sup>.  $\text{K}^+/\text{Cl}^-$  co-transporter (KCC) mediates the coupled efflux of  $\text{K}^+$  and  $\text{Cl}^-$ , and together with NKCC, they maintain  $\text{Cl}^-$  concentration. This transporter gets its energy from the  $\text{K}^+$  gradient, which is ensured by the  $\text{Na}^+/\text{K}^+/\text{ATPase}$  <sup>50</sup>. It was shown, that among others, KCC is also important in regulatory volume decrease (RVD) mechanism, which functions as a cell restitution process after hyposmolar stress. RVD is carried out via pH-dependent  $\text{K}^+$  and  $\text{Cl}^-$  efflux coupled with water transport through the basolateral membrane. Snow et al. have found, that at acidic pH RVD is inhibited, assuming that disturbances in cell restitution mechanisms can distribute to the state of acid injury of the oesophagus <sup>51</sup>. Orlando et al. have confirmed the hypothesis, that KCC function is in connection with RVD; they used a specific KCC inhibitor on human OECs and RVD was also inhibited <sup>52</sup>.

$\text{HCO}_3^-$  transporter proteins participate in maintaining the body's main buffering system,  $\text{CO}_2/\text{HCO}_3^-$  balance, which is essential for the pH homeostasis.  $\text{HCO}_3^-$  transporters are encoded by *SLC4A* and *SLC26A* gene families, and subfamilies are distinguished, as follows. *SLC4A* family involves  $\text{Na}^+/\text{HCO}_3^-$  co-transporters (NBCs),  $\text{Na}^+$  dependent  $\text{Cl}^-/\text{HCO}_3^-$  transporters (NDCBE and NCBE), and  $\text{Na}^+$  independent  $\text{Cl}^-/\text{HCO}_3^-$  transporters (AE1, AE2 and AE3). The *SLC26A* family comprises five  $\text{Cl}^-/\text{HCO}_3^-$  exchangers (SLC26A3, SLC26A4, SLC26A6, SLC26A7 and SLC26A9). AEs mediate the  $\text{Cl}^-$  and  $\text{HCO}_3^-$  exchange through the basolateral membrane, preserve physiological pH, and they also regulate cell volume and acidification/alkalisation depending on the direction of  $\text{HCO}_3^-$  movement. These proteins show differences in tissue expression, apical or basolateral localisation,  $\text{Cl}^- : \text{HCO}_3^-$  stoichiometry, electrogenicity and roles <sup>53</sup>. Tobey et al. have described the function of two AEs in cultured rabbit oesophageal epithelial basal cells that influence cell  $\text{pH}_i$ .  $\text{Na}^+$  dependent  $\text{Cl}^-/\text{HCO}_3^-$  exchangers are active after the cell achieving low  $\text{pH}_i$ , which have a significant role in case of

contact with acidic luminal content. In spite of this,  $\text{Na}^+$  independent  $\text{Cl}^-/\text{HCO}_3^-$  exchangers operates in cellular alkalisiation by exchanging 1  $\text{Cl}^-$  to 1  $\text{HCO}_3^-$ . Both mentioned AEs are electroneutral and located on the basolateral membrane <sup>54</sup>. Oesophageal SMGs secrete  $\text{HCO}_3^-$  and mucus-rich alkaline fluid to the lumen to prevent oesophageal acidic damage. NBCe1 and AE2 are found to be expressed in the basolateral membranes of duct cells using IHC and ensure  $\text{HCO}_3^-$  secretion on the luminal side, which is fulfilled by the coordinated function of SLC26A6 and CFTR <sup>43</sup>.

### Squamous epithelial cell

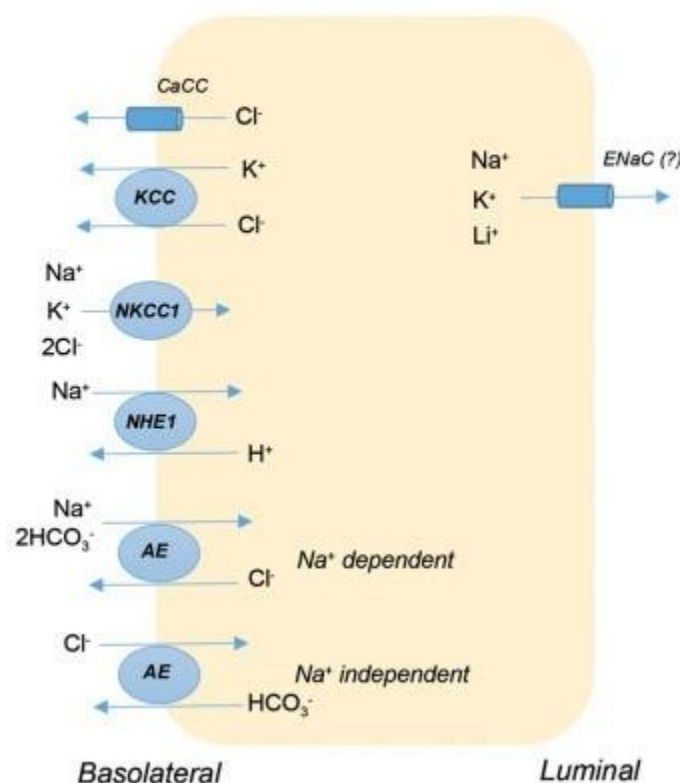


**Figure 1. Ion transporters of rabbit squamous epithelial cells (SECs).** AE, anion exchanger; CaCC,  $\text{Ca}^{2+}$ -activated  $\text{Cl}^-$  channel; CFTR, cystic fibrosis transmembrane conductance regulator; KCC,  $\text{K}^+/\text{Cl}^-$  co-transporter; NBC,  $\text{Na}^+/\text{HCO}_3^-$  co-transporter; NHE,  $\text{Na}^+/\text{H}^+$  exchanger; NKCC,  $\text{Na}^+/\text{K}^+/2\text{Cl}^-$  co-transporter.

$\text{Na}^+/\text{K}^+/\text{ATPase}$  can be found in SECs and also in acinar and ductal cells of SMGs, and provides  $\text{Na}^+$ -gradient through basolateral membrane <sup>43,55,56</sup>. In rabbit OECs, three subunits of epithelial  $\text{Na}^+$  channel (ENaC) were identified by Western blotting, however, they do not show the features that ENaC have and it cannot be inhibited by amiloride. They found, that this channel regulate cation influx, and is equally permeable for monovalent cation, such as  $\text{Li}^+$ ,

$\text{Na}^+$  and  $\text{K}^+$  <sup>57</sup>. In addition to the ion transporters mentioned above, there is another essential transporter that occurs in almost every cell, namely, the  $\text{Na}^+/\text{H}^+$ -exchanger-1 (NHE-1), the role of which is detailed in the next chapter.

#### 1.2.4 Physiological function of $\text{Na}^+/\text{H}^+$ -exchanger-1 in oesophageal epithelial cells

$\text{Na}^+/\text{H}^+$ -exchangers (NHEs) are integral membrane proteins, that mediate  $\text{Na}^+$  influx and  $\text{H}^+$  efflux in 1:1 stoichiometry in cells, using the energy of electrochemical  $\text{Na}^+$  gradient provided by  $\text{Na}^+/\text{K}^+/\text{ATPase}$  <sup>58</sup>. Solute carrier nine (*SLC9*) gene family encodes human NHEs, and to date, nine members (*SLC9A1-9* encoding NHE1-9) of the *SLC9A* subfamily have been identified. Expression of given NHE isoforms is specific for different tissues, whereas NHE1 is expressed in most mammalian cells, and also referred as a housekeeping gene <sup>59,60</sup>.

NHEs are mainly responsible for maintaining  $\text{pH}_i$  homeostasis, but have a role in several other cell functions such as cell growth, differentiation, proliferation, cell migration, and controlling cell volume <sup>34-36,39,61-63</sup>. Powell et al. have observed, that mucosal-to-serosal  $\text{Na}^+$  transport is responsible for the potential difference and short-circuit current in rabbit oesophagus and it could be inhibited by amiloride <sup>64</sup>. In 1990, Layden et al. have described for the first time functioning NHE in rabbit oesophagus <sup>65</sup>, later other studies have strengthened this finding <sup>66,67</sup> and characterized NHE on the basolateral membrane <sup>66</sup>. Since then, it is well known, that subcellular localisation of NHEs is specific for the isoform, can be expressed on basolateral or apical plasma membranes, and also on cellular organelles, e.g. endosomes or trans-Golgi network <sup>68,69</sup>. Tobey et al. have identified NHE-1 in human OECs for the first time, as this ion transporter activity stands in the background of a  $\text{H}^+$  extrusion mechanism <sup>70</sup>.

NHE-1 (encoded by *SLC9A1*) is the most common isoform among NHEs, it is virtually expressed in all tissues, except macula densa and  $\alpha$ - and  $\beta$ -intercalated cells in the kidney <sup>59</sup>. In oesophageal epithelium, Shallat et al. have identified the NHE-1 messenger RNA in rabbit and rat with reverse transcription polymerase chain reaction (RT-PCR), but no other NHE isoform was detected in OECs <sup>71</sup>. It is located on the basolateral plasma membrane of the OECs. This phosphoprotein is 815 amino acids long, and consists of a 500-amino-acid-long hydrophobic N-terminal membrane domain, and a hydrophilic C-terminal, cytoplasmic domain <sup>72</sup>.

Under physiological conditions, it performs an electroneutral exchange of one extracellular  $\text{Na}^+$  and one intracellular  $\text{H}^+$ , thus regulates  $\text{pH}_i$  by extruding  $\text{H}^+$ . Since the main  $\text{Na}^+$  uptake happens through NHE-1,  $\text{Na}^+$  couples with  $\text{Cl}^-$  and it consequently leads to osmotic  $\text{H}_2\text{O}$  uptake of the cell, therefore this isoform has a major role in regulating cell volume <sup>59</sup>.

Besides these 'housekeeping' processes, NHE-1 has additional functions in cells; it is involved in e.g. cell proliferation, migration and differentiation, indicating its complex role. However, in the oesophageal epithelium, the main function of NHE-1 is to prevent intracellular acidification by extruding  $H^+$ , therefore maintain the  $pH_i$  homeostasis of the cell in case of acidic luminal content.

Several factors are associated with the regulation of this isoform. Primarily, it is activated by intracellular acidification<sup>73</sup>. NHE-1 has a low basal activity within physiological pH range. When intracellular pH drops, the accumulated  $H^+$  provokes NHE-1 activation with the maximal response in over one pH unit<sup>74,75</sup>. Aronson et al. have described, that  $H^+$  activates NHE-1 in an allosteric way. Based on their observations, the N-terminal transmembrane domain possesses a distinct so-called ' $H^+$  - sensing' site, which binds intracellular  $H^+$  that activates the exchanger, but this  $H^+$  would not be transported. Therefore, presumably more than one  $H^+$  is involved in this process<sup>74</sup>. This mechanism can be an explanation for the greater response of NHE-1 than it would be predicted<sup>76</sup>. It was also confirmed, that N-terminal transmembrane domain and cytoplasmic domain functions separately; the complete deletion of the encoding region of cytoplasmic domain does not alter the  $Na^+/H^+$  exchange, nor the  $H^+$  sensing site, but reduces its affinity, and the growth factor-induced alkalisation disappears. These findings have led to the conclusions, that cytoplasmic domain is not required for the ion transport, but indispensable for regulation, such as growth factor activation<sup>72</sup>. Since NHEs are secondary active transporters, ion fluxes are driven by  $Na^+$  gradient that is maintained by the  $Na^+/K^+/ATPase$ <sup>58</sup>. Therefore, in the absence of adenosine triphosphate (ATP), the activity of NHE-1 is inhibited. Besides, Aharonovitz et al. have found a significant decrease in plasmalemmal phosphatidylinositol-4,5-bisphosphate ( $PIP_2$ ) levels parallel to the ATP depletion and have also identified two  $PIP_2$ -binding motifs on the C-terminal of the exchanger. In *in vitro* studies, NHE-1 activity was decreased in those mutant forms of NHE-1, which lacked these  $PIP_2$ -binding domains indicating, that phosphoinositides have a major role in the regulation and optimal function of NHE-1<sup>77</sup>. In addition, the C-terminal part of the exchanger contains serine and threonine residues and their phosphorylation by protein kinases can also influence the function of the exchanger. The protein kinases that take part in regulation were summarized by Slepnev, are the followings: ERK1/2 (extracellular signal-regulated kinase 1/2),  $p90^{rsk}$  (p90 ribosomal S6 kinase),  $p160^{ROCK}$ , NIK (Nck-interacting kinase); and CaMKII ( $Ca^{2+}$ /calmodulin-dependent kinase II), p38 MAPK, protein kinases C, D. Dephosphorylation by protein phosphatase I has also a role in regulation<sup>58</sup>.

NHE-1 is specifically sensitive for amiloride, a potassium-sparing diuretic, and it was the first drug among NHE inhibitors, described by Benos in 1982 <sup>78</sup>. This drug also has an inhibitory effect on epithelial Na<sup>+</sup> channel (ENaC), Na<sup>+</sup>/Ca<sup>2+</sup> exchanger (NCX), nonselective cation channels and transient receptor potential polycystin-3 (TRPP3) <sup>79</sup>. Amiloride derivatives, such as ethylisopropylamiloride (EIPA), dimethylamiloride (DMA) and 5-N-(methylpropyl)amiloride (HMA), does not affect Na<sup>+</sup> channel and NCX, but they are weak NHE-1 inhibitors. Benzoylguanidine derivatives, HOE694, HOE642 (also known as cariporide), eniporide, and BIIB-513 can be also mentioned among selective NHE-1 inhibitors, with a higher specificity compared to EIPA <sup>80</sup>. However, amiloride derivatives and HOE694 or HOE642 also block NHE-2 and NHE-8, therefore they cannot be used for selective NHE-1 inhibition *in vivo* <sup>81</sup>.

### **1.2.5 Pathophysiological relevance of Na<sup>+</sup>/H<sup>+</sup>-exchanger-1 in the oesophagus**

#### **1.2.5.1 Na<sup>+</sup>/H<sup>+</sup>-exchanger-1 in gastro-oesophageal reflux disease and Barrett's oesophagus**

When the balance between damaging and protective factors is upset, the epithelium can no more resist acid injury. First of all, impaired anti-reflux mechanisms predispose patients to have more frequent reflux episodes. These factors are incompetent LOS function, increased intra-abdominal pressure, which weakens LOS, and frequent transient LOS relaxation. The existence of one of these three factors is enough for pathologic reflux, and elevates the number of reflux episodes and the contact time with gastric volume <sup>10</sup>. Barrett's oesophagus (BO) is a disease, in which the stratified squamous epithelium is replaced by columnar metaplasia in the lower section of the oesophagus. This condition develops primarily as a result of long-term gastro-oesophageal reflux disease (GORD) <sup>82</sup> and it can be considered as an adaptive alteration to the acidic environment <sup>83</sup>. The underlying mechanisms are not completely clear yet, thus, this topic stands in the centre of numerous GI investigations. Lin et al. have described, that short administration of acid to the luminal surface of rat oesophagus caused elevated function of ion transporters. As these ion fluxes were HCO<sub>3</sub><sup>-</sup> dependent or could be inhibited by 4,4'-Diisothiocyano-2,2'-stilbenedisulfonic acid (DIDS; an inhibitor of HCO<sub>3</sub><sup>-</sup> dependent ion transporters) and EIPA, respectively, it was suggested, that NHEs and AEs have a role in response to acidic pH<sub>e</sub> <sup>84</sup>. Fujiwara et al. have suggested, that in acidic environment, EGF activates NHEs through Ca<sup>2+</sup>/calmodulin and protein kinase C (PKC) pathways, thus protects OECs from cell damage <sup>85</sup>. Park et al. have strengthened the importance of NHE-1 in acidic



injury. They found that in normal OECs acid treatment induced intrinsic survival mechanisms, and described the protective role of NHE-1 in acidic injury <sup>86</sup>. In contrast, Fitzgerald et al. have suggested, that hyperproliferative response to low pH<sub>e</sub> may be mediated by NHE in BO, as this process could be inhibited by amiloride analogs and PKC inhibitors <sup>87</sup>. As regurgitating gastric content often contains BAs the effect of bile exposure on OECs have also been intensively examined. In a study by Goldman et al., normal and metaplastic oesophageal cell lines were treated with BAs alone or in combination with acid, in the presence or absence of nitric oxide synthase (NOS) and NHE inhibitors. BA treatment caused intracellular acidification and DNA damage. It has been shown that BAs elevated nitric oxide (NO) levels through NOS-activation, that led to NHE-1 inhibition, and DNA damage as a result of consequent intracellular acidification <sup>88</sup>.

Some studies have showed elevated NHE-1 expression in GORD and BO. Elevated mRNA and protein levels of NHE-1 was found in GORD patients both in the presence and absence of oesophagitis <sup>89</sup>. Goldman et al. have found increased mRNA and protein expression of NHE-1 in BO cell line and tissue samples, whereas in normal tissue samples and cell lines only weak NHE-1 expression could be detected <sup>88</sup>. Similarly to these results, our workgroup has previously shown an increased mRNA and protein expression of NHE-1 and NHE-2 isoforms, after treating metaplastic and dysplastic cell lines with BAs, acid or together in combination <sup>90</sup>. In contrast, NHE-1 staining was almost absent in normal oesophageal samples <sup>90</sup>.

### **1.2.5.2 Na<sup>+</sup>/H<sup>+</sup>-exchanger-1 in oesophageal cancer**

Oesophageal cancer is the 8<sup>th</sup> most common cancer around the world, takes the 6<sup>th</sup> place in cancer mortality, and has a poor, 5-year survival rate <sup>91,92</sup>. Oesophageal squamous cell carcinoma (OSCC) is considered to be the predominant subtype of oesophageal cancer worldwide, but in the latter decades, the incidence of oesophageal adenocarcinoma (OAC) has started rising in the western countries <sup>93</sup>. The prevalence of the two histological subtypes also shows a geographical distribution: OAC is more common in the developed countries, whereas OSCC is the prevalent subtype in Eastern, South-East Asia, Central Asia and sub-Saharan Africa <sup>94</sup>. There are also differences among the cancer types in risk factors. OSCC is more common in black individuals and men. Smoking and alcohol consumption are considered the main risk factors in OSCC. Smoking increases the risk by 5-fold and by 10-fold in heavy smokers compared to non-smokers. Tar fraction contains the main carcinogenic substances, and

polynuclear aromatic hydrocarbons and volatile nitrosamines can be the initiators <sup>95</sup>. In other regions of the world, dietary factors and habits have more impact on risk.

In recent decades, several articles have been published about the relevance of ion transporters in cancerous diseases <sup>96-100</sup>. Aberrant function, expression of ion transporters and their involvement in signalling pathways can influence among others cell cycle, proliferation, migration, invasion and adhesion of tumour cells <sup>100,101</sup>. NHE-1 is a well-studied ion transporter in cancer research and numerous cancer types and mechanisms have been described in which NHE-1 is included. Current research data in this field were reviewed recently by Hu <sup>102</sup>. NHE-1 has an anti-apoptotic effect, participates in cancer cell migration, invasion, proliferation and most importantly, both  $\text{pH}_i$  and  $\text{pH}_e$  regulation <sup>101</sup>. Solid tumour growth and angiogenesis happens slipped in time, therefore hypoxia, elevated glycolysis and ATP depletion occurs, and lactate and  $\text{H}^+$  accumulates in the cytosol. Intracellular acidification activates NHE-1 allosterically on the  $\text{H}^+$  modifying site and changes set point higher, more alkaline than physiological  $\text{pH}_i$ . Thus, activation and overexpression of NHE-1 establishes an alkaline intracellular and an acidic extracellular microenvironment, thereby ensures an optimal  $\text{pH}_i$  for malignant cells <sup>101</sup>. Pedersen and Stock summarized, pH changes are well-controlled during cell cycle, and G2-M transition is highly pH-sensitive, therefore the role of NHE-1 is especially important considering that increased NHE-1 expression can be detected in many types of cancers <sup>96</sup>.

In oesophageal malignancies, there are less experimental data is available about the molecular mechanisms in association with NHE-1 and the results are contradictory. Goldman et al. have detected elevated NHE-1 expression in BO, and described BA-induced NO production and consequential NHE-1 inhibition, which causes DNA damage via intracellular acidification in cells and elevates the risk of mutations and tumour progression <sup>88</sup>. As an interesting hypothesis, later they have suggested, that by pharmacological inhibition of NHE-1 cells can avoid BA-induced apoptosis and establish an apoptosis resistance <sup>103</sup>. Guan et al. found increased NHE-1 expression in OAC tissues compared to the normal epithelium and shown, that cell viability and proliferation were suppressed and apoptosis could be induced in oesophageal cancer cell lines by inhibition of NHE-1 function and NHE-1 knockdown <sup>104</sup>. Ariyoshi et al. claimed that in OSCC cells, inhibition of NHE-1 increased migration, proliferative and invasive potentials and this was in association with PI3K/AKT and Notch signalling pathway. It was also shown, that NHE-1 expression was increased in well-differentiated primary OSCC, and the 5-year overall survival was higher of these patients <sup>105</sup>.

Although there are more and more results are published about NHE-1 in connection with oesophageal malignancies, there are no clear evidence of its etiological role.

### **1.2.6 The effect of smoking on the oesophagus**

Along with alcohol, smoking is one of the most important etiological factors in the development of oesophageal diseases. During smoking, the oesophageal epithelium is directly exposed to cigarette smoke, which contains numerous toxic substances and is known to play a prominent role in the development of many cancer types. Therefore, numerous clinical studies were conducted that ascertain the relation between oesophageal diseases and smoking <sup>106-110</sup>. Genetic liability to smoking was also associated with GORD and oesophageal cancer <sup>111</sup>. In a review, Kahrilas has summarised the results of publications that studied the effects of smoking on the development of GORD. He summarized, that smoking causes a lower LOS pressure on a long term, and increase the frequency of acid reflux events. Smoking also has an impact on oesophageal clearance mechanisms via the reduced salivary functions <sup>112</sup>. Clinical studies presented clear results, that smoking elevates the risk of BO <sup>107</sup> and OAC <sup>106</sup>. In BO patients, smoking promotes progression and doubles the risk to high-grade dysplasia or cancer <sup>110</sup>. A meta-analysis pointed out, that current and former smokers diagnosed with OSCC had poorer prognosis compared to those OSCC patients, who has no smoking history <sup>108</sup>. In addition, it has been shown, that the risk of cancer development decreased in a time-dependent way after cessation. However, in OAC there was no significant reduction after giving up smoking <sup>109</sup>. Surprisingly, the effect of smoking on OECs has been investigated in only one basic research study. In 1986, Orlando et al. have performed an interesting experiment on rabbit oesophageal mucosa. Oesophageal epithelium was exposed to acute cigarette smoke extract (CSE) *in vivo* and *in vitro* that caused a decreased potential difference across the plasma membrane due to the inhibition of mucosal Na<sup>+</sup> transport <sup>113</sup>.

Although this study suggested the role of ion transporters in the effects of tobacco smoke, it did not identify the transporters involved, so the exact mechanism remains unknown.

**Since smoking is an important factor in the development of oesophageal diseases, it is important to understand the underlying mechanism that leads to the altered functioning of OECs, because it may even represent a starting point for the development of new therapeutic attack points.**

### **1.3 The pancreas**

#### **1.3.1 Anatomy and function of the pancreas**

The pancreas is an elongated, retroperitoneal, accessory digestive gland, which is situated transversely between duodenum and spleen. This organ can be divided to head, neck, body and tail. The head of the pancreas is slightly enlarged and it is surrounded by the curve of the duodenum, then continues in the relatively short neck. The body that lies over the aorta and L2 vertebra, and the tail is located near the left kidney, splenic hilum and left colic flexure<sup>114,115</sup>. Anterior and posterior pancreaticoduodenal arterial arcades supply the head and neck of the pancreas, which, through the superior and inferior pancreaticoduodenal arteries, are in connection with the gastroduodenal artery, that is a branch of the common hepatic artery, and superior mesenteric artery. The body and the tail of the pancreas get their blood supply from the splenic artery, the major terminal branch of the coeliac trunk. The venous blood of the pancreas is drained to the superior and inferior pancreaticoduodenal veins; the superior veins connect the right gastroepiploic vein or the portal vein directly, whereas the inferior pancreaticoduodenal veins reach the superior mesenteric vein. Lymphatic vessels drain to the retropancreatic nodes, coeliac lymph nodes and superior mesenteric nodes.<sup>115</sup> The pancreas has both exocrine and endocrine functions. The exocrine part of the pancreas is comprised of acinar and ductal cells and gives the main part of the organ<sup>116</sup>. Acinar cells secrete digestive enzymes, whereas ductal cells produce  $\text{HCO}_3^-$ -rich fluid, and this pancreatic juice is drained by a ductal system of the organ. The main duct called the duct of Wirsung, which runs almost all along the organ collecting pancreatic juice, and ends in the hepatopancreatic ampulla, as known as the ampulla of Vater. Here, the duct of Wirsung joins (or opens near) the common bile duct, and pancreatic juice together with bile discharge in the duodenum. There can also be an accessory pancreatic duct, called duct of Santorini<sup>115</sup>. The lesser part of the organ is responsible for the endocrine function, where so-called Langerhans-islets produce essential hormones for glucose homeostasis, namely insulin, glucagon and somatostatin<sup>117</sup>.

#### **1.3.2 Role of epithelial cells in the pancreas**

Approximately 2,5 L of alkaline, isotonic pancreatic juice is produced by the human pancreas per day, which has a main role in the normal function of the organ<sup>118</sup>. Acinar cells are polarized epithelial cells and create an acinar segment, where they produce isotonic fluid containing NaCl. Pancreatic duct can absorb  $\text{Cl}^-$  and secrete a relatively high, 140 mM

concentration of  $\text{HCO}_3^-$  and water, with which it neutralizes the acidic acinar fluid <sup>118,119</sup>. Intercalated ducts collect acinar fluid, then the fluid flows in to intra-lobular, inter-lobular and inter-lobar ducts and finally reaches the main duct. Pancreatic fluid secretion is under neuro-humoral and hormonal control. Basal secretion is very low, and together with digestive enzyme production, it increases in response to a meal. The main regulators of secretion are vagal tone, cholecystokinin, secretin, in addition, insulin, somatostatin, and paracrine agonists also regulate this process <sup>119</sup>.

### **1.3.3 Duct-related pancreatic diseases**

Pancreatic cancer (PC) is the most common disease related to pancreatic ducts. PC is an aggressive, highly malignant cancer type in the GI tract, which has a very low 5-year survival rate. The diagnosis is difficult and often late, since there is lack of symptoms and due to retroperitoneal location of the pancreas, it can be problematic to examine this organ <sup>120</sup>. More than 80% of PC are ductal adenocarcinoma (PDAC) and in 60% located in the head of the pancreas <sup>121</sup>. As they grow, they cause an obstruction of the common bile tract and so-called obstructive jaundice (OJ) occurs, which means a poor prognostic sign. Metastatic regional lymph nodes can be found nearly in 80% by surgeries, and it creates metastatic lesions in the liver, peritoneum, lung, pleura and adrenals <sup>122</sup>. Pancreatic intraepithelial neoplasia (PanIN) and intraductal papillary mucinous neoplasm (IPMN) are considered the precursor lesions of PDAC. Genetic mutations of *KRAS*, *TP53*, *CDKN2A/p16* and *SMAD4* is associated with PDAC <sup>123</sup>. Obesity, chronic pancreatitis, smoking, diabetes or inherited DNA mutations are also considered as risk factors of PDAC <sup>124</sup>.

### **1.3.4 Bile acids as etiological factor in pancreatic cancer**

Bile acids (BAs) play a significant role in lipid digestion, absorption of fat-soluble vitamins and they are also key molecules in signalling pathways related to metabolism, gene expression or cell proliferation. BAs are produced in the liver, and in the human body, cholic acid (CA) and chenodeoxycholic acid (CDCA) are the primary BAs, which are present mostly in glycin-or taurine-conjugated form. In addition, among secondary BAs, deoxycholic acid (DCA) also occurs in human bile, which is formed from primary BAs as a result of intestinal bacterial enzymes and returns to the bile via the enterohepatic cycle <sup>125</sup>.

The effect of BAs on pancreatic cells is a highly important topic in PC research. Feng and Chen have summarized in their review, that smoking can stimulate BA secretion, and

elevated secretion combined with a long common channel may consequently lead to BA reflux. This can also cause pancreatitis and initiate cell dedifferentiation. BAs are also connected with obesity, diabetes and hypertriglyceridaemia, that are well-known risk factors of PC <sup>120</sup>. Farnesoid X receptor (FXR) was described as a key receptor of BAs <sup>126</sup>. Hu et al. observed that high FXR expression was associated with poor prognosis, as elevated FXR contributed to proliferation and migration of the PC cells <sup>127</sup>. Joshi et al. have demonstrated, that BA levels rise in the serum and the pancreatic juice of PC patients with OJ, and oncogenic MUC4 expression is also upregulated via FAK-dependent c-Jun activation <sup>128</sup>.

**Although numerous studies described, that BAs, especially hydrophobic BAs, may contribute to the development and progression of GI cancers, there is no such a study that investigated the effect of the most common human BAs in PC.**

## 2. Aims of the study

In the present thesis, I attempted to summarize the effect of well-known risk factors, smoking and BAs in oesophageal and pancreatic malignancies, respectively.

Since, there is a lack of information about the effect of smoking on the pathophysiology of BO and its progression. As we have seen in the introduction, ion transporters have a highlighted role in the prevention of oesophageal injury. Based on this, we hypothesized, that expression and function of the main epithelial ion transporter, namely NHE-1, alters by a harmful action such as smoking and it has a significance in the pathophysiology of smoke-induced oesophageal injury. Therefore, our aims in the first part of the thesis were:

- I. to investigate the effect of CSE on the activity and expression of NHE-1 in primary OECs originated from guinea pig, in human metaplastic and dysplastic BO cell lines *in vitro*
- II. to examine the impact of smoking on NHE-1 function in guinea pig model *in vivo*
- III. to analyse the effect of smoking on NHE-1 expression in healthy and BO patients
- IV. to investigate the role of NHE-1 in the effect of CSE

Numerous scientific articles have explained the carcinogenic feature of BAs. The majority of PC is located in the head of the pancreas, the growing tumour causes an obstruction of the common channel and provoke an OJ. The exact effects of certain BAs are not clearly understood on the progression of PC.

Therefore, our aim in this study was:

- V. to estimate proliferative activity of PDAC cells after treatment with various BAs.

### **3. Materials and Methods**

#### **3.1 Human samples**

Retrospective data collection of patients was performed by the approval of the Ethics Committee of the University of Szeged (No. 4658), according to Helsinki Declaration and GDPR. Patient information was retrieved concerning the histopathological samples collected between January 2018 and May 2021 from a medical database used in Albert Szent-Györgyi Medical School, University of Szeged, eMedSolution. BO patients were included based on age, diagnosis, state of the disease, smoking history, histopathological description of oesophageal lesion. Exclusion criteria was age under 18 years and missing or incomplete smoking history. Formalin-fixed, paraffin-embedded oesophageal tissue samples of patients were retrieved from the Archive of Department of Pathology, University of Szeged. Samples were analysed and diagnosis were validated by pathologists earlier. Patients were basically classified into two groups: smoking group with a smoking history of more than 20 years and non-smoking group who had never smoked or had not smoked for at least a year. As a control, tumour-free resection margins and normal oesophageal biopsy samples were used. The average age of BO patients was  $55.1 \pm 4.6$  years in the smoking group ( $n = 7$ ), and  $57.3 \pm 3.8$  years in the non-smoking group ( $n = 20$ ). The average age in the control group was  $38.5 \pm 11.5$  years in the smoking group ( $n = 3$ ), and  $59.7 \pm 3.8$  years in the non-smoking group ( $n = 7$ ).

#### **3.2 Animals**

4-12 week-old, male guinea pigs were used for our experiments. Animals were kept at room temperature ( $23 \pm 1^\circ\text{C}$ ), at 12:12 h light-dark cycle in plastic cages and had free access to laboratory chow and water completed with Vitamin C. All animal experiments were performed in accordance the Guide for the Care and Use of Laboratory Animals (United States, Department of Health and Human Services) and by the approval of the local Ethical Board of the University of Szeged, Hungary.

#### **3.3 Cell lines**

CP-A (human metaplastic oesophageal epithelial cell line), CP-D (human dysplastic oesophageal epithelial cell line) and Capan-1 (human PDAC) cells were purchased from American Type Culture Collection (Manassas, VA, USA). The complete growth medium of CP-A and CP-D consisted of MCDB-153 basal medium, 5% fetal bovine serum, 4 mM L-



glutamine, 1x ITS supplement (Sigma I1884; 5 µg/ml Insulin, 5 µg/ml Transferrin, 5 ng/ml Sodium Selenite), 140 µg/ml Bovine Pituitary Extract (Sigma P1476), 20 mg/L adenine, 0,4 µg/ml hydrocortisone, 8,4 µg/L cholera toxin (Sigma C8052), 20 ng/ml recombinant human Epidermal Growth Factor (hEGF), 1% (v/v) penicillin/streptomycin. The complete medium of Capan-1 cells comprised of RPMI-1640 media, 15% (v/v) fetal bovine serum (FBS); 1% (v/v) L-glutamine and 2% (v/v) antimycoticum/antibioticum. Cells were seeded when being 90-100% confluent and CP-A and CP-D cells were used between 3-19 passage numbers, and Capan-1 cells between 30-35 passage numbers.

### **3.4 Chemicals and Solutions**

All general laboratory chemicals and BAs (glycocholic acid (GCA); taurocholic acid (TCA); taurodeoxycholic acid (TDCA); glycochenodeoxycholic acid (GCDCA); taurochenodeoxycholic acid (TCDCA)) were purchased from Sigma-Aldrich (Budapest, Hungary). Glycodeoxycholic acid (GDCA) was from Cayman Chemical Company (Michigan, MI, USA). 2,7-bis-(2-carboxyethyl)-5(6)-carboxyfluorescein acetoxymethyl ester (BCECF-AM) was obtained from Invitrogen (Waltham, MA, USA), prepared (2 µmol/L) in dimethyl sulfoxide and stored at -20°C. Nigericin (10 µM) was dissolved in ethanol and stored at -20°C. High-Capacity Reverse Transcription Kit, TaqMan gene expression Master Mix, TaqMan probes, Lipofectamine 2000 transfection reagents were purchased from Thermo Fisher Scientific (Waltham, MA, USA). Cell Counting Kit-8 was from Dojindo Molecular Technologies (Rockville, MD, USA). Cytotoxicity Detection Kit Plus (Cat.No.: 4744926001) was obtained from Roche. SLC9A1 siRNAs (siRNA ID: 119643) was from Life Technologies. The standard Na<sup>+</sup>-HEPES solution contained (in mM): 130 NaCl, 5 KCl, 1 CaCl<sub>2</sub>, 1 MgCl<sub>2</sub>, 10 D-glucose, and 10 Na-HEPES. NH<sub>4</sub>Cl-HEPES solution was supplemented with 20 mM NH<sub>4</sub>Cl, while NaCl concentration was lowered to 110 mM. HEPES-buffered solutions were gassed with 100% O<sub>2</sub>, and their pH was set to 7.5 with HCl.

### **3.5 Cigarette smoke exposure**

The effect of chronic cigarette smoke exposure was studied using smoking chamber at the Department of Pharmacology and Pharmacotherapy, University of Pécs. Male guinea pigs were divided into three groups according to the period of cigarette smoke exposure (1-, 2- and 4-months exposure, n=3/group). All animals were 5 months old at the time of sacrifice. Animals were exposed to whole body cigarette smoke exposure 5 times a day, 10 minutes each time

using a TE2 closed-chamber manual smoking system (Teague Enterprises, Woodland). During the experiment, 3R4F Kentucky Research Cigarettes (Kentucky Tobacco Research and Development Center, Lexington, KY, USA) were smoked and ventilated inside the chamber. 24-48 hours after the last cigarette smoke exposure, animals were sacrificed, and OECs were isolated. Age-matched control animals were exposed to air. Guinea pigs were kept under standard laboratory conditions, at 12:12 hours light/dark cycle and with free access to food and drinking solutions. All experiments were performed in accordance with the institutional guidelines under approved protocols (No.: XII./2222/2018, University of Pécs).

### **3.6 Cigarette smoke extract and treatment**

Cigarette smoke extract (CSE) was prepared at the Department of Pharmacognosy, University of Szeged. Briefly, mainstream smoke from 15 filterless 3R4F Kentucky Research Cigarettes (12 mg tar and 1.0 mg nicotine/cigarette), was continuously bubbled through 20 mL of distilled water. CSE was then sterile-filtered through a 0.22- $\mu$ m filter (Millipore, Bedford, MA, USA) and the dry weight was measured. CSE solution was then diluted to the desired concentration using HEPES or culture media. CSE was freshly prepared for each experiments or used within 2 days of preparation. Cells were treated with cigarette smoke extract for 6, 24 and 72 hours in concentrations of 1, 10 and 100  $\mu$ g/mL.

### **3.7 Isolation of guinea pig oesophageal epithelial cells**

Our workgroup optimized a protocol for guinea pig OECs based on the work Kalabis et al.<sup>129</sup>. Briefly, animals were sacrificed by cervical dislocation, the oesophagus was removed, cut longitudinally, rinsed in Hank's Balanced Salt Solution (HBSS, Sigma H9269) and digested in dispase I solution (2 U/mL, Sigma D4818) for 40 minutes. After digestion, the inner, epithelial layer of the oesophagus was detached from the submucosa and rinsed in fresh HBSS. Then the epithelial layer was incubated in 0,25% Trypsin-EDTA solution supplemented with 1% (v/v) antimycoticum/antibioticum for 2  $\times$  15 minutes, and the Eppendorf tube was vortexed several times during the incubation period to promote tissue disintegration. Filtered Soybean trypsin inhibitor (Gibco, Cat. No.: 10684033) solution was added to the tube and the whole lysate was centrifuged for 5 minutes at 1000 rpm. The cell pellet was diluted in keratinocyte serum free media (KSFM, Gibco, Cat. No.: 17005042) supplemented with 1% (v/v) antimycoticum/antibioticum and seeded onto cover glasses and incubated until use.

### **3.8 Immunohistochemistry**

Immunohistochemical analysis of NHE-1 expressions was performed on 4% buffered formalin-fixed sections of human oesophageal samples embedded in paraffin. The 5 µm-thick sections were stained in an automated system (Autostain, Dako, Glostrup, Denmark). Briefly, the slides were deparaffinised, and endogenous peroxidase activity was blocked by incubation with 3% H<sub>2</sub>O<sub>2</sub> (10 min). Antigenic sites were disclosed by applying citrate buffer in a pressure cooker (120 °C, 3 min). To minimize non-specific background staining, the sections were then pre-incubated with milk (30 min). Subsequently, the sections were incubated with a human anti-NHE-1 (1:100 dilution, 30 min, Alomone Laboratories) primary polyclonal antibody and exposed to LSAB2 labeling (Dako, Glostrup, Denmark) for 2 × 10 min. The immunoreactivity was visualized with 3,3'-diaminobenzidine (10 min); then the sections were dehydrated, mounted and examined. NHE-1 expressing cells were identified by the presence of a dark red/brown chromogen. A semi-quantitative scoring system was used to evaluate the expression of NHE-1. The intensity of staining (0 = negative, 1 = weak, 2 = moderate and 3 = strong) and the percentage of positive cells (1 = 0–25% of the cells are positive, 2 = 25–50% of the cells are positive, 3 = 50–75% of the cells are positive and 4 = 75–100% of the cells are positive) were scored and then the composite score was obtained by multiplying the intensity of staining and the percentage of immunoreactive cells.

### **3.9 Western blot**

Cells were lysed in Cell Lysis Buffer (Catalogue No. 9803, Cell Signalling Technology, Danvers, MA, USA) supplemented with complete EDTA-free protease inhibitor (Roche, Catalogue No. 11873580001). Then samples were centrifuged at 2500 rpm for 20 minutes at 4 °C, and the supernatants were used. Protein concentration in the samples was determined by using a BCA assay (Pierce Chemical, Rockford, IL, USA) or Bradford reagent (Bio-Rad Laboratories, Hercules, CA, USA), and equal amounts of proteins (20 or 30 µg) were resolved on polyacrylamide gel and transferred onto Protran (GE Healthcare Amersham™) or PVDF (Invitrogen, Watham, MA, USA) membranes. Membranes were incubated overnight with rabbit polyclonal anti-NHE-1 (Catalogue No. ANX-010, Alomone Labs, Jerusalem, Israel), mouse monoclonal anti-GAPDH (Catalogue No. MAB 374, Sigma Aldrich, Hungary) or mouse monoclonal anti-α-Tubulin antibody (Catalogue No. T9026, Merck, Darmstadt, Germany) followed by the incubation with the appropriate HRP-conjugated secondary antibody (Catalogue No. P0448 goat anti-rabbit and P0161 rabbit anti-mouse, DAKO, Glostrup,

Denmark or G-21040 goat anti-mouse, Invitrogen, Waltham, MA, USA). The peroxidase activity was visualized by using the enhanced chemiluminescence assay (Advansta, Menlo Park, CA, USA) or with Clarity Chemiluminescence Substrate (Bio-Rad Laboratories, Hercules, CA, USA). Signal intensities were quantified by using the QuantityOne software (Bio-Rad, Hercules, CA, USA) or Image Lab Software, version 5.2 (Bio-Rad Laboratories, Hercules, CA, USA). The results from each membrane were normalized to the GAPDH or  $\alpha$ -Tubulin values and compared to the 6-hour control.

### **3.10 Measurement of intracellular pH**

Cells were seeded onto 24 mm cover glasses which was placed on the stage of an inverted microscope (IX-71) connected with an Xcellence imaging system (Olympus, Budapest, Hungary). Cells were incubated with a pH-sensitive fluorescence dye, BCECF-AM for 30-60 minutes according to cell type. Cells were perfused with solutions at 37°C at a 5-6 ml/min perfusion rate. Average 5-12 regions of interest (ROIs) were marked in each measurement and one image was taken per second using a CCD camera. The cells were excited with 440 and 495 nm wavelengths, and the 440/495 ratio was detected at 535 nm. One  $\text{pH}_i$  measurement was obtained per second. *In situ* calibration of the fluorescence signal was performed using the high  $\text{K}^+$ -nigericin technique.

### **3.11 Determination of buffering capacity**

The total buffering capacity ( $\beta_{\text{total}}$ ) of cells was estimated according to the  $\text{NH}_4\text{Cl}$  pre-pulse technique, as previously described. Briefly, OECs were exposed to various concentrations of  $\text{NH}_4\text{Cl}$  in a  $\text{Na}^+$ - and  $\text{HCO}_3^-$ -free solutions. The total buffering capacity of the cells was calculated using the following equation:  $\beta_{\text{total}} = \beta_i + \beta_{\text{HCO}_3^-} = \beta_i + 2.3 \times [\text{HCO}_3^-]_i$ , where  $\beta_i$  refers to the ability of intrinsic cellular components to buffer changes of  $\text{pH}_i$  and was estimated by the Henderson–Hasselbach equation.

### **3.12 Measurement of $\text{Na}^+/\text{H}^+$ -exchanger-1 activity**

For evaluating the activity of NHE-1,  $\text{NH}_4\text{Cl}$  pre-pulse technique was used. Cells were exposed to  $\text{NH}_4\text{Cl}$  (20 mM) for 3 minutes, which caused a sudden  $\text{pH}_i$  elevation due to the diffusion of  $\text{NH}_3$  into the cells. After the removal of  $\text{NH}_4\text{Cl}$ , the  $\text{pH}_i$  decreased rapidly followed by a  $\text{pH}_i$  regeneration. The rate of the acid regeneration (the first 60 s) reflects the activity of NHEs in standard HEPES-buffered solutions. In order to quantify NHE-1 activity, the measured

rates of  $\text{pH}_i$  change ( $\Delta\text{pH}/\Delta t$ ) were converted to transmembrane base flux  $J(\text{B}^-)$  using the equation:  $J(\text{B}^-) = \Delta\text{pH}/\Delta t \times \beta_i$ , where  $\beta_i$  is the intrinsic buffering capacity. For the calculation of  $J(\text{B}^-)$ , the  $\beta_i$  value at the start point  $\text{pH}_i$  was used.

### 3.13 RT-qPCR

Total mRNA was isolated using RNA isolation kit of Macherey-Nagel (Nucleospin RNA Plus kit, Macherey-Nagel, Germany) according to manufacturer's instructions. The concentration of RNA was determined by spectrophotometry (NanoDrop 3.1.0, Rockland, DE). Two micrograms of total RNA were reverse transcribed using High-Capacity cDNA Archive Kit (Applied Biosystems) according to manufacturer's instructions. Quantitative real-time PCR was carried out on a Roche LightCycler 96 SW (Roche, Basel, Switzerland). TaqMan probe set of *SLC9A1* was used to check gene expression. Target gene expression levels were normalised to a human housekeeping gene,  $\beta$ -actin (*ACTB*), and then using the  $\Delta\Delta C_T$  method, relative gene expression was calculated. Fold changes were represented ( $2^{-\Delta\Delta C_T}$ ). Values below 0.5 and above 2.0 were considered significant.

### 3.14 *SLC9A1* gene silencing

*SLC9A1* gene silencing was performed on the cell lines as follows.  $3 \times 10^5$  cells were seeded on a 6-well plate in antibiotic free growth medium, incubated overnight and then medium was changed to 800  $\mu\text{L}$ /well fresh, complete growth medium without antibiotics. *SLC9A1* gene silencing was performed at 40-50% confluency. 100 pmol *SLC9A1* siRNA was dissolved in 250  $\mu\text{L}$  Opti-MEM (Gibco, Cat. No 31985070) serum free media. Depending on the transfection length and cell line, 5-7.5  $\mu\text{L}$  Lipofectamine 2000 was added to 250  $\mu\text{L}$  Opti-MEM and incubated for 5 minutes at room temperature. Then prepared siRNA solution and Lipofectamine 2000 were mixed and incubated at room temperature for 20 minutes to form complexes. Complexes were added to the wells, mixed gently by rocking the plate back and forth, and incubated for 72 hours at  $37^\circ\text{C}$ . After transfection, RT-qPCR and immunocytochemistry was performed to estimate mRNA and protein levels.

### 3.15 Evaluation of cytotoxicity

For cytotoxicity assay Cytotoxicity Detection Kit Plus (Cat.No.: 4744926001, Roche) was used, according to the kit instructions. 100  $\mu\text{L}$  of cell suspension was seeded into a 96-well cell culture plate at a  $2 \times 10^4$  cells/well density and incubated overnight. On the following day,

the cells were incubated with CSE (1, 10 or 100 µg/mL) for 6, 24 and 72 hours, then 100 µL reaction mixture was added to the wells. Lactate dehydrogenase (LDH) activity was measured at 490 nm using a FLUOstar OPTIMA Spectrophotometer (BMG Labtech, Ortenberg, Germany). Control groups (background controls, low controls and high controls) were determined according to kit instructions. The LDH release induced by Triton-X 100 was assigned as 100%. The average absorbance values of each of the triplicates were calculated and the average value of the background control was subtracted from each of the samples to reduce background noises. Percentage of cytotoxicity was calculated using the following formula: Cytotoxicity (%) = (exp. value – low control / high control – low control) × 100.

### **3.16 Proliferation**

10<sup>3</sup> CP-A or CP-D cells per well were seeded into a 96-well plate (100 µl/well) in complete growth medium and allowed to attach overnight. Cells were then treated with CSE (1 and 10 µg/mL) for 6, 24 and 72 hours. After the treatments, 10 µL of CCK8 solution was added to each well and the cells were incubated for further 3 hours. Absorbance was detected at 450 nm using a FLUOstar OPTIMA Spectrophotometer (BMG Labtech, Ortenberg, Germany). For determining the proliferation of Capan-1 cells, 5 × 10<sup>3</sup> cells per well were seeded into a 96-well plate (100 µl/well) in complete growth medium and allowed to attach overnight. Cells were then treated with BAs (glycocholic acid (GCA); taurocholic acid (TCA); Glycodeoxycholic acid (GDCA); taurodeoxycholic acid (TDCA); glycochenodeoxycholic acid (GCDCA); taurochenodeoxycholic acid (TCDCA)) in two different concentrations (100 and 500 µM), for 24, 48 and 72 hours. After treatments, all steps were performed as described above.

### **3.17 Statistical analysis**

Results were described as means ± SEM. For statistical analysis, one-way ANOVA, and Student's t-test were used.  $p \leq 0,05$  were considered significant.

## 4. Results

### 4.1 Effect of smoking on the proliferation and viability of oesophageal cells

In the first step we have examined the viability and proliferative activity of CP-A and CP-D cells in the presence of CSE. To determine cytotoxic potential of CSE, cells were seeded in 96-well plates, allowed to adhere overnight and treated with 1, 10 and 100  $\mu\text{g/mL}$  CSE for 6, 24 and 72 hours (Figure 2A). At the end of the incubation period, cell viability was investigated using Cytotoxicity Detection Kit Plus from Roche.

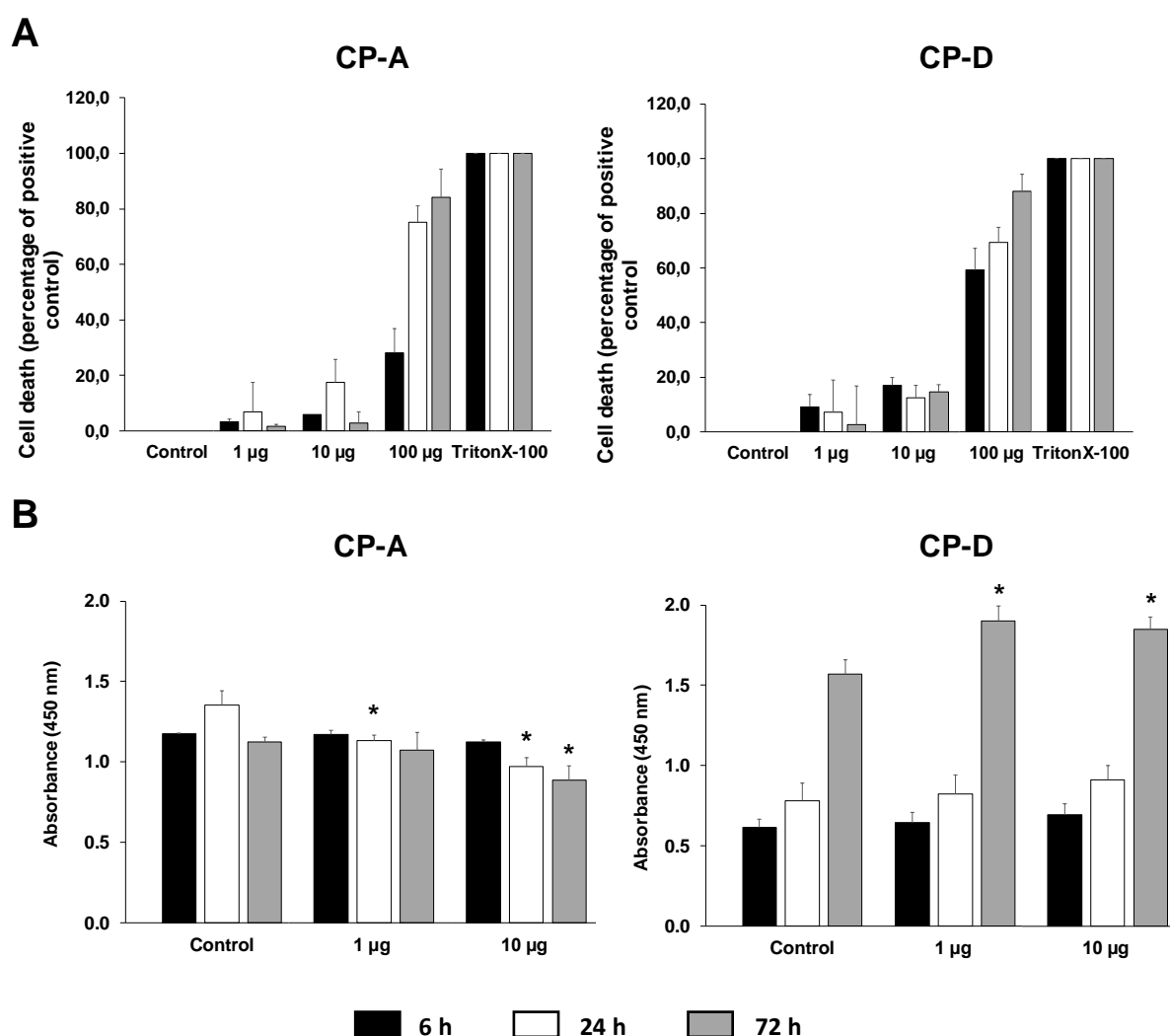


**Figure 2. Effects of cigarette smoke extract (CSE) treatment on cell viability and proliferation.** Metaplastic (CP-A) and dysplastic (CP-D) oesophageal cell lines were exposed to different concentration of CSE for 6, 24 and 72 hours and the effects on cellular viability (A) and proliferation (B) were studied using LDH and CCK8 assays, respectively. In the case of viability assay, as a positive control, 0.1% Triton X-100 was used. Data represent mean  $\pm$  SEM of three, independent experiments. \*= $p \leq 0.05$  vs. Control.

We have found that in case of both cell lines, lower concentrations of CSE (1 and 10  $\mu\text{g/mL}$ ) caused moderate cell death, around 20% in all three incubation periods. In contrast, 100  $\mu\text{g/mL}$  CSE induced a time-dependent, high cell death rate. 72 hours after the CSE treatment, cell death was above 80%. As 100  $\mu\text{g/mL}$  concentration of CSE was toxic for the cells, we continued investigating the proliferative activity only in lower concentrations (1 and 10  $\mu\text{g/mL}$ ) of CSE.

After treating the cells with CSE for 6, 24, and 72 hours, proliferative activity of the cells was estimated using CCK-8 assay according to manufacturer's instructions. Proliferation of CP-A cells dose-dependently decreased after 24 and 72 hours CSE treatment compare to control. In CP-D cells proliferative rate increased in the 72 hours treatment groups, at both concentrations (Figure 2B).

#### **4.2 $\text{Na}^+/\text{H}^+$ -exchanger-1 activity and expression in metaplastic and dysplastic Barrett cell lines**

For investigating the function of NHE,  $\text{NH}_4\text{Cl}$  pre-pulse technique was performed. Briefly, cells were perfused with standard HEPES solution and when 20 mM  $\text{NH}_4\text{Cl}$  was added to the system, after that, an intracellular alkalinisation was observed. Withdrawal of  $\text{NH}_4\text{Cl}$  caused a sudden drop in  $\text{pH}_i$  followed by an elevation in the following 60 s, which is called recovery. In the absence of  $\text{HCO}_3^-$ , the rate of recovery from acidosis reflects the activity of NHEs (Figure 3A). Our workgroup has previously shown that the primary NHE isoform is NHE-1 in CP-A and CP-D cell lines, and NHE-1 has the greatest role in  $\text{pH}_i$  regeneration<sup>90</sup>. Recovery rate from acidosis, consequently functional activity of NHE-1, was significantly higher in CP-A cells (BF:  $5.47 \pm 0.52$ ) than in CP-D cells (BF:  $3.36 \pm 0.24$ ) (Figure 3B). We have also examined the mRNA and protein expression of NHE-1 in these cell lines at certain time points (6, 24 and 72 hours). RT-qPCR was performed for investigating mRNA expression, and data were normalized to  $\beta$ -actin (*ACTB*) (Figure 4A). We have found that there was no significant difference between mRNA expression of NHE-1 in CP-A and CP-D cells, neither between incubation times. Similarly, to RT-qPCR results, Western blot analysis showed that protein levels were entirely the same at both cell lines and time points (Figure 4B).



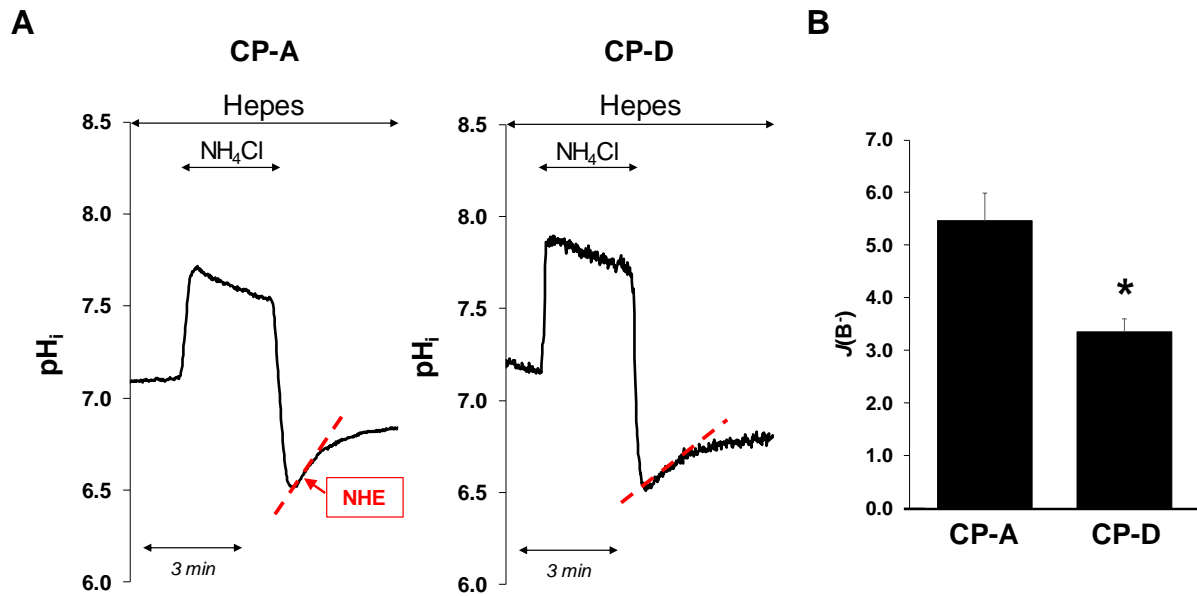


**Figure 3. Activity of  $Na^+/H^+$  exchanger-1 (NHE-1) in human Barrett's oesophageal cell lines.** (A) Representative intracellular pH ( $pH_i$ ) curves present the recovery from acidosis in CP-A and CP-D cells. (B) Summary data of the calculated activity of NHE-1 in the different cell lines. The rate of pH recovery ( $J(B^-)$ ) was calculated from the  $\Delta pH/\Delta t$  obtained via linear regression analysis of the  $pH_i$  measurement performed over the first 60 s of recovery from the lowest  $pH_i$  level (initial  $pH_i$ ). The buffering capacity at the initial  $pH_i$  was used to calculate  $J(B^-)$ . Data are presented as the mean  $\pm$  SEM. \*:  $p \leq 0.05$  vs. CP-A.  $n = 5-11$  experiments/26-91 ROIs.

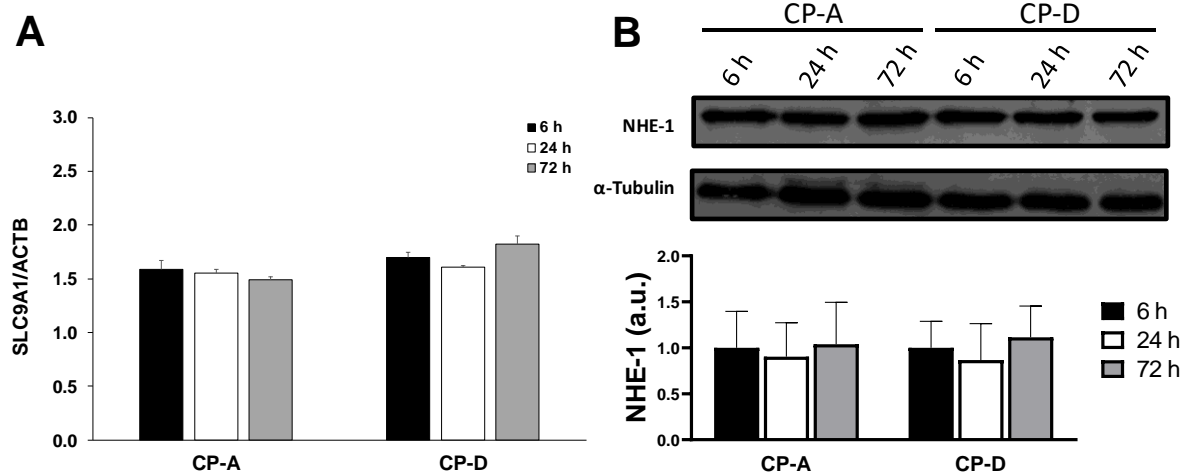


**Figure 4. mRNA and protein expression of  $Na^+/H^+$  exchanger-1 (NHE-1) in oesophageal cell lines.** (A) mRNA and (B) protein expression of NHE-1 in the CP-A and CP-D cells.  $\alpha$ -Tubulin was used as a protein-loading control. Data represent mean  $\pm$  SEM of three independent experiments.

### 4.3 Effect of cigarette smoke extract on $\text{Na}^+/\text{H}^+$ -exchanger-1 activity and expression in metaplastic and dysplastic Barrett cell lines

We have studied the acute effects of CSE on NHE-1 activity by performing the above mentioned  $\text{NH}_4\text{Cl}$  pre-pulse technique. Since CSE can cause disturbances of fluorescence signals, we incubated the cells with CSE (1, 10 and 100  $\mu\text{g}/\text{mL}$ ) for one hour, then changed the incubation solution to HEPES solution before the measurements. As it can be seen on Figure 5A and B, in CP-A cells we have observed that 1  $\mu\text{g}/\text{mL}$  CSE reduced the activity of NHE-1 compared to the control ( $5.47 \pm 0.52$  to  $3.08 \pm 0.55$ ). However, treatment with higher concentrations of CSE provoked an elevated function of this exchanger, and 100  $\mu\text{g}/\text{mL}$  CSE pre-treatment caused a more than 2-fold elevation ( $8.18 \pm 1.3$  at 10  $\mu\text{g}/\text{mL}$  CSE and  $12.28 \pm 0.73$  at 100  $\mu\text{g}/\text{mL}$  CSE). In case of CP-D cells, CSE decreased the activity of NHE-1 in all three groups.

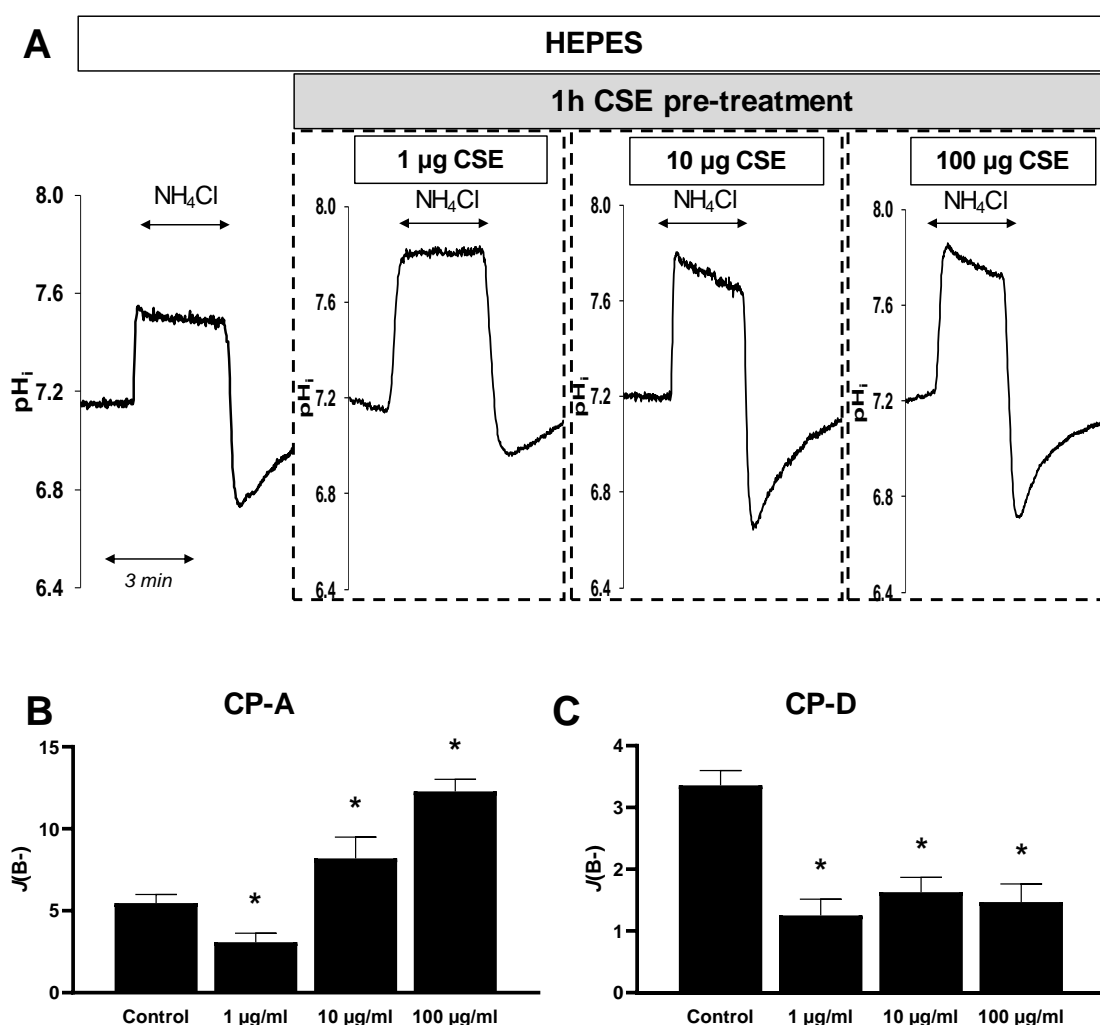


**Figure 5. Effects of cigarette smoke extract (CSE) treatment on the activity of  $\text{Na}^+/\text{H}^+$  exchanger-1 (NHE-1) in oesophageal cell lines. Metaplastic (CP-A) and dysplastic (CP-D)**

oesophageal cell lines were pre-treated with different concentration of CSE (1, 10 and 100  $\mu\text{g/mL}$ ) for 1 hour and the activity of NHE-1 was measured. (A) Representative intracellular pH ( $\text{pH}_i$ ) curves present the recovery from acidosis in CP-A cells. (B) Summary data of the calculated activity of NHE-1 in the different cell lines. The rate of pH recovery ( $J(\text{B}^-)$ ) was calculated from the  $\Delta\text{pH}/\Delta t$  obtained via linear regression analysis of the  $\text{pH}_i$  measurement performed over the first 60 s of recovery from the lowest  $\text{pH}_i$  level (initial  $\text{pH}_i$ ). Data are presented as the mean  $\pm$  SEM. \*:  $p \leq 0.05$  vs. Control.  $n = 12-14$  experiments/66-68 ROIs.

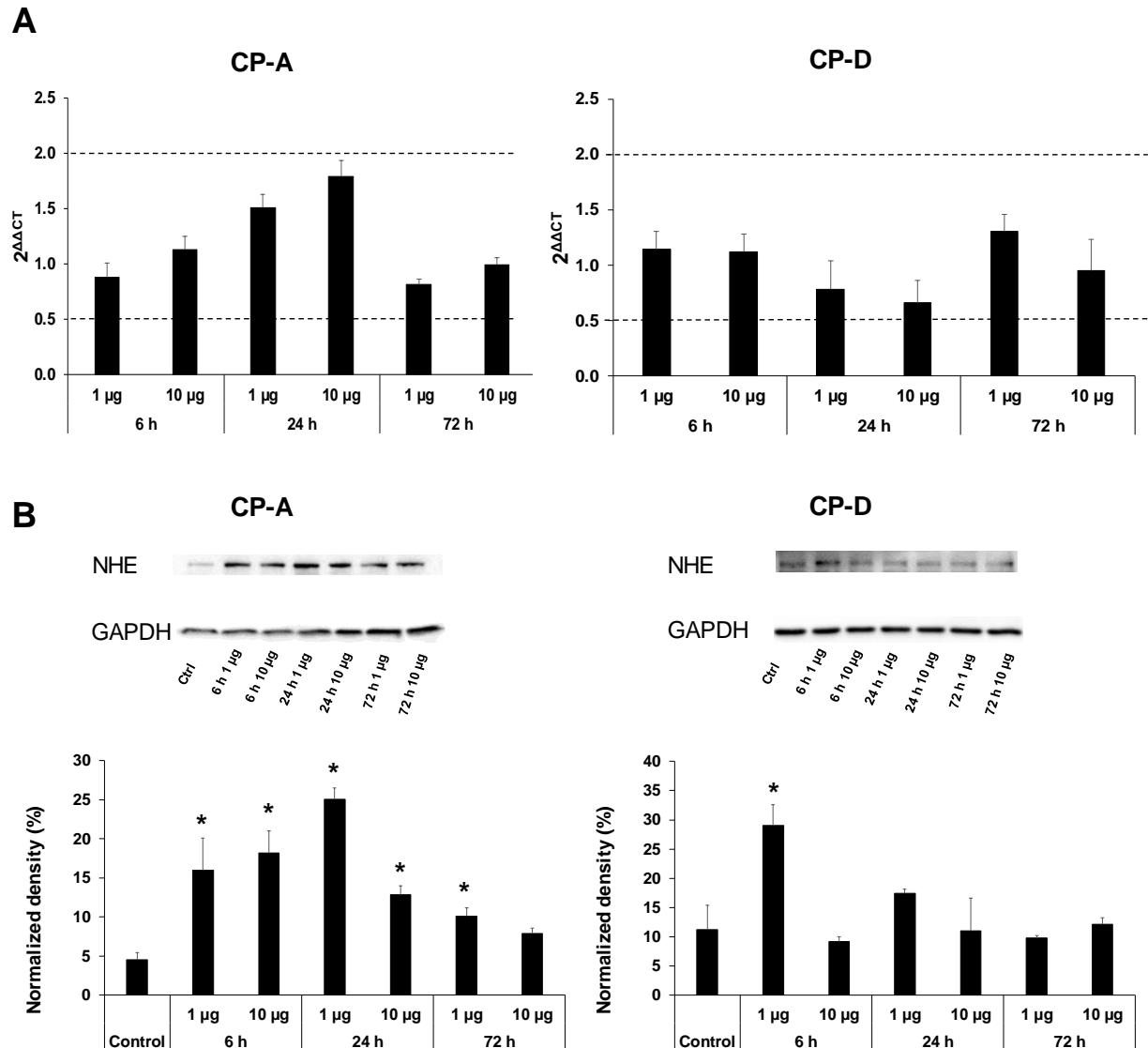


**Figure 6. Effects of cigarette smoke extract (CSE) treatment on the mRNA and protein expression of  $\text{Na}^+/\text{H}^+$  exchanger-1 (NHE-1) in oesophageal cell lines.** Metaplastic (CP-A) and dysplastic (CP-D) oesophageal cell lines were treated with different concentration of CSE (1 and 10  $\mu\text{g}$ ) for 6, 24 and 72 hours and the relative gene (A) and protein (B) expression of NHE-1 were investigated by real-time PCR and Western blot, respectively. Data represent mean  $\pm$  SEM of three, independent experiments. \*:  $p \leq 0.05$  vs. Control.

For expressional studies, we have treated the cells with 1 and 10  $\mu\text{g/mL}$  of CSE for 6, 24 and 72 hours and implemented qPCR and Western blot analysis. We did not detect any significant changes in mRNA expression of NHE-1 after CSE treatment in any of the cell lines (Figure 6A). In spite of these results, in CP-A cells protein levels were elevated in almost all groups. Surprisingly, in CP-D cells there was an elevated protein level only in the 6-hour 1  $\mu\text{g/mL}$  CSE treatment group, and no significant differences could be seen in the other groups (Figure 6B).

#### **4.4 Effect of smoking on $\text{Na}^+/\text{H}^+$ -exchanger-1 activity in normal oesophageal cells**

In order to investigate how CSE affects NHE activity under physiological conditions, we studied the effect of CSE on normal OECs isolated from guinea pigs. The same concentrations were used as for the cell lines, and the cells were pre-treated with CSE in the same manner. As shown in Figure 7A-B, NHE-1 activity was significantly reduced by CSE treatment (from  $12.19 \pm 0.46$  to  $4.64 \pm 0.94$  at 1  $\mu\text{g/mL}$  CSE, to  $3.96 \pm 0.43$  at 10  $\mu\text{g/mL}$  CSE and to  $4.49 \pm 0.4$  at 100  $\mu\text{g/mL}$  CSE, respectively). In chronic studies, we have investigated the long-term effects of smoking on OECs using a guinea pig model. Male guinea pigs were selected for three groups depending on the period of cigarette smoke exposure. Animals were exposed to cigarette smoke in a smoking chamber 4 times a day, 5 times a week for one, two and four months, respectively. All animals were 5 months old at the time of sacrifice. Control animals were age-matched with the treated group and not exposed to cigarette smoke. OECs were isolated according to the isolation protocol mentioned earlier and  $\text{NH}_4\text{Cl}$  pre-pulse technique was performed in order to estimate changes in NHE-1 function. Results were similar to the acute experiment results; after long-term cigarette smoke exposure the recovery rate was reduced in all three groups, compared to their own control groups, hence cigarette smoke exposure decreased NHE-1 activity (Figure 7C).

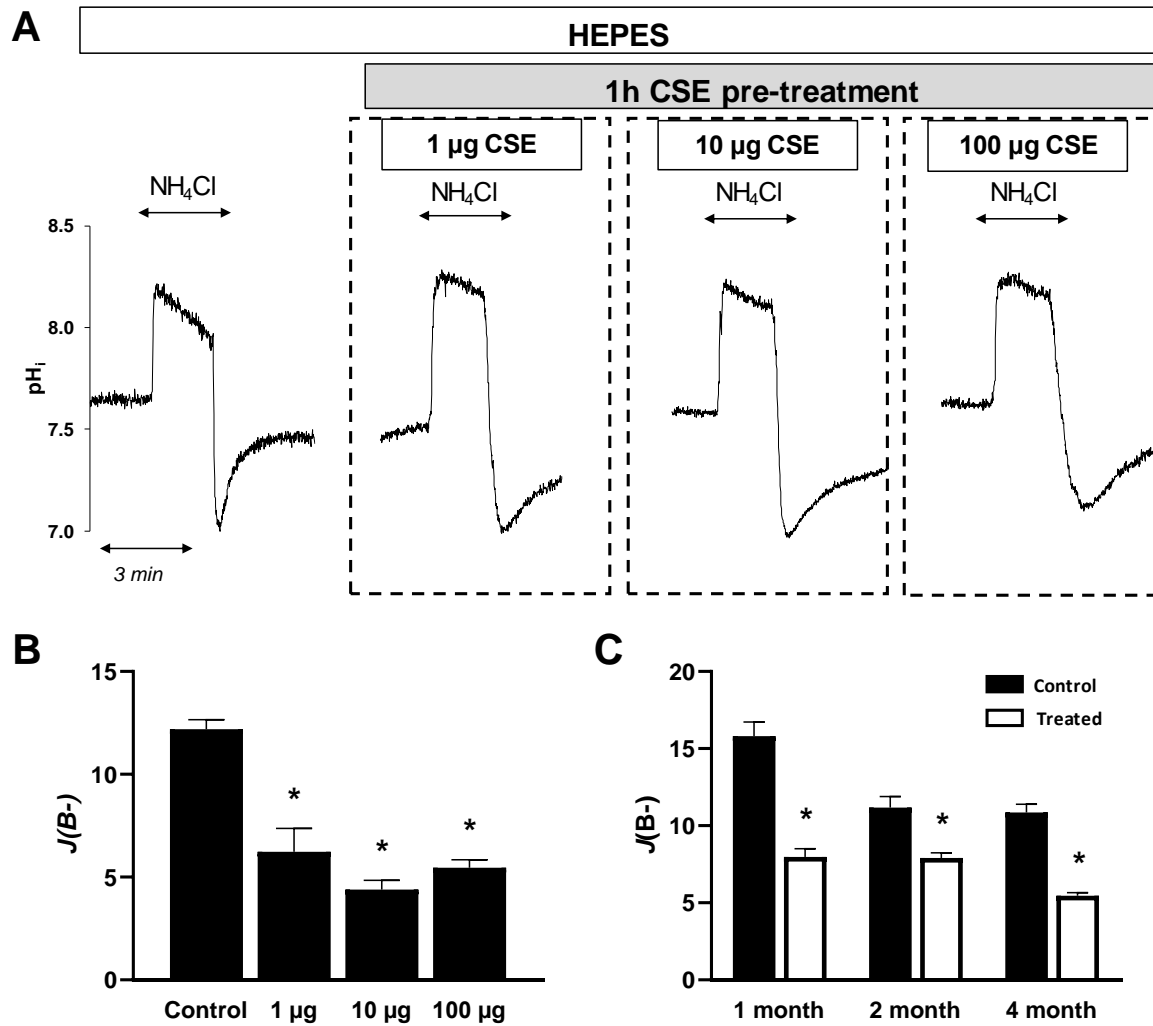


**Figure 7. Effects of cigarette smoke extract (CSE) treatment and smoking on the activity of Na<sup>+</sup>/H<sup>+</sup> exchanger-1 (NHE-1) in guinea pig oesophageal epithelial cells (OECs).** (A) Normal guinea pig OECs were pre-treated with different concentration of CSE (1, 10 and 100 µg/mL) for 1 hour and the activity of NHE-1 was measured. Representative intracellular pH (pH<sub>i</sub>) curves show the recovery from acidosis. (B) Summary data of the calculated activity of NHE-1 in guinea pig OECs. The rate of pH recovery ( $J(B^-)$ ) was calculated as described in the method section. Data are presented as the mean ± SEM. \*:  $p \leq 0.05$  vs. Control.  $n = 13-18$  experiments/86-99 ROIs. (C) Summary data of the calculated activity of NHE-1 in guinea pig OECs. The rate of pH recovery ( $J(B^-)$ ) was calculated from the  $\Delta pH/\Delta t$  obtained via linear regression analysis of the pH<sub>i</sub> measurement performed over the first 60 s of recovery from the lowest pH<sub>i</sub> level (initial pH<sub>i</sub>). Data are presented as the mean ± SEM. \*:  $p \leq 0.05$  vs. Control.  $n = 8-16$  experiments/81-211 ROIs.

#### 4.5 Effect of long-term smoking on Na<sup>+</sup>/H<sup>+</sup>-exchanger-1 expression in human oesophageal samples

NHE-1 immunostaining of biopsy samples from normal squamous epithelia and BO was performed. Patients were classified into four groups based on their diagnosis and smoking history. Those patients, who had been smoking for minimum of 20 years were classified as

smokers, and those, who have never smoked or have not smoked for one year before the biopsy sampling were classified as non-smokers. Normal epithelium and the intact margin of resected oesophageal cancer section were used as controls. Protein expression was determined with a semi-quantitative scoring system, and DAB intensities were calculated for quantification. In normal, non-smoker group, low NHE-1 expression could be detected and it was even lower in the smoker group. On the contrary, in BO patients' samples there was a strong NHE-1 expression, which was further increased by smoking (Figure 8A and B).

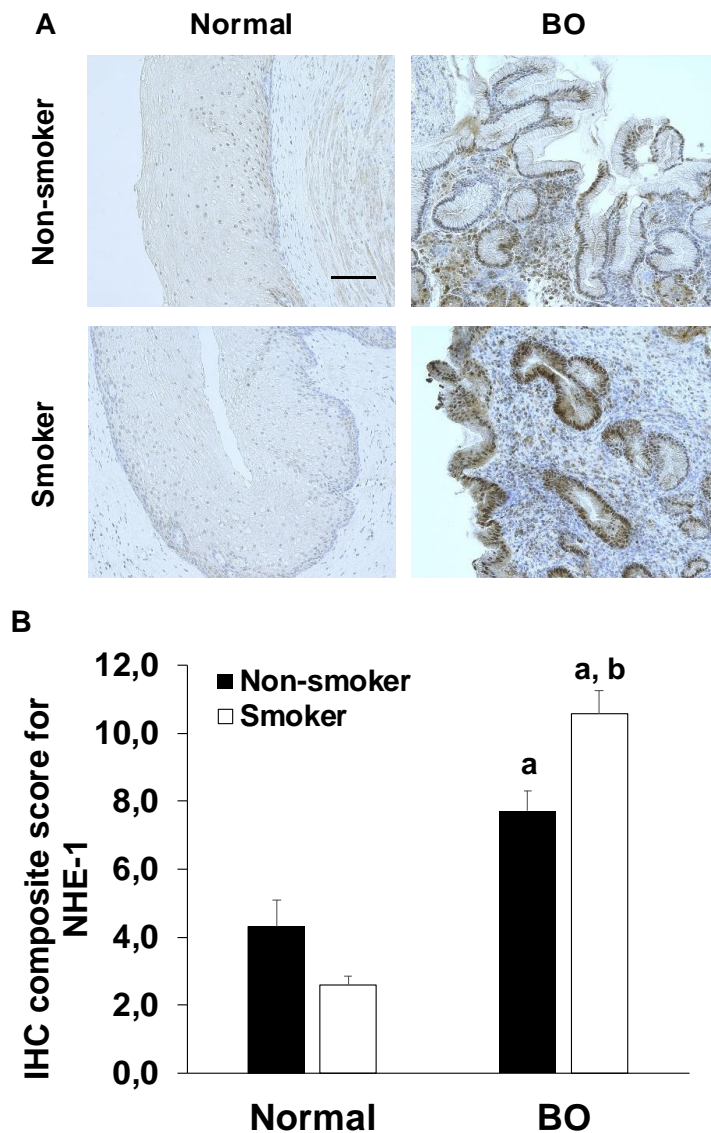


**Figure 8. Expression of Na<sup>+</sup>/H<sup>+</sup> exchanger-1 (NHE-1) in human oesophageal samples.** (A) Representative

immunohistochemical stainings show the presence of NHE-1 in human oesophageal samples. (B) Quantification of DAB intensities were calculated using a semiquantitative scoring system. Data represent mean  $\pm$  SEM of 23-25 specimens/3-6 patients each group. a= $p \leq 0.05$  vs. normal, b= $p \leq 0.05$  vs. non-smoker. Scale bar represents 100  $\mu$ m.

#### 4.6 Effect of knockdown of *SLC9A1* gene on the proliferation of metaplastic and dysplastic oesophageal epithelial cell lines

In order to investigate whether the altered expression or activity of NHE-1 has any role in the effect of CSE on proliferation, we silenced the *SLC9A1* gene, using specific siRNA. The efficiency of silencing was investigated at both mRNA and protein levels (Figure 9A and B). In CP-A cells, NHE-1 knockdown reduced the rate of proliferation at each incubation time, suggesting that NHE-1 is essential for the normal function of the cells. In the CP-D cells, the lack of NHE-1 protein initially increased the rate of proliferation, whereas no significant difference was observed with additional incubation times (Figure 9C). In the absence of NHE-1, CSE treatment increased the rate of proliferation in the CP-A cells in almost all treated groups. For CP-D cells, proliferation increased alone in the 72 hours treatment group (Figure 9D).

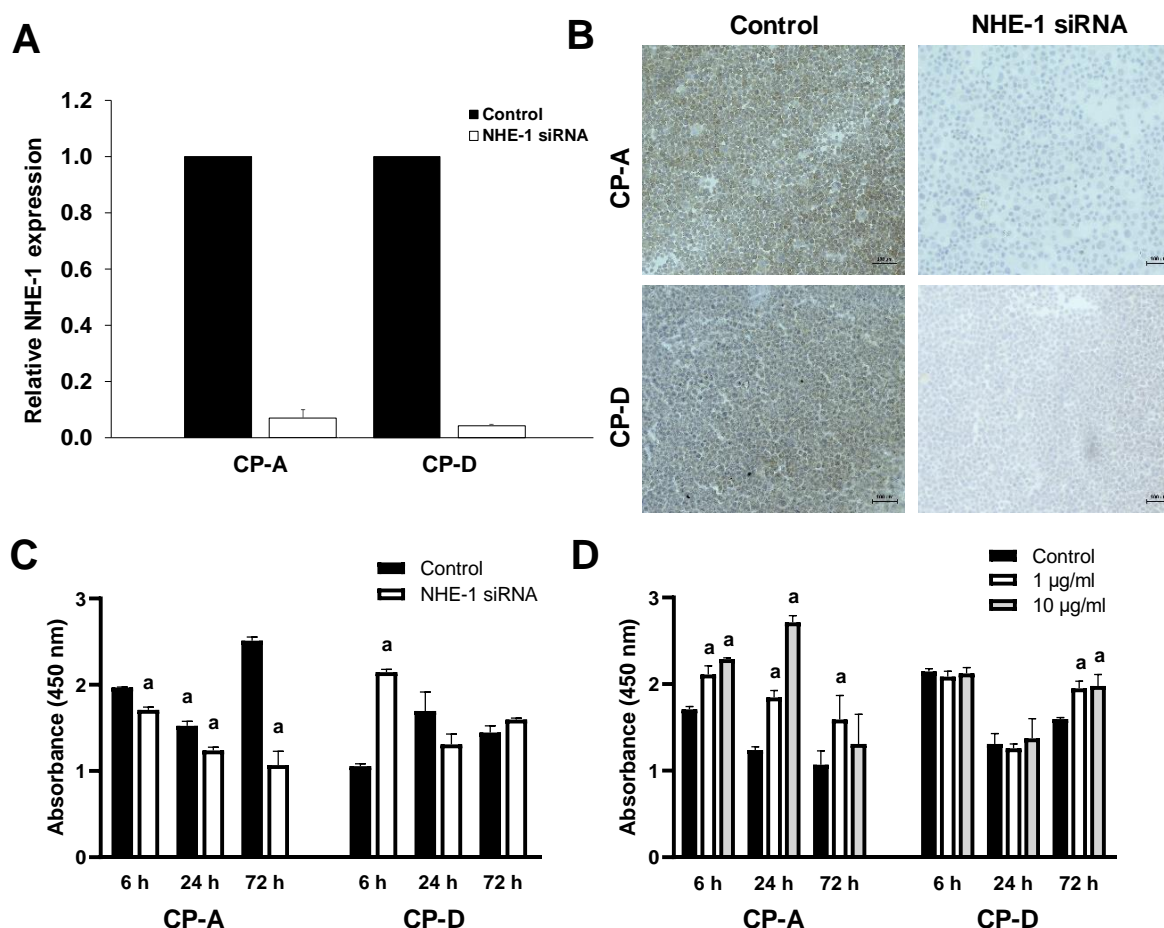


**Figure 9.** Expression of  $\text{Na}^+/\text{H}^+$  exchanger-1 (NHE-1) and proliferative activity of cells after *SLC9A1* knockdown in human Barrett's oesophageal cell lines.. The expression levels of NHE-1 were investigated by RT-PCR (A) and immunohistochemistry (B) in control cells and in cells treated with specific siRNA for *SLC9A1*. The rate of proliferation was determined

in the non-treated (**C**) and cigarette smoke extract-treated (**D**) CP-A and CP-D cells. Data represent mean  $\pm$  SEM of three independent experiments;  $a = p \leq 0.05$  vs. control.

#### 4.7 Effect of bile acids on the proliferation of Capan-1 cells

Cells were incubated with GCA, TCA, GDCA, TDCA, GCDCA and TCDCA for 24, 48 and 72 hours in two different concentrations (100 and 500  $\mu$ M), then we estimated proliferative activity of the cells. BAs increased proliferation of Capan-1 cells almost in all treated groups (Figure 10.). TDCA dose-dependently decreased proliferative activity of the cells, especially after 24 hours ( $0.83 \pm 0.06$ ) at 100  $\mu$ M, and increased it ( $1.64 \pm 0.02$ ) at 500  $\mu$ M at each incubation time.

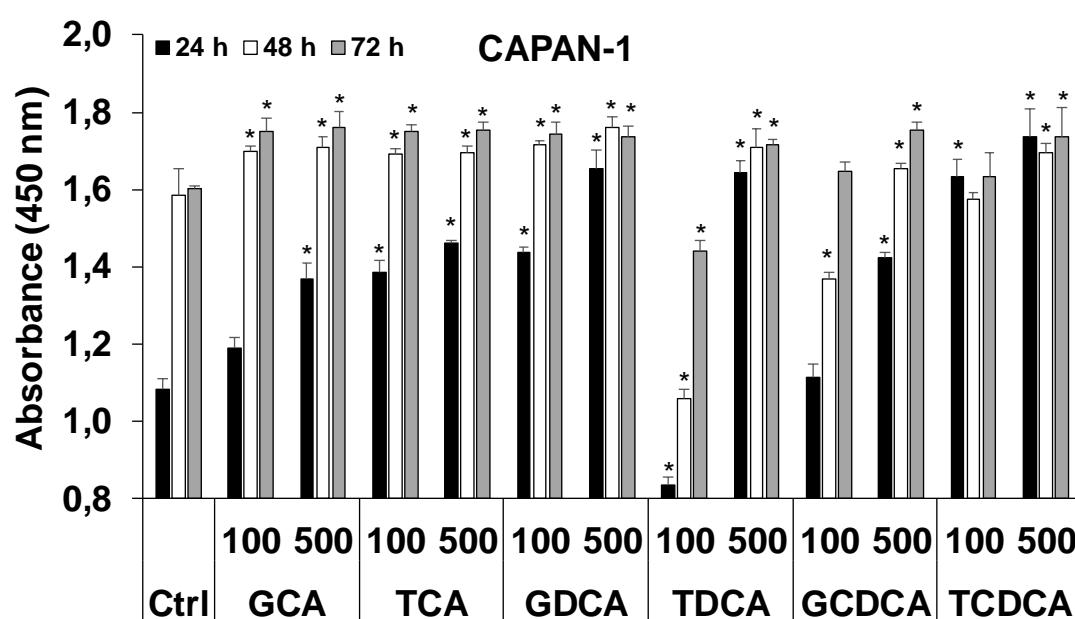


**Figure 10. Proliferative activity of Capan-1 cells after bile acid (BA) treatment.** Capan-1 cells were treated with 100 and 500  $\mu$ M of BAs for 24, 48 and 72 hours, then the rate of proliferation was determined with CCK8 assay as it was described in the Methods section. Data represent mean  $\pm$  SEM of three independent experiments;  $* = p \leq 0.05$  vs. control. Ctrl, control; GCA, glycocholic acid; TCA, taurocholic acid; GDCA, glycodeoxycholic acid; TDCA, taurodeoxycholic acid; GCDCA, glycochenodeoxycholic acid; TCDCA, taurochenodeoxycholic acid.



## 5. Discussion

Orlando et al. has summarized the pathogenesis of GORD as the imbalance of defence and offensive factors <sup>10</sup>. Weakening of the defence mechanisms of the oesophagus may contribute to the development of both BO and GORD <sup>130</sup>. In GORD or duodeno-gastrooesophageal reflux (DGOR), the regurgitating acidic gastric content, which usually contains gastric acid, pepsin, bile salts or pancreatic enzymes, damages the oesophageal mucosa, and on a long-term it causes oesophagitis and BO <sup>15</sup>. BO refers to a state, when oesophageal squamous epithelium is replaced by intestine-type columnar metaplasia as a consequence of repeated reflux episodes over a long period of time. The explanation of cell replacement might be a chronic injury caused by the regurgitating acid, which induces trans-differentiation by the alteration in transcription factors or prompts immature oesophageal progenitor cells to form to columnar cells <sup>131,132</sup>. BO has no symptoms, and this condition has a high malignant potential and predisposes to oesophageal adenocarcinoma <sup>83</sup>.

Among risk factors we can mention several elements: older age, male sex, white race, smoking, hiatal hernia, metabolic syndrome, chronic heartburn, GORD, BO or OAC in family history <sup>83</sup>. Smoking is one of the most harmful habits that increases the risk of many diseases, including oesophageal diseases. It was shown, that smoking weakens oesophageal defence mechanisms, such as oesophageal clearance by reducing saliva production or anti-reflux mechanisms by relaxation of LOS, and causing more frequent reflux episodes and a prolonged clearance time <sup>112</sup>. After swallowing, substances from tobacco smoke mixed with saliva can directly contact the oesophageal lining, which might be also harmful for the OECs. Clinical studies have also shown that smoking elevates the risk for BO and OAC, and enhances the progression of BO to dysplasia and OAC <sup>106,107,110</sup>.

From oesophageal defence processes, ion transporters have a great importance, especially NHE-isoforms. NHEs exchange extracellular  $\text{Na}^+$  and intracellular  $\text{H}^+$ , therefore maintain a physiological  $\text{pH}_i$  and regulate cell volume. The most common NHE isoform is NHE-1, which is ubiquitously expressed in human tissues, and besides the above mentioned functions, it is involved in cell proliferation, migration and differentiation. The presence of NHE-1 isoform was described in both rodent and human oesophageal epithelium <sup>65,67,70,71</sup>. It has been shown that compared to the other NHE isoforms, NHE-1 is most responsible for the regulation of  $\text{pH}_i$  in OECs. The role of NHE-1 under physiological conditions is largely

clarified, but it is less studied under pathological conditions. In the present study, we investigated for the first time how CSE affects NHE-1 activity in normal oesophageal epithelium and in BO cell lines.

As a first step of experiments, we have checked the cytotoxic and proliferative potential of CSE on OECs. A massive cell death was observed in case of 100 µg/mL in both CP-A and CP-D cells, therefore we administered only the lower, 1 and 10 µg/mL concentrations in the further experiments. We have also investigated proliferative activity of CP-A and CP-D cells after 6-, 24- and 72 hours long CSE treatment, and we experienced a significant reduction in proliferation of CP-A cells after 24 hours incubation with 1 µg/mL CSE, and after the same or longer incubation with 10 µg/mL CSE. In contrast, a marked increase was observed after 72 hours in both CSE concentrations in CP-D.

In the first step of functional studies, we compared the activity of NHE in different oesophageal cell types. We have compared the base flux values of acid regeneration in normal, metaplastic and dysplastic cells. For modelling the physiological circumstances, we chose primary, freshly isolated guinea pig OECs. The reason why we used primer guinea pig OECs instead of human OECs or human oesophageal cell lines is that the human cells are highly sensitive, and difficult to maintain them in cell culture. Therefore, they are not suitable for long-term studies or functional measurements. Primary cell cultures isolated from rodents are much more resistant, retain their viability for a longer period of time and are suitable for functional measurements<sup>37,133,134</sup>. We chose guinea pig, because compared to rats and mice, (i) the oesophageal mucosa can be removed more easily, (ii) more cells can be isolated from its oesophageal epithelium and (iii) it's oesophagus shows more similarities to humans, e.g. SMGs are present also in guinea pigs.<sup>135</sup> In the functional studies we have found, that normal OECs are more active, than BO cells, and a dynamic reduction in NHE activity can be seen from normal to dysplastic state. CSE pre-treatment reduced NHE-1 activity in normal and dysplastic cells, whereas in metaplastic cells we could detect a marked elevation in the 10 and 100 µg/mL groups. The reduced activity of NHE-1 in normal and dysplastic cells may be explained by the observation of Orlando et al. They found that CSE inhibits the Na<sup>+</sup> transport of normal oesophageal epithelia in rabbit which is presumably due to the reduced function of NHE-1<sup>113</sup>. In the case of BO cells, the increased NHE activity can presumably be explained by the fact that metaplastic cells have a greater adaptation potential to the changed environment than dysplastic cells, as we previously demonstrated it in the case of BAs<sup>90</sup>.

For expressional studies, BO cells were incubated for 6, 24 and 72 hours with CSE, then alterations in mRNA and protein levels were investigated with RT-qPCR and Western blotting, respectively. In general, we could not detect significant changes in mRNA expression after treatment in any groups; although, there was an elevation after 24 hours in CP-A cells, but it was not significant either. On protein level, we have seen marked elevation in almost every treated group in the CP-A cells. It is not entirely clear why the changes experienced at the protein level were not detectable at the mRNA level. Although there was an increase in mRNA levels, particularly in the 1 and 10 µg/mL 24 hours CP-A groups, this was not significant. A possibly explanation is, that there can be transcriptional changes that influenced protein levels and resulted significant alterations.

A highly important part of our study is examining the NHE-1 activity after long-term smoking. We have exposed guinea pigs to cigarette smoke for 1, 2 and 4 months, sacrificed them, and checked NHE-1 activity with NH<sub>4</sub>Cl technique. Age- and sex-matched controls were used, and all animals were at the same age at the time of sacrifice. In all treated groups, pH<sub>i</sub> recovery curves rose merely slowly, ergo smoking considerably decreased NHE-1 activity under normal conditions. At the 2-month group the base flux values after exposure were nearly the same, like in the 1-month group, so a classic time-dependent manner could not be detected. The cause of this finding might be that the ion transport processes, like NHE activity may vary at different ages in guinea pigs considering that base flux of control groups also show differences. In this part of our study, it would be more favourable to perform functional measurements also on human OECs to get a more accurate view of NHE-1 activity in the human oesophagus. For this measurements freshly isolated primary human OECs or human oesophageal organoids would be needed, that to date, are not available in our laboratory. Creating human oesophageal organoids is a challenging process and these organoids are difficult to maintain and seed. However, our laboratory team have successfully established mouse oesophageal organoids, these organoids are viable for a longer time, can be seeded, and are also suitable for examining ion transport processes <sup>136</sup>.

For examining the long-term effects of smoking on the NHE-1 in human OECs, we have decided to investigate alterations of NHE-1 expression in human oesophageal samples. Four groups were created based on the smoking history and histology: patients were classified as smoker or non-smoker, and samples as normal and Barrett's metaplasia. Dysplastic samples were not included due to the low number of patients. Patients with a 20-year-long continuous

smoking history were classified as smokers, and patients who have never smoked or stopped smoking minimum one year before the biopsy sampling were considered as non-smokers. Due to the literature data, in human oesophageal epithelia, NHE-1 shows a low expression, but an increased expression can be detected in GORD, BO and oesophageal cancer<sup>88,90,104,105</sup>. Similarly, to earlier studies, we also detected that in healthy, normal epithelium NHE-1 showed a relatively weak expression and a high expression was found in BO samples. During investigation of the relation of smoking status and NHE-1 expression, we observed, that in normal epithelium NHE-1 staining were even weaker in smokers, in spite of this in BO samples, smoking further increased the elevated NHE-1 expression.

Based on the functional and expression results, we can conclude that, **in normal state**, acute CSE treatment decreased NHE function, and in accordance with this, on a long-term smoking also significantly decreased the activity of NHE-1 in guinea pig. These results are also consistent with human data, where NHE-1 expression was also reduced by smoking in normal samples. **In metaplastic state**, acute administration of CSE induced a robust elevation of the functional activity of NHE-1 and long-term CSE exposure caused higher NHE-1 protein levels. The same results can be seen after examining human samples, namely the high NHE-1 expression in BO becomes even higher in smokers. As it was described earlier, NHE-1 has only a weak expression in normal epithelium or in normal cell line, and in metaplastic state NHE-1 is more active and highly expressed<sup>88,90</sup>. According to the most accepted hypothesis, NHE-1 protein upregulates as a result of long-term acid exposure in order to handle intracellular acidification, this phenomenon may be an adaptive response<sup>88,90,103,130</sup>. Smoking induced an even higher NHE-1 upregulation in BO patients, indicating that similarly to acid, smoking also switch on an adaptive, protective response in order to avoid cellular acidification. Although, it should be also mention that Coleman et al. have stated, that smoking raises the chance in BO for high-grade dysplasia and cancer. This suggest that although increased NHE activity attempts to maintain normal pH homeostasis within the cell, other mechanisms nevertheless contribute to the cancerous transformation of BO cells<sup>110</sup>.

An important finding of our study is that smoking influenced the proliferation of the BO cells in absence of NHE-1. We performed NHE-1 knockdown using specific siRNA oligonucleotids. In absence of NHE-1, proliferative activity of CP-A cells decreased, whereas in case of CP-D, we could detect increased proliferation only after 6 hours. After CSE administration, we observed a massive change. In NHE-1 silenced, CP-A cells smoking induced

a considerable increase in proliferation, in almost each groups. In spite of this, in CP-D cells the proliferation did not change in the presence of CSE after 6 and 24 hours, proliferation elevated only after 72 hours. It is well-known that NHE-1 promotes cell proliferation in normal cells <sup>62</sup>. Fitzgerald et al have shown, that short-term acid-pulses provoke hyperproliferation, whereas long-term acid exposure induces differentiation in BO <sup>87</sup>. Ariyoshi et al have described that in OSCC cells NHE-1 knockdown caused an inhibition of apoptosis and induced proliferation <sup>105</sup>. In our study we have observed that metaplastic cells proliferate slower after CSE treatment, but in NHE-1 silenced cells, CSE increased proliferative activity. Therefore, NHE-1 has a highlighted, presumably protective role in metaplastic state. **In dysplastic cells**, longer incubation with CSE caused an increase in proliferation. After NHE-1 knockdown, proliferative activity remained high after 72 hours. These results indicate, that in CP-D cells, smoking induces proliferation on long-term, but NHE-1 might not be involved.

We should also mention the limitations of our research. The first one is that only normal and metaplastic biopsy samples were analysed, dysplastic samples were not included. Increasing the number of patients and samples would also be reasonable. Secondly, as we conducted retrospective data collection, there was often a lacking information about the details of smoking in patients' medical history, thus, we could not calculate package years, which would be a valuable information. Thirdly, as I have mentioned above, since human OECs and normal cell lines are sensitive, we could not perform functional and expressional studies on them, which has a bigger relevance in investigating the pathophysiology of BO.

These results strengthen the observation, that smoking has a significant role in the pathomechanism of BO. NHE-1 has an essential function in pH homeostasis of the cells. In normal OECs, smoking reduces the activity of NHE-1, and on a long-term NHE-1 expression is also reduced. The worsening alkalising function can no more maintain normal pH range, and this state leads to metaplastic transformation of the oesophageal epithelium. In metaplastic cells, NHE-1 expression and activity is also higher in order to compensate the pH alterations, that smoking or other toxic agents caused. NHE-1 also participates in proliferation, and in absence of NHE-1, metaplastic cells react with high proliferative activity for smoking. All these results confirm that metaplastic cells attempt to compensate the effect of toxic agent, such as smoking. These cells have a high potential to malignant transformation and dysplastic state can easily occur. In dysplastic cells, the activity of NHE-1 is significantly lower than in metaplastic cells, and smoking does not influence expression or the activity of this ion transporter. In NHE-1

knockdown dysplastic cells proliferation does not change, but a long-term treatment enhances it. Based on these findings, NHE-1 has a protective role in metaplastic state, but dysplastic cells do not respond to CSE treatment indicating, that these changes would be not alterable in this cell type. It would be an interesting question, if NHE-1 expression or activity would change in case of cessation of smoking, or whether these alterations are reversible, since a clinical study indicated the decrease in risk for OSCC after cessation of smoking <sup>109</sup>. Nevertheless, it is highly recommended for every smoker patient to quit smoking as soon as possible to reduce the chances of oesophageal malignancies.

In the second part of this thesis, we investigated the effect of BAs on the proliferation of PC cells. Capan-1 is an aggressive, human PDAC cell line used for modelling the most common PC type. We incubated the cells with GCA, TCA, GDCA, TDCA, GCDCA and TCDCA for 24, 48 and 72 hours in two different concentrations, then we estimated proliferative activity of the cells. BAs were selected based on literature data; it was shown that certain BAs occur in the serum and pancreatic juice of PC patients <sup>120,128,137</sup>. As we expected, almost all BAs elevated the proliferative activity of Capan-1 cells, except TDCA, which in low concentration suppressed the proliferative rate, but elevated it at higher dose, depending on time. This result strengthens the data that were published in this topic, that hydrophobic BAs have a tumorigenic activity and promote proliferation of cancerous cells <sup>127,138</sup>.

## 6. Conclusion

In this research we attempted to describe possible alterations in epithelial cell functions induced by risk factors such as smoking in the oesophagus and BAs in the pancreas.

New findings of our study are the followings:

- Activity of NHE-1 varies in normal, metaplastic and dysplastic oesophageal cells and smoking influences NHE-1 differently in each cell type.
- **Under physiological circumstances**, both the activity and expression of NHE-1 is reduced by smoking, resulting in an intracellular acidosis. According to scientific literature, alterations in pH optimum can induce apoptosis, or via trans-differentiation, the appearance of metaplasia, in which the cells are more prone to malignant transformation.
- **In the metaplastic state**, smoking increases the function of NHE-1, which is presumably a compensatory mechanism that prevents the onset of cancerous processes by keeping the intracellular pH in the normal range. As the expression of NHE-1 decreases, this protective mechanism disappears and the proliferative potential of the cells increases.
- In contrast to BO, decreased activity or expression of NHE-1 had no effect on smoking-induced proliferation **in the dysplastic state** indicating the involvement of other mechanisms.

Taken together, we propose that upregulation of NHE-1 is the part of a protective mechanism against the harmful effects of smoking; however, further investigation would be needed to support this hypothesis. Nevertheless, the present results indicate that direct augmentation of NHE-1 function may provide new avenues for decreasing the damaging effect of smoking.

- The carcinogenic effect of BAs was strengthened by our results, as they elevated proliferative activity, an important character of cancerous cells. This feature may make the PC more aggressive. This additional observation might be a relevant information in terms of therapy.

## 7. Acknowledgements

Words cannot express my gratitude to my supervisor, Dr. Viktória Venglovecz, who taught and guided me all along my PhD training. Her professional guidance, logical way of thinking and encouragement helped me in my development and in acquiring a scientific mindset.

I would like to thank for Professor Dr. István Baczkó and Professor Dr. András Varró for giving the opportunity to fulfil my PhD training in the Department of Pharmacology and Pharmacotherapy, Albert Szent-Györgyi Medical School, University of Szeged. I could not have undertaken this journey without the professional support and advices of Professor Dr. Peter Hegyi.

I had a pleasure of collaborating with our co-authors of the published articles from Department of Pharmacognosy, Department of Biochemistry, Department of Pathology and Department of Pharmacology, University of Pécs. Special thanks go to Zoltán Márton Köhler, Dr. Kata Csekő, Krisztián Daru and Attila Horváth.

I would like to extend my sincere thanks to Eleonóra Gál, Tünde Pritz, Attila Ébert, Dr. Réka Molnár, Margaréta Korsós, Emese Tóth, Miklósné Árva, Edit Magyarné Pálfi, Zsolt Tóth and all of my colleagues. This thesis would not have been possible without their help, advices and generous support.

I am grateful for the financial support from the National Research, Development and Innovation Office (FK123982), the Economic Development and Innovation Operative Programme Grants (GINOP-2.3.2-15-2016-00015), the National Research, Development and Innovation Office, the Ministry of Human Capacities (EFOP 3.6.2-16-2017-00006), the Bolyai Postdoctoral Fellowship of the Hungarian Academy of Sciences (HAS) to Viktória Venglovecz (00509/16), the HAS-USZ Momentum Grant (LP2014-10/2017) and UNKP-18-4 New National Excellence Program Of The Ministry of Human Capacities.

Thanks should also go to my family and friends for encouragement and all of their support.



## 8. References

- 1 Mahadevan, V. Anatomy of the oesophagus. *Surgery (Oxford)* **38**, 677-682 (2020).
- 2 Sivarao, D. & Goyal, R. K. Functional anatomy and physiology of the upper esophageal sphincter. *The American journal of medicine* **108**, 27-37 (2000).
- 3 Al Yassin, T. M. & Toner, P. G. Fine structure of squamous epithelium and submucosal glands of human oesophagus. *Journal of Anatomy* **123**, 705 (1977).
- 4 Zhang, X. *et al.* The microscopic anatomy of the esophagus including the individual layers, specialized tissues, and unique components and their responses to injury. *Annals of the New York Academy of Sciences* **1434**, 304-318 (2018).
- 5 Németh, A., L. Kiss, A. in *Szövektan* (ed Pál Röhlich) Ch. Nyelöcső, 284-285 (Semmelweis Kiadó, 2006).
- 6 Oezcelik, A. & DeMeester, S. R. General anatomy of the esophagus. *Thoracic surgery clinics* **21**, 289-297 (2011).
- 7 Sachdeva, U. M. *et al.* Understanding the cellular origin and progression of esophageal cancer using esophageal organoids. *Cancer Letters* **509**, 39-52 (2021).
- 8 Becskeházi, E., Korsós, M. M., Eröss, B., Hegyi, P. & Venglovecz, V. OEsophageal ion transport mechanisms and significance under pathological conditions. *Frontiers in physiology* **11**, 855 (2020).
- 9 Antal, M., Liposits, Z., Oláh, I., Réthelyi, M., Sétáló, G. in *Funkcionális anatómia* (ed Miklós Réthelyi) 994 (Medicina Könyvkiadó Rt., 2006).
- 10 Orlando, R. C. Pathogenesis of gastroesophageal reflux disease. *The American journal of the medical sciences* **326**, 274-278 (2003).
- 11 Mittal, R. K., Holloway, R. H., Penagini, R., Blackshaw, L. A. & Dent, J. Transient lower esophageal sphincter relaxation. *Gastroenterology* **109**, 601-610 (1995).
- 12 Helm, J. F. *et al.* Effect of esophageal emptying and saliva on clearance of acid from the esophagus. *New England Journal of Medicine* **310**, 284-288 (1984).
- 13 Orlando, R. C. *Esophageal mucosal defense mechanisms*, <<https://www.nature.com/gimo/contents/pt1/full/gimo15.html>> (2006).
- 14 Dixon, J. *et al.* A mucus gel barrier is present in Barrett's oesophagus but is not present in normal oesophagus. *Gut* (1999).
- 15 Sarosiek, J. & McCallum, R. W. Mechanisms of oesophageal mucosal defence. *Best Practice & Research Clinical Gastroenterology* **14**, 701-717 (2000).
- 16 Namiot, Z., Sarosiek, J., Rourk, R. M., Hetzel, D. P. & McCallum, R. W. Human esophageal secretion: mucosal response to luminal acid and pepsin. *Gastroenterology* **106**, 973-981 (1994).
- 17 Sarosiek, J. & McCallum, R. The evolving appreciation of the role of esophageal mucosal protection in the pathophysiology of gastroesophageal reflux disease. *PRACTICAL GASTROENTEROLOGY* **18**, 20J-20J (1994).
- 18 Sarosiek, J. & McCallum, R. W. What is the secretory potential of submucosal mucous glands within the human gullet in health and disease? *Digestion* **56**, 15-23 (1995).

- 19 Arul, G. *et al.* Mucin gene expression in Barrett's oesophagus: an in situ hybridisation and immunohistochemical study. *Gut* **47**, 753-761 (2000).
- 20 Guillem, P. *et al.* Mucin gene expression and cell differentiation in human normal, premalignant and malignant esophagus. *International journal of cancer* **88**, 856-861 (2000).
- 21 Günther, C., Neumann, H. & Vieth, M. Esophageal epithelial resistance. *Digestive Diseases* **32**, 6-10 (2014).
- 22 Carney, C., Orlando, R., Powell, D. & Dotson, M. Morphologic alterations in early acid-induced epithelial injury of the rabbit esophagus. *Laboratory investigation; a journal of technical methods and pathology* **45**, 198-208 (1981).
- 23 Hopwood, D., Logan, K. R., Coghill, G. & Bouchier, I. Histochemical studies of mucosubstances and lipids in normal human oesophageal epithelium. *The Histochemical journal* **9**, 153-161 (1977).
- 24 Bass, B. L., Schweitzer, E., Harmon, J. & Kraimer, J. H<sup>+</sup> back diffusion interferes with intrinsic reactive regulation of esophageal mucosal blood flow. *Surgery* **96**, 404-413 (1984).
- 25 Hollwarth, M. E., Smith, M., Kvietys, P. R. & Granger, D. N. Esophageal blood flow in the cat: normal distribution and effects of acid perfusion. *Gastroenterology* **90**, 622-627 (1986).
- 26 Feldman, M., Morris, G. & Paterson, W. Role of substance P and calcitonin gene-related peptide in acid-induced augmentation of opossum esophageal blood flow. *Digestive diseases and sciences* **46**, 1194-1199 (2001).
- 27 Feldman, M. J., Morris, G., Dinda, P. & Paterson, W. Mast cells mediate acid-induced augmentation of opossum esophageal blood flow via histamine and nitric oxide. *Gastroenterology* **110**, 121-128 (1996).
- 28 Orlando, R. C. Esophageal epithelial defense against acid injury. *Journal of clinical gastroenterology* **13**, S1-5 (1991).
- 29 Jessica, L. L. & Charles, H. S. Integrins and epithelial cell polarity. *Journal of Cell Science* (2014).
- 30 Etienne-Manneville, S. Microtubules in cell migration. *Annual review of cell and developmental biology* **29**, 471-499 (2013).
- 31 Krogh, S. A. S. Croonian Lecture-The active and passive exchanges of inorganic ions through the surfaces of living cells and through living membranes generally. *Proceedings of the Royal Society of London. Series B-Biological Sciences* **133**, 140-200 (1946).
- 32 Frizzell, R. A. & Hanrahan, J. W. Physiology of epithelial chloride and fluid secretion. *Cold Spring Harbor perspectives in medicine* **2**, a009563 (2012).
- 33 Koefoed-Johnsen, V. & Ussing, H. H. The nature of the frog skin potential. *Acta physiologica scandinavica* **42**, 298-308 (1958).
- 34 Denker, S. P., Huang, D. C., Orlowski, J., Furthmayr, H. & Barber, D. L. Direct binding of the Na-H exchanger NHE1 to ERM proteins regulates the cortical cytoskeleton and cell shape independently of H<sup>+</sup> translocation. *Molecular cell* **6**, 1425-1436 (2000).

- 35 Demaurex, N. & Grinstein, S. Na<sup>+</sup>/H<sup>+</sup> antiport: modulation by ATP and role in cell volume regulation. *The Journal of experimental biology* **196**, 389-404 (1994).
- 36 Grinstein, S., Rotin, D. & Mason, M. J. Na<sup>+</sup>/H<sup>+</sup> exchange and growth factor-induced cytosolic pH changes. Role in cellular proliferation. *Biochimica et Biophysica Acta (BBA)-Reviews on Biomembranes* **988**, 73-97 (1989).
- 37 Venglovecz, V. *et al.* Effects of bile acids on pancreatic ductal bicarbonate secretion in guinea pig. *Gut* **57**, 1102-1112 (2008).
- 38 Farkas, K. *et al.* New therapeutic targets in ulcerative colitis: the importance of ion transporters in the human colon. *Inflammatory bowel diseases* **17**, 884-898 (2011).
- 39 Czepán, M. *et al.* NHE1 activity contributes to migration and is necessary for proliferation of human gastric myofibroblasts. *Pflügers Archiv-European Journal of Physiology* **463**, 459-475 (2012).
- 40 Judák, L. *et al.* Ethanol and its non-oxidative metabolites profoundly inhibit CFTR function in pancreatic epithelial cells which is prevented by ATP supplementation. *Pflügers Archiv-European Journal of Physiology* **466**, 549-562 (2014).
- 41 Russell, J. M. Sodium-potassium-chloride cotransport. *Physiological reviews* (2000).
- 42 Shiozaki, A. *et al.* Role of the Na<sup>+</sup>/K<sup>+</sup>/2Cl<sup>-</sup>-cotransporter NKCC1 in cell cycle progression in human esophageal squamous cell carcinoma. *World Journal of Gastroenterology: WJG* **20**, 6844 (2014).
- 43 Abdulnour-Nakhoul, S. *et al.* Ion transport mechanisms linked to bicarbonate secretion in the esophageal submucosal glands. *American Journal of Physiology-Regulatory, Integrative and Comparative Physiology* **301**, R83-R96 (2011).
- 44 Rocha-González, H. I., Mao, S. & Alvarez-Leefmans, F. J. Na<sup>+</sup>, K<sup>+</sup>, 2Cl<sup>-</sup> cotransport and intracellular chloride regulation in rat primary sensory neurons: thermodynamic and kinetic aspects. *Journal of neurophysiology* **100**, 169-184 (2008).
- 45 Tobey, N., Reddy, S. & Keku, T. Cragoe EJ Jr, Orlando RC. *HCl-induced cell edema in rabbit esophageal epithelium: a bumetanide-sensitive process. Gastroenterology* **109**, 414-421 (1995).
- 46 Abdulnour-Nakhoul, S., Nakhoul, N. L., Caymaz-Bor, C. & Orlando, R. C. Chloride transport in rabbit esophageal epithelial cells. *American Journal of Physiology-Gastrointestinal and Liver Physiology* **282**, G663-G675 (2002).
- 47 Goldstein, J. L. *et al.* Rabbit esophageal cells possess K<sup>+</sup> channels: effect of hyposmotic stress on channel activity. *Gastroenterology* **104**, 417-426 (1993).
- 48 Khalbuss, W., Alkiek, R., Marousis, C. & Orlando, R. Potassium conductance in rabbit esophageal epithelium. *American Journal of Physiology-Gastrointestinal and Liver Physiology* **265**, G28-G34 (1993).
- 49 Cotton, C. U. Basolateral potassium channels and epithelial ion transport. *American Journal of Respiratory Cell and Molecular Biology* **23**, 270-272 (2000).
- 50 Haas, M. & Forbush, B. The na-k-cl cotransporters. *Journal of bioenergetics and biomembranes* **30**, 161-172 (1998).
- 51 Snow, J. C., Goldstein, J. L., Schmidt, L. N., Lisitza, P. & Layden, T. J. Rabbit esophageal cells show regulatory volume decrease: ionic basis and effect of pH. *Gastroenterology* **105**, 102-110 (1993).

- 52 Orlando, G. S., Tobey, N. A., Wang, P., Abdalnour-Nakhoul, S. & Orlando, R. C. Regulatory volume decrease in human esophageal epithelial cells. *American Journal of Physiology-Gastrointestinal and Liver Physiology* **283**, G932-G937 (2002).
- 53 Bonar, P. T. & Casey, J. R. Plasma membrane Cl<sup>-</sup>/HCO<sub>3</sub><sup>-</sup>-exchangers: structure, mechanism and physiology. *Channels* **2**, 337-345 (2008).
- 54 Tobey, N. A. *et al.* Na<sup>+</sup>-dependent and-independent C<sup>-</sup>/HCO<sub>3</sub><sup>-</sup> exchangers in cultured rabbit esophageal epithelial cells. *Gastroenterology* **104**, 185-195 (1993).
- 55 Orlando, R., Powell, D. & Carney, C. N. Pathophysiology of acute acid injury in rabbit esophageal epithelium. *The Journal of clinical investigation* **68**, 286-293 (1981).
- 56 Orlando, R., Bryson, J. C. & Powell, D. Mechanisms of H<sup>+</sup> injury in rabbit esophageal epithelium. *American Journal of Physiology-Gastrointestinal and Liver Physiology* **246**, G718-G724 (1984).
- 57 Awayda, M. S., Bengrine, A., Tobey, N. A., Stockand, J. D. & Orlando, R. C. Nonselective cation transport in native esophageal epithelia. *American Journal of Physiology-Cell Physiology* **287**, C395-C402 (2004).
- 58 Slepko, E. R., Rainey, J. K., Sykes, B. D. & Fliegel, L. Structural and functional analysis of the Na<sup>+</sup>/H<sup>+</sup> exchanger. *Biochemical Journal* **401**, 623-633 (2007).
- 59 Donowitz, M., Tse, C. M. & Fuster, D. SLC9/NHE gene family, a plasma membrane and organellar family of Na<sup>+</sup>/H<sup>+</sup> exchangers. *Molecular aspects of medicine* **34**, 236-251 (2013).
- 60 Orłowski, J. & Grinstein, S. Diversity of the mammalian sodium/proton exchanger SLC9 gene family. *Pflügers Archiv* **447**, 549-565 (2004).
- 61 Stock, C. & Schwab, A. Role of the Na<sup>+</sup>/H<sup>+</sup> exchanger NHE1 in cell migration. *Acta physiologica* **187**, 149-157 (2006).
- 62 Pouyssegur, J., Sardet C, Franchi A, L'Allemain G, Paris S. A specific mutation abolishing Na<sup>+</sup>/H<sup>+</sup> antiport activity in hamster fibroblasts precludes growth at neutral and acidic pH. *Proc Natl Acad Sci USA* **81**, 4833-4837 (1984).
- 63 Shi, Y. *et al.* Stimulation of Na<sup>+</sup>/H<sup>+</sup> exchanger isoform 1 promotes microglial migration. *PLoS One* **8**, e74201 (2013).
- 64 Powell, D., Morris SM, Boyd DD. Water and electrolyte transport by rabbit esophagus. *American Journal of Physiology* **229**, 438-443 (1975).
- 65 Layden, T. J., Agnone, L. M., Schmidt, L. N., Hakim, B. & Goldstein, J. L. Rabbit esophageal cells possess an Na<sup>+</sup>, H<sup>+</sup> antiport. *Gastroenterology* **99**, 909-917 (1990).
- 66 Abdalnour-Nakhoul, S., Bor, S., Imeryuz, N. & Orlando, R. C. Mechanisms of basolateral Na<sup>+</sup> transport in rabbit esophageal epithelial cells. *American Journal of Physiology-Gastrointestinal and Liver Physiology* **276**, G507-G517 (1999).
- 67 Layden, T. J. *et al.* Rabbit esophageal cell cytoplasmic pH regulation: role of Na (+)-H<sup>+</sup> antiport and Na (+)-dependent HCO<sub>3</sub><sup>-</sup>-transport systems. *American Journal of Physiology-Gastrointestinal and Liver Physiology* **263**, G407-G413 (1992).
- 68 Pedersen, S. & Counillon, L. The SLC9A-C mammalian Na<sup>+</sup>/H<sup>+</sup> exchanger family: molecules, mechanisms, and physiology. *Physiological reviews* (2019).
- 69 Nakamura, N., Tanaka, S., Teko, Y., Mitsui, K. & Kanazawa, H. Four Na<sup>+</sup>/H<sup>+</sup> exchanger isoforms are distributed to Golgi and post-Golgi compartments and are

- involved in organelle pH regulation. *Journal of Biological Chemistry* **280**, 1561-1572 (2005).
- 70 Tobey, N. A., Koves, G. & Orlando, R. C. Human esophageal epithelial cells possess an Na<sup>+</sup>/H<sup>+</sup> exchanger for H<sup>+</sup> extrusion. *The American journal of gastroenterology* **93**, 2075-2081 (1998).
  - 71 Shallat, S. *et al.* NHE-1 isoform of the Na<sup>+</sup> H<sup>+</sup> antiport is expressed in the rat and rabbit esophagus. *Gastroenterology* **109**, 1421-1428 (1995).
  - 72 Wakabayashi, S., Fafournoux, P., Sardet, C. & Pouyssegur, J. The Na<sup>+</sup>/H<sup>+</sup> antiporter cytoplasmic domain mediates growth factor signals and controls "H (+)-sensing". *Proceedings of the National Academy of Sciences* **89**, 2424-2428 (1992).
  - 73 Lacroix, J. m., Poet, M., Maehrel, C. & Counillon, L. A mechanism for the activation of the Na/H exchanger NHE-1 by cytoplasmic acidification and mitogens. *EMBO reports* **5**, 91-96 (2004).
  - 74 Aronson, P. S., Nee, J. & Suhm, M. A. Modifier role of internal H<sup>+</sup> in activating the Na<sup>+</sup>-H<sup>+</sup> exchanger in renal microvillus membrane vesicles. *Nature* **299**, 161-163 (1982).
  - 75 Paris, S. & Pouyssegur, J. Growth factors activate the Na<sup>+</sup>/H<sup>+</sup> antiporter in quiescent fibroblasts by increasing its affinity for intracellular H<sup>+</sup>. *Journal of Biological Chemistry* **259**, 10989-10994 (1984).
  - 76 Avkiran, M. & Haworth, R. S. Regulatory effects of G protein-coupled receptors on cardiac sarcolemmal Na<sup>+</sup>/H<sup>+</sup> exchanger activity: signalling and significance. *Cardiovascular research* **57**, 942-952 (2003).
  - 77 Aharonovitz, O. *et al.* Intracellular pH regulation by Na<sup>+</sup>/H<sup>+</sup> exchange requires phosphatidylinositol 4, 5-bisphosphate. *The Journal of cell biology* **150**, 213-224 (2000).
  - 78 Benos, D. J. Amiloride: a molecular probe of sodium transport in tissues and cells. *American Journal of Physiology-Cell Physiology* **242**, C131-C145 (1982).
  - 79 Dai, X.-Q. *et al.* Inhibition of TRPP3 channel by amiloride and analogs. *Molecular pharmacology* **72**, 1576-1585 (2007).
  - 80 Masereel, B., Pochet, L. & Laeckmann, D. An overview of inhibitors of Na<sup>+</sup>/H<sup>+</sup> exchanger. *European journal of medicinal chemistry* **38**, 547-554 (2003).
  - 81 Nikolovska, K., Seidler, U. E. & Stock, C. The Role of Plasma Membrane Sodium/Hydrogen Exchangers in Gastrointestinal Functions: Proliferation and Differentiation, Fluid/Electrolyte Transport and Barrier Integrity. *Frontiers in Physiology*, 896 (2022).
  - 82 Jain, S. & Dhingra, S. Pathology of esophageal cancer and Barrett's esophagus. *Annals of cardiothoracic surgery* **6**, 99 (2017).
  - 83 Spechler, S. J. a. S. R. F. Barrett's Esophagus. *New England Journal of Medicine* **371**, 836-845, doi:10.1056/nejmra1314704 (2014).
  - 84 Lin, B. *et al.* Luminal hydrochloric acid stimulates rapid transepithelial ion fluxes in rodent esophageal stratified squamous epithelium. *Acta physiologica Polonica* **59**, 525 (2008).

- 85 Fujiwara, Y. *et al.* Epidermal growth factor protects human esophageal epithelial cells against acid-induced damage through the activation of Na<sup>+</sup>/H<sup>+</sup> exchangers. *Gastroenterology* **5**, A145 (2001).
- 86 Park, S. Y., Lee, Y. J., Cho, E. J., Shin, C. Y. & Sohn, U. D. Intrinsic resistance triggered under acid loading within normal esophageal epithelial cells: NHE1-and ROS-mediated survival. *Journal of Cellular Physiology* **230**, 1503-1514 (2015).
- 87 Fitzgerald, R., Omary, M. B. & Triadafilopoulos, G. Altered sodium-hydrogen exchange activity is a mechanism for acid-induced hyperproliferation in Barrett's esophagus. *American Journal of Physiology-Gastrointestinal and Liver Physiology* **275**, G47-G55 (1998).
- 88 Goldman, A. *et al.* A novel mechanism of acid and bile acid-induced DNA damage involving Na<sup>+</sup>/H<sup>+</sup> exchanger: implication for Barrett's oesophagus. *Gut* **59**, 1606-1616 (2010).
- 89 Siddique, I. & Khan, I. Regulation of Na/H exchanger-1 in gastroesophageal reflux disease: possible interaction of histamine receptor. *Digestive diseases and sciences* **48**, 1832-1838 (2003).
- 90 Laczkó, D. *et al.* Role of ion transporters in the bile acid-induced esophageal injury. *American Journal of Physiology-Gastrointestinal and Liver Physiology* **311**, G16-G31 (2016).
- 91 Arnal, M. J. D., Arenas, Á. F. & Arbeloa, Á. L. Esophageal cancer: Risk factors, screening and endoscopic treatment in Western and Eastern countries. *World journal of gastroenterology: WJG* **21**, 7933 (2015).
- 92 Zhang, Y. Epidemiology of esophageal cancer. *World journal of gastroenterology: WJG* **19**, 5598 (2013).
- 93 Edgren, G., Adami, H.-O., Weiderpass, E. & Nyrén, O. A global assessment of the oesophageal adenocarcinoma epidemic. *Gut* **62**, 1406-1414 (2013).
- 94 Arnold, M., Soerjomataram, I., Ferlay, J. & Forman, D. Global incidence of oesophageal cancer by histological subtype in 2012. *Gut* **64**, 381-387 (2015).
- 95 Wheeler, J. B. & Reed, C. E. Epidemiology of esophageal cancer. *Surgical Clinics* **92**, 1077-1087 (2012).
- 96 Pedersen, S. F. & Stock, C. Ion Channels and Transporters in Cancer: Pathophysiology, Regulation, and Clinical Potential Ion Channels and Transporters in Cancer. *Cancer research* **73**, 1658-1661 (2013).
- 97 Oosterwijk, E. & Gillies, R. Targeting ion transport in cancer. *Philosophical Transactions of the Royal Society B: Biological Sciences* **369**, 20130107 (2014).
- 98 Djamgoz, M. B., Coombes, R. C. & Schwab, A. Vol. 369 20130092 (The Royal Society, 2014).
- 99 Martial, S. Involvement of ion channels and transporters in carcinoma angiogenesis and metastasis. *American Journal of Physiology-Cell Physiology* **310**, C710-C727 (2016).
- 100 Kunzelmann, K. Ion channels and cancer. *The Journal of membrane biology* **205**, 159-173 (2005).
- 101 Cong, D., Zhu, W., S Kuo, J., Hu, S. & Sun, D. Ion transporters in brain tumors. *Current medicinal chemistry* **22**, 1171-1181 (2015).

- 102 Hu, Y. *et al.* Advances in research on the regulatory mechanism of NHE1 in tumors. *Oncology Letters* **21**, 1-1 (2021).
- 103 Goldman, A. *et al.* The Na<sup>+</sup>/H<sup>+</sup> exchanger controls deoxycholic acid-induced apoptosis by a H<sup>+</sup>-activated, Na<sup>+</sup>-dependent ionic shift in esophageal cells. *PLoS One* **6**, e23835 (2011).
- 104 Guan, B., Hoque, A. & Xu, X. Amiloride and guggulsterone suppression of esophageal cancer cell growth in vitro and in nude mouse xenografts. *Frontiers in biology* **9**, 75-81 (2014).
- 105 Ariyoshi, Y. *et al.* Na<sup>+</sup>/H<sup>+</sup> exchanger 1 has tumor suppressive activity and prognostic value in esophageal squamous cell carcinoma. *Oncotarget* **8**, 2209 (2017).
- 106 Cook, M. B. *et al.* Cigarette smoking and adenocarcinomas of the esophagus and esophagogastric junction: a pooled analysis from the international BEACON consortium. *Journal of the National Cancer Institute* **102**, 1344-1353 (2010).
- 107 Cook, M. B. *et al.* Cigarette smoking increases risk of Barrett's esophagus: an analysis of the Barrett's and Esophageal Adenocarcinoma Consortium. *Gastroenterology* **142**, 744-753 (2012).
- 108 Kuang, J.-j. *et al.* Smoking exposure and survival of patients with esophagus cancer: a systematic review and meta-analysis. *Gastroenterology research and practice* **2016** (2016).
- 109 Wang, Q.-L., Xie, S.-H., Li, W.-T. & Lagergren, J. Smoking cessation and risk of esophageal cancer by histological type: systematic review and meta-analysis. *JNCI: Journal of the National Cancer Institute* **109**, d1115 (2017).
- 110 Coleman, H. G. *et al.* Tobacco smoking increases the risk of high-grade dysplasia and cancer among patients with Barrett's esophagus. *Gastroenterology* **142**, 233-240 (2012).
- 111 Larsson, S. C. & Burgess, S. Appraising the causal role of smoking in multiple diseases: A systematic review and meta-analysis of Mendelian randomization studies. *EBioMedicine* **82**, 104154 (2022).
- 112 Kahrilas, P. J. Cigarette smoking and gastroesophageal reflux disease. *Digestive Diseases* **10**, 61-71 (1992).
- 113 Orlando, R. C., Bryson, J. C. & Powell, D. W. Effect of cigarette smoke on esophageal epithelium of the rabbit. *Gastroenterology* **91**, 1536-1542 (1986).
- 114 Talathi, S. S., Zimmerman, R. & Young, M. Anatomy, abdomen and pelvis, pancreas. (2018).
- 115 Mahadevan, V. Anatomy of the pancreas and spleen. *Surgery (Oxford)* **37**, 297-301 (2019).
- 116 Zhou, Q. & Melton, D. A. Pancreas regeneration. *Nature* **557**, 351-358 (2018).
- 117 Khan, D., Moffet, C. R., Flatt, P. R. & Kelly, C. Role of islet peptides in beta cell regulation and type 2 diabetes therapy. *Peptides* **100**, 212-218 (2018).
- 118 Hegyi, P. & Rakonczay Jr, Z. The role of pancreatic ducts in the pathogenesis of acute pancreatitis. *Pancreatology* **15**, S13-S17 (2015).
- 119 Lee, M. G., Ohana, E., Park, H. W., Yang, D. & Muallem, S. Molecular mechanism of pancreatic and salivary gland fluid and HCO<sub>3</sub><sup>-</sup> secretion. *Physiological reviews* **92**, 39-74 (2012).

- 120 Feng, H.-Y. & Chen, Y.-C. Role of bile acids in carcinogenesis of pancreatic cancer: An old topic with new perspective. *World journal of gastroenterology* **22**, 7463 (2016).
- 121 Winter, J. M., Maitra, A. & Yeo, C. J. Genetics and pathology of pancreatic cancer. *Hpb* **8**, 324-336 (2006).
- 122 Wilentz, R. E. & Hruban, R. H. Pathology of cancer of the pancreas. *Surgical oncology clinics of North America* **7**, 43-65 (1998).
- 123 Esposito, I., Konukiewitz, B., Schlitter, A. M. & Klöppel, G. Pathology of pancreatic ductal adenocarcinoma: facts, challenges and future developments. *World journal of gastroenterology: WJG* **20**, 13833 (2014).
- 124 Wood, L. D., Canto, M. I., Jaffee, E. M. & Simeone, D. M. Pancreatic cancer: pathogenesis, screening, diagnosis, and treatment. *Gastroenterology* **163**, 386-402. e381 (2022).
- 125 Di Ciaula, A. *et al.* Bile acids and cancer: direct and environmental-dependent effects. *Annals of hepatology* **16**, S87-S105 (2017).
- 126 Parks, D. J. *et al.* Bile acids: natural ligands for an orphan nuclear receptor. *Science* **284**, 1365-1368 (1999).
- 127 Hu, H. *et al.* Correlated high expression of FXR and Sp1 in cancer cells confers a poor prognosis for pancreatic cancer: a study based on TCGA and tissue microarray. *Oncotarget* **8**, 33265 (2017).
- 128 Joshi, S. *et al.* Bile acids-mediated overexpression of MUC4 via FAK-dependent c-Jun activation in pancreatic cancer. *Molecular oncology* **10**, 1063-1077 (2016).
- 129 Kalabis, J. *et al.* Isolation and characterization of mouse and human esophageal epithelial cells in 3D organotypic culture. *Nature protocols* **7**, 235-246 (2012).
- 130 Fujiwara, Y. *et al.* Functional oesophageal epithelial defense against acid. *Inflammopharmacology* **13**, 1-13 (2005).
- 131 Burke, Z. D. & Tosh, D. Barrett's metaplasia as a paradigm for understanding the development of cancer. *Current opinion in genetics & development* **22**, 494-499 (2012).
- 132 Wang, D. H. *et al.* Aberrant epithelial–mesenchymal Hedgehog signaling characterizes Barrett's metaplasia. *Gastroenterology* **138**, 1810-1822. e1812 (2010).
- 133 Pallagi, P. *et al.* Trypsin reduces pancreatic ductal bicarbonate secretion by inhibiting CFTR Cl<sup>−</sup> channels and luminal anion exchangers. *Gastroenterology* **141**, 2228-2239. e2226 (2011).
- 134 Venglovecz, V. *et al.* Pathophysiological relevance of apical large-conductance Ca<sup>2+</sup>-activated potassium channels in pancreatic duct epithelial cells. *Gut* **60**, 361-369 (2011).
- 135 Long, J. D. & Orlando, R. C. Esophageal submucosal glands: structure and function. *The American journal of gastroenterology* **94**, 2818-2824 (1999).
- 136 Korsós, M. M. *et al.* Mouse organoid culture is a suitable model to study esophageal ion transport mechanisms. *American Journal of Physiology-Cell Physiology* **321**, C798-C811 (2021).
- 137 Tucker, O. N., Dannenberg, A. J., Yang, E. K. & Fahey III, T. J. Bile acids induce cyclooxygenase-2 expression in human pancreatic cancer cell lines. *Carcinogenesis* **25**, 419-423 (2004).



- 138 Rees, D. O. *et al.* Comparison of the composition of bile acids in bile of patients with adenocarcinoma of the pancreas and benign disease. *The Journal of steroid biochemistry and molecular biology* **174**, 290-295 (2017).

## **9. Annex**

# **I.**



Article

# Inhibition of NHE-1 Increases Smoke-Induced Proliferative Activity of Barrett's Esophageal Cell Line

Eszter Becskeházi <sup>1</sup>, Marietta Margaréta Korsós <sup>1</sup> , Eleonóra Gál <sup>1</sup>, László Tiszlavicz <sup>2</sup>, Zsófia Hoyk <sup>3</sup>,  
Mária A. Deli <sup>3</sup> , Zoltán Márton Köhler <sup>4</sup> , Anikó Keller-Pintér <sup>4</sup> , Attila Horváth <sup>5</sup> , Kata Csekő <sup>6,7</sup>,  
Zsuzsanna Helyes <sup>6,7</sup>, Péter Hegyi <sup>8,9,10</sup> and Viktória Venglovecz <sup>1,\*</sup>

- <sup>1</sup> Department of Pharmacology and Pharmacotherapy, University of Szeged, H-6721 Szeged, Hungary; eszter.becskehazi@gmail.com (E.B.); margaretakorsos@gmail.com (M.M.K.); galeleonora@gmail.com (E.G.)  
<sup>2</sup> Department of Pathology, University of Szeged, H-6725 Szeged, Hungary; tiszlavicz.laszlo@med.u-szeged.hu  
<sup>3</sup> Biological Research Centre, Institute of Biophysics, H-6726 Szeged, Hungary; hoyk.zsofia@brc.hu (Z.H.); deli.maria@brc.hu (M.A.D.)  
<sup>4</sup> Department of Biochemistry, University of Szeged, H-6720 Szeged, Hungary; kohler.zoltan.marton@gmail.com (Z.M.K.); keller.aniko@med.u-szeged.hu (A.K.-P.)  
<sup>5</sup> Department of Pharmacognosy, University of Szeged, H-6720 Szeged, Hungary; horvath.attila@pharmacognosy.hu  
<sup>6</sup> Department of Pharmacology and Pharmacotherapy, Medical School & Szentágotthai Research Centre, University of Pécs, H-7624 Pécs, Hungary; csekoe.kata@gmail.com (K.C.); zsuzsanna.helyes@aok.pte.hu (Z.H.)  
<sup>7</sup> PharmInVivo Ltd., H-7629 Pécs, Hungary  
<sup>8</sup> First Department of Medicine, University of Szeged, H-6720 Szeged, Hungary; hegyi.peter@pte.hu  
<sup>9</sup> Medical School & Szentágotthai Research Centre, Institute for Translational Medicine, University of Pécs, H-7624 Pécs, Hungary  
<sup>10</sup> Division of Gastroenterology, First Department of Medicine, Medical School, University of Pécs, H-7624 Pécs, Hungary  
\* Correspondence: venglovecz.viktoria@med.u-szeged.hu; Tel.: +36-62-545-677



**Citation:** Becskeházi, E.; Korsós, M.M.; Gál, E.; Tiszlavicz, L.; Hoyk, Z.; Deli, M.A.; Köhler, Z.M.; Keller-Pintér, A.; Horváth, A.; Csekő, K.; et al. Inhibition of NHE-1 Increases Smoke-Induced Proliferative Activity of Barrett's Esophageal Cell Line. *Int. J. Mol. Sci.* **2021**, *22*, 10581. <https://doi.org/10.3390/ijms221910581>

Academic Editor: Robert Y. Tsai

Received: 31 August 2021

Accepted: 27 September 2021

Published: 30 September 2021

**Publisher's Note:** MDPI stays neutral with regard to jurisdictional claims in published maps and institutional affiliations.



**Copyright:** © 2021 by the authors. Licensee MDPI, Basel, Switzerland. This article is an open access article distributed under the terms and conditions of the Creative Commons Attribution (CC BY) license (<https://creativecommons.org/licenses/by/4.0/>).

**Abstract:** Several clinical studies indicate that smoking predisposes its consumers to esophageal inflammatory and malignant diseases, but the cellular mechanism is not clear. Ion transporters protect esophageal epithelial cells by maintaining intracellular pH at normal levels. In this study, we hypothesized that smoking affects the function of ion transporters, thus playing a role in the development of smoking-induced esophageal diseases. Esophageal cell lines were treated with cigarettes smoke extract (CSE), and the viability and proliferation of the cells, as well as the activity, mRNA and protein expression of the Na<sup>+</sup>/H<sup>+</sup> exchanger-1 (NHE-1), were studied. NHE-1 expression was also investigated in human samples. For chronic treatment, guinea pigs were exposed to tobacco smoke, and NHE-1 activity was measured. Silencing of NHE-1 was performed by using specific siRNA. CSE treatment increased the activity and protein expression of NHE-1 in the metaplastic cells and decreased the rate of proliferation in a NHE-1-dependent manner. In contrast, CSE increased the proliferation of dysplastic cells independently of NHE-1. In the normal cells, the expression and activity of NHE-1 decreased due to in vitro and in vivo smoke exposure. Smoking enhances the function of NHE-1 in Barrett's esophagus, and this is presumably a compensatory mechanism against this toxic agent.

**Keywords:** esophagus; ion transport; smoking; NHE-1; Barrett's esophagus

## 1. Introduction

Cigarette smoking is responsible for the development of many diseases, especially different types of cancers. Since smoking primarily affects the lungs, the effects of smoking have been most intensively studied on this organ. However, other organs may also be affected, such as the esophagus, which is directly exposed to cigarette smoke. For this reason, a number of clinical studies have been conducted to examine the connection between

smoking and esophageal diseases. These studies have shown that smoking strongly correlates with the development of esophageal adenocarcinoma (EAC) and Barrett's esophagus (BE) and also increases the risk of progression from BE to EAC [1–5]. In contrast, only a few data are available regarding the cellular mechanism of smoking-induced lesions. In an older study, Orlando et al. showed that the esophageal potential difference is reduced by cigarette smoke extract (CSE), in which inhibition of  $\text{Na}^+$  transport plays an important role [6]. This study suggests that smoking alters the ion transport processes in esophageal epithelial cells (EECs); however, it is not known whether this takes part in the development of BE or EAC.

Ion transport processes through the esophageal mucosa play an important protective role, as they greatly contribute to the maintenance of normal intracellular pH ( $\text{pH}_i$ ). Several ion transporters have been identified on EECs in recent years, and their role has been characterized both under physiological and pathophysiological conditions [7,8]. Our workgroup showed that acid and/or bile acids alters the activity and expression of ion transporters, which may be important in the development and progression of esophageal diseases [8]. Among the acid–base transporters, the  $\text{Na}^+/\text{H}^+$  exchanger (NHE) is one of the most important transmembrane protein that mediates the exchange of  $\text{Na}^+$  and  $\text{H}^+$ . In addition to playing an important role in the alkalization of the  $\text{pH}_i$ , it also regulates cell volume, proliferation, migration, and invasion [9–11]. Several members of the NHE family are known, of which NHE-1 is the most common, ubiquitously expressed isoform. The presence of NHE-1 has been shown in the esophagus of several species, such as rat and rabbit, where it is essentially involved in the regulation of  $\text{pH}_i$  [12]. In contrast, the expression of this isoform in the normal human esophagus is controversial, and its importance is more highlighted under pathological conditions [8,13–17]. Increased NHE-1 expression has been shown in BE, which probably plays a protective role against the acid- or bile-induced injury by enhancing the cellular resistance of the cells [8,15,18]. The role of NHE-1 in EAC is controversial. Some studies suggest that NHE-1 enhances the growth of esophageal cancer cells, while other studies have shown that NHE-1 expression is associated with longer postoperative survival [13,16].

There is no information on how smoking affects NHE-1 activity or expression in the esophagus. Since  $\text{Na}^+$  transport is inhibited by smoking [6], it is conceivable that NHE-1 plays a role in the pathogenesis of cigarette-smoke-induced esophageal diseases. Therefore, the objective of the present study was to investigate the effect of tobacco smoke on normal, metaplastic and dysplastic cells and to investigate the role of NHE-1 in it.

## 2. Results

### 2.1. Effect of CSE on Esophageal Epithelial Cell Proliferation

To examine the effect of CSE on cell proliferation, first we determined the concentrations of CSE at which the cells retained their viability. CSE concentrations were chosen based on the literature data [19,20]. Cytotoxicity studies showed that both CP-A and CP-D cells mostly tolerated CSE at 1 and 10  $\mu\text{g}/\text{mL}$  concentrations, at each incubation time (6, 24 and 72 h). In contrast, 100  $\mu\text{g}/\text{mL}$  CSE induced a high degree of cell death, especially during longer incubation (Figure 1a). Therefore, in the proliferation assays, the effect of 1 and 10  $\mu\text{g}/\text{mL}$  CSE was examined for 6, 24 and 72 h (Figure 1b). In the metaplastic, CP-A cells, CSE treatment dose-dependently reduced cell proliferation in the 24 and 72 h treatment groups. In contrast, in the dysplastic, CP-D cells 72 h CSE treatment significantly increased the proliferation.

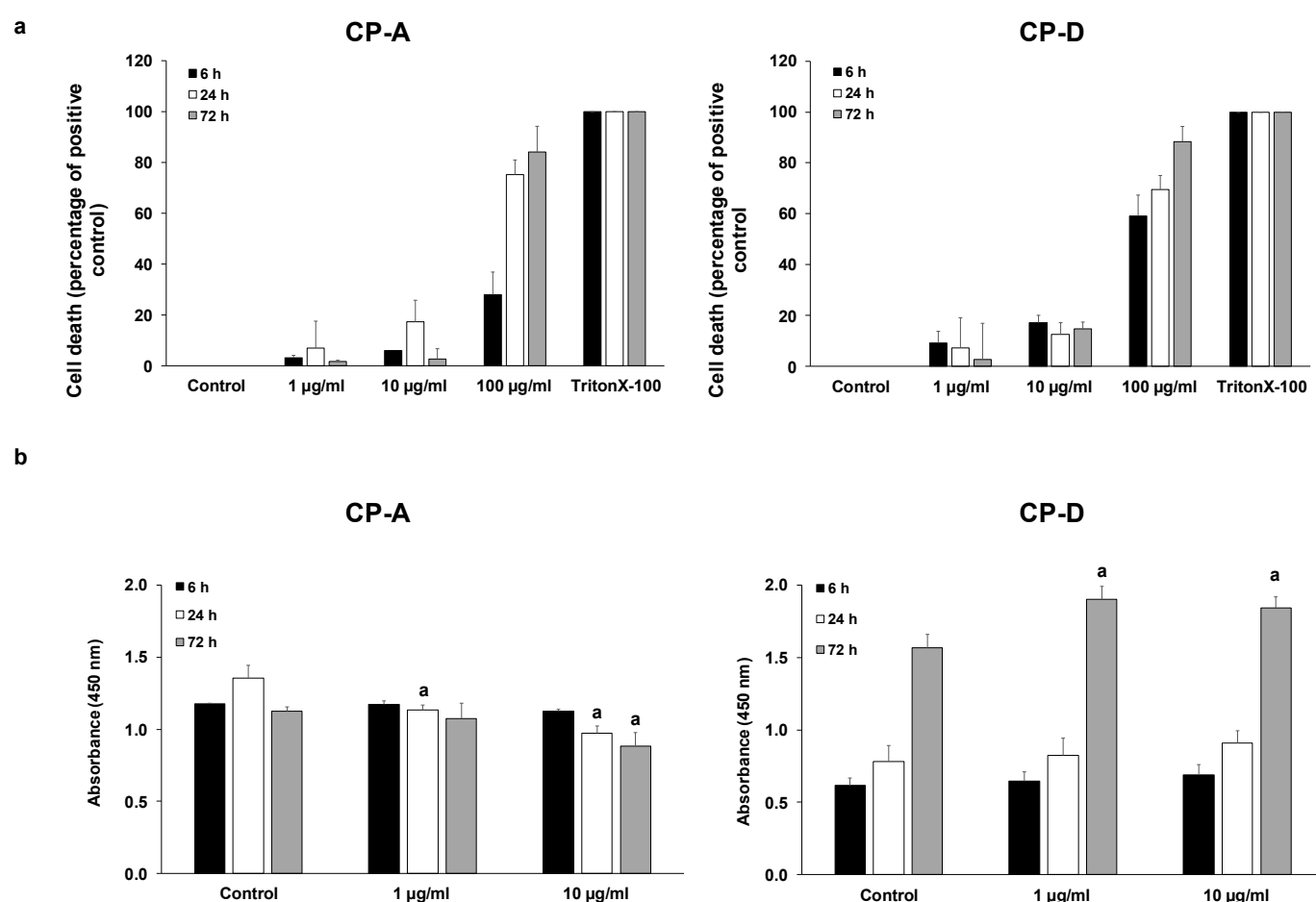


**Figure 1.** Effects of cigarette smoke extract (CSE) treatment on cell viability and proliferation. Metaplastic (CP-A) and dysplastic (CP-D) esophageal cell lines were exposed to different concentrations of CSE for 6, 24 and 72 h and the effects on cellular viability (a) and proliferation (b) were studied, using LDH and CCK8 assays, respectively. In the case of viability assay, 0.1% Triton X-100 was used as a positive control. Data represent mean  $\pm$  SEM of three independent experiments;  $a = p \leq 0.05$  vs. control.

## 2.2. Activity and Expression of NHE-1 in the Metaplastic and Dysplastic Cells

Next, we examined the rate of NHE activity in the CP-A and CP-D cell lines, using the  $\text{NH}_4\text{Cl}$  pre-pulse technique (Figure 2a,b). As shown in Figure 2a, in the absence of  $\text{HCO}_3^-$  the initial rate of regeneration from acidosis reflects the activity of NHE. Currently, nine NHE isoforms are known, and among them the presence of NHE-1 and NHE-2 was confirmed in the esophageal mucosa [8,12,21]. Our previous studies showed that NHE-1 displays greater activity and is better expressed than NHE-2 both in the metaplastic and dysplastic cells [8], indicating that NHE-1 is primarily responsible for the regeneration from acidosis. As shown in Figure 2a,b, regeneration from acidosis was higher in CP-A (BF:  $5.47 \pm 0.52$ ) than in CP-D cells (BF:  $3.36 \pm 0.24$ ), indicating that CP-A cells have higher NHE-1 activity. We have also compared the mRNA and protein expressions of NHE-1 between the metaplastic and dysplastic cells at different time points (6, 24 and 72 h). In addition, mRNA expression of NHE-1 (*SLC9A1*) was investigated by RT-PCR 24 h after plating the cells. As an internal gene, human beta actin (*ACTB*) was used. RT-PCR analysis revealed that there was no significant difference in NHE-1 expression among CP-A and CP-D cells, and no difference was observed between the different incubation times (Figure 2c). Similar to RT-PCR, the Western blot analysis showed no difference in the protein expression of NHE-1 between the CP-A and CP-D cells (Figure 2d).

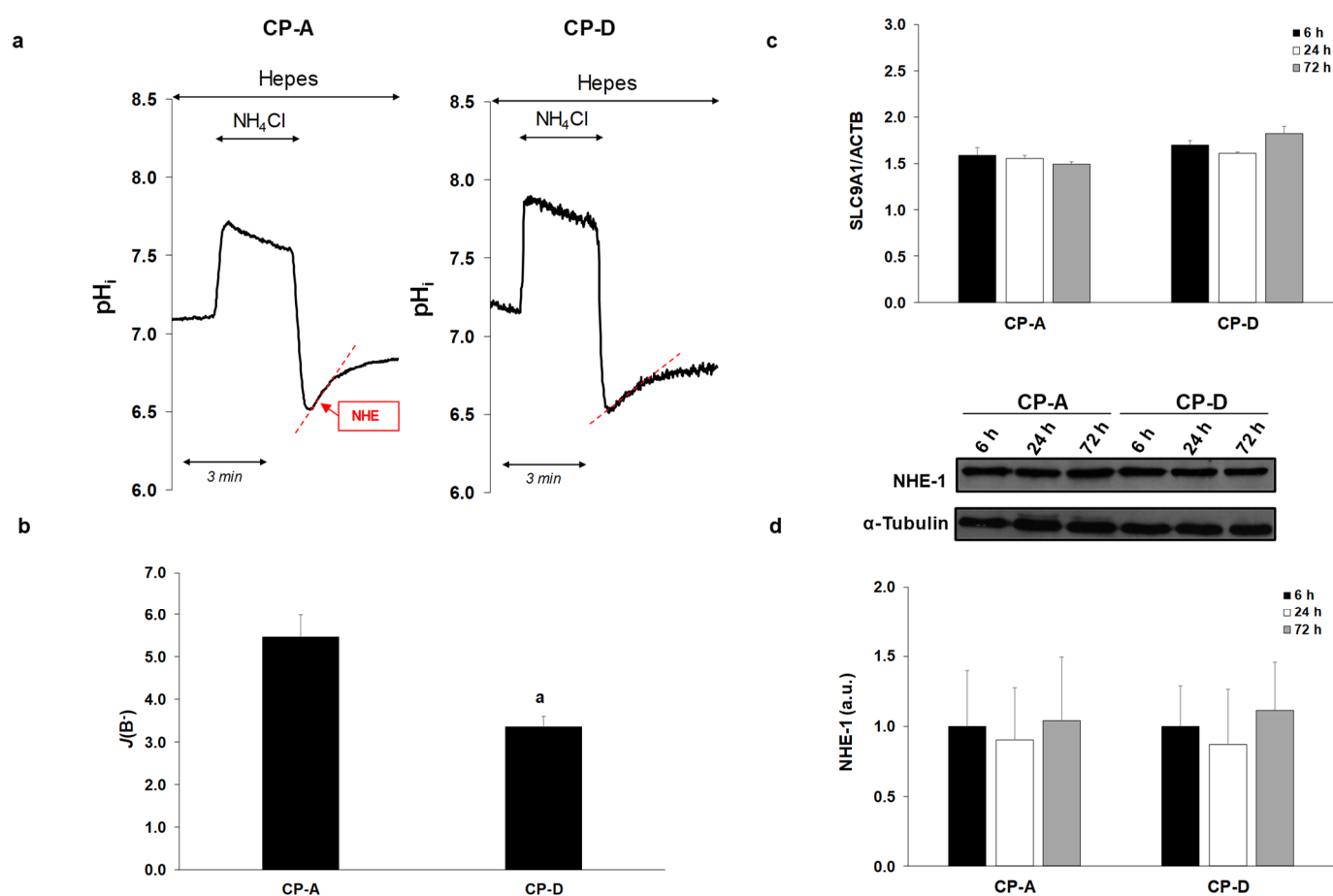


**Figure 2.** Activity, mRNA and protein expression of Na<sup>+</sup>/H<sup>+</sup> exchanger-1 (NHE-1) in esophageal cell lines. (a) Representative intracellular pH (pH<sub>i</sub>) curves present the recovery from acidosis in CP-A and CP-D cells. (b) Summary data of the calculated activity of NHE-1 in the different cell lines. The rate of pH recovery ( $J(B^-)$ ) was calculated from the  $\Delta pH_i / \Delta t$  obtained via linear regression analysis of the pH<sub>i</sub> measurement performed over the first 60 s of recovery from the lowest pH<sub>i</sub> level (initial pH<sub>i</sub>). The buffering capacity at the initial pH<sub>i</sub> was used to calculate  $J(B^-)$ . Data are presented as the mean  $\pm$  SEM. a:  $p \leq 0.05$  vs. CP-A;  $n = 5\text{--}11$  exp./26–91 region of interests (ROIs). (c) mRNA and (d) protein expression of NHE-1 in the CP-A and CP-D cells.  $\alpha$ -Tubulin was used as a protein-loading control. Data represent mean  $\pm$  SEM of three independent experiments.

### 2.3. Effect of CSE on The Activity and Expression of NHE-1

In order to investigate the effect of CSE on the activity of NHE-1, the previously mentioned NH<sub>4</sub>Cl pre-pulse technique was used. Since CSE alone can affect the fluorescence signals, cells were pretreated with 1, 10 or 100  $\mu\text{g/mL}$  CSE for 1 h, and then NHE activity was measured (Figure 3a,b). Control cells were incubated in HEPES solution without CSE. In the case of CP-A cells, pretreatment with 1  $\mu\text{g/mL}$  CSE decreased NHE activity from  $5.47 \pm 0.52$  to  $3.08 \pm 0.55$ . In contrast, at higher concentrations (10 and 100  $\mu\text{g/mL}$ , respectively) the activity of the exchanger increased ( $8.18 \pm 1.3$  at 10  $\mu\text{g/mL}$  CSE and  $12.28 \pm 0.73$  at 100  $\mu\text{g/mL}$  CSE). In CP-D cells, CSE strongly reduced NHE-1 activity at all three concentrations (from  $3.36 \pm 0.24$  to  $1.25 \pm 0.26$  at 1  $\mu\text{g/mL}$  CSE,  $1.62 \pm 0.23$  at 10  $\mu\text{g/mL}$  CSE and  $1.46 \pm 0.29$  at 100  $\mu\text{g/mL}$  CSE, respectively).

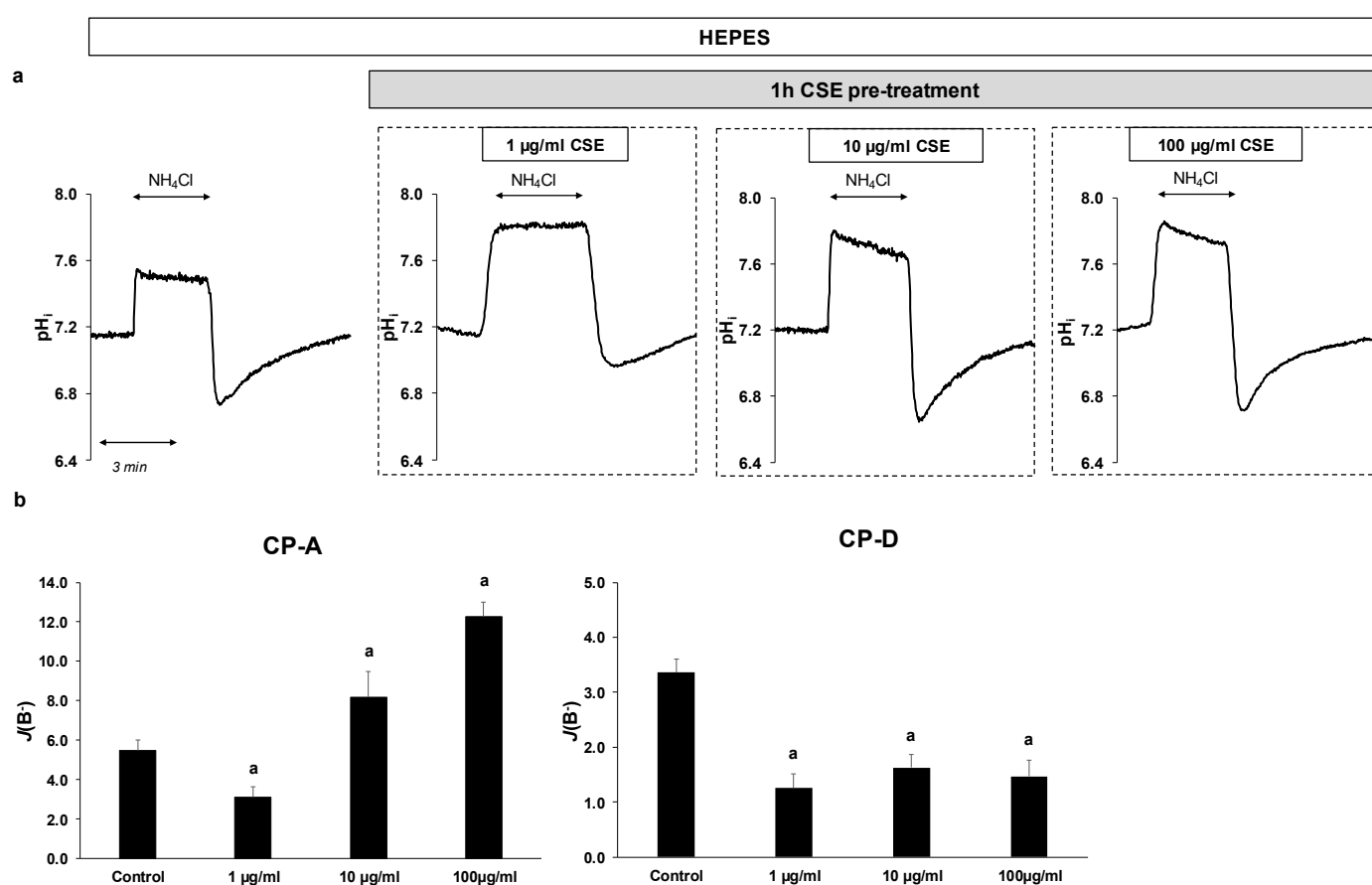


**Figure 3.** Effects of cigarette smoke extract (CSE) treatment on the activity of Na<sup>+</sup>/H<sup>+</sup> exchanger-1 (NHE-1) in esophageal cell lines. Metaplastic (CP-A) and dysplastic (CP-D) esophageal cell lines were pretreated with different concentrations of CSE (1, 10 and 100 µg/mL) for 1 h, and the activity of NHE-1 was measured. (a) Representative intracellular pH (p<sub>Hi</sub>) curves present the recovery from acidosis in CP-A cells. (b) Summary data of the calculated activity of NHE-1 in the different cell lines. The rate of pH recovery (J(B<sup>-</sup>)) was calculated as described in Figure 2b. Data are presented as the mean ± SEM; a  $p \leq 0.05$  vs. control;  $n = 12$ –14 exp./66–68 ROIs.

The CSE treatment did not cause significant differences in mRNA expression of NHE-1 in any of the cell lines (Figure 4a). In contrast, the protein expression was increased in the CP-A cells upon CSE treatment, almost in all treated groups (Figure 4b). In the CP-D cells, CSE treatment caused a robust increase at 1 µg/mL concentration in the 6 h treatment group, while no significant change was detected in the other groups.

#### 2.4. Smoking Decreases NHE-1 Activity on Normal Esophageal Epithelial Cells

In order to investigate how CSE affects NHE activity under physiological conditions, we studied the effect of CSE on normal EECs isolated from guinea pigs. The same concentrations were used as for the cell lines, and the cells were pretreated with CSE in the same manner. As shown in Figure 5a,b, NHE activity was significantly reduced by CSE treatment (from  $12.19 \pm 0.46$  to  $4.64 \pm 0.94$  at 1 µg/mL CSE, to  $3.96 \pm 0.43$  at 10 µg/mL CSE and to  $4.49 \pm 0.4$  at 100 µg/mL CSE, respectively). In order to investigate the chronic effects of smoking, guinea pigs were exposed to cigarette smoke for one, two and four months, respectively, and then NHE activity was examined (Figure 5c). Guinea pigs of the same age were used as controls. Similar to acute CSE treatment, chronic treatment decreased NHE activity from  $15.81 \pm 0.91$  to  $7.98 \pm 0.52$  in the 1-month group, from  $9.92 \pm 0.78$  to  $7.9 \pm 0.33$  in the 2-month group and from  $10.86 \pm 0.54$  to  $5.46 \pm 0.19$  in the 4-month group (Figure 5d). These data indicate that smoking decreases the activity of NHE-1 in the normal esophageal mucosa.

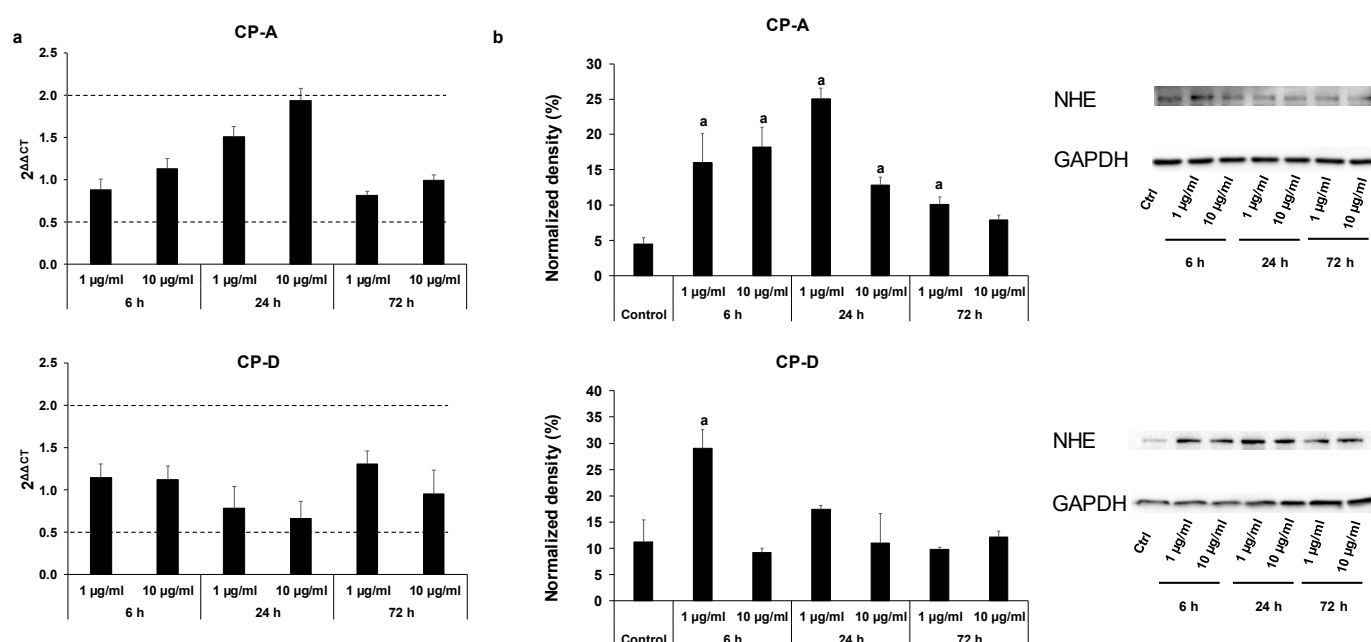


**Figure 4.** Effects of cigarette smoke extract (CSE) treatment on the mRNA and protein expression of Na<sup>+</sup>/H<sup>+</sup> exchanger-1 (NHE-1) in esophageal cell lines. Metaplastic (CP-A) and dysplastic (CP-D) esophageal cell lines were treated with different concentrations of CSE (1 and 10 μg/mL) for 6, 24 and 72 h, and the relative gene (a) and protein (b) expressions of NHE-1 were investigated by real-time PCR and Western blot, respectively. GAPDH was used as a protein-loading control. Data represent mean ± SEM of three independent experiments; a =  $p \leq 0.05$  vs. control.

### 2.5. Effect of Smoking on NHE-1 Protein Expression in Human Esophageal Samples

Protein expression of NHE-1 was investigated in normal squamous epithelium and in BE samples obtained from patients with smoking and non-smoking history (Figure 6a,b). Patients who had never smoked or not smoked for more than a year were classified as non-smokers, while patients who had been smokers for at least 20 years were classified as smokers. Only patients with known smoking status were included in the analysis. As controls, normal esophageal biopsy samples and the intact tumor-free margin of surgically resected esophageal cancer were used. Weak NHE-1 expression was detected in the normal esophageal epithelium, and it was further reduced by smoking. In BE, strong NHE-1 expression was observed, mainly at the basolateral membrane of the columnar cells. In smokers, NHE-1 expression increased, and staining was detected not only in the plasma membrane but in the cytoplasm as well. Interestingly, strong NHE-1 staining was also observed in the glands. There was no significant difference between the intestinal and non-intestinal metaplasia, neither in the smoker nor in the non-smoker group.

### 2.6. Role of NHE-1 in The CSE-Induced Proliferation

In order to investigate whether the altered expression or activity of NHE-1 has any role in the effect of CSE on proliferation, we silenced the *SLC9A1* gene, using specific siRNA (Figure 7a–d). The efficiency of silencing was investigated at both mRNA and protein levels (Figure 7a,b). In CP-A cells, NHE-1 knockdown reduced the rate of proliferation at each incubation time, suggesting that NHE-1 is essential for the normal function of the cells (Figure 7c). In the CP-D cells, the lack of NHE-1 protein initially increased the rate of proliferation, whereas no significant difference was observed with additional incubation times (Figure 7c). In the absence of NHE-1, CSE treatment increased the rate of proliferation in the CP-A cells in almost all treated groups. For CP-D cells, proliferation increased alone in the 72h treatment group (Figure 7d).



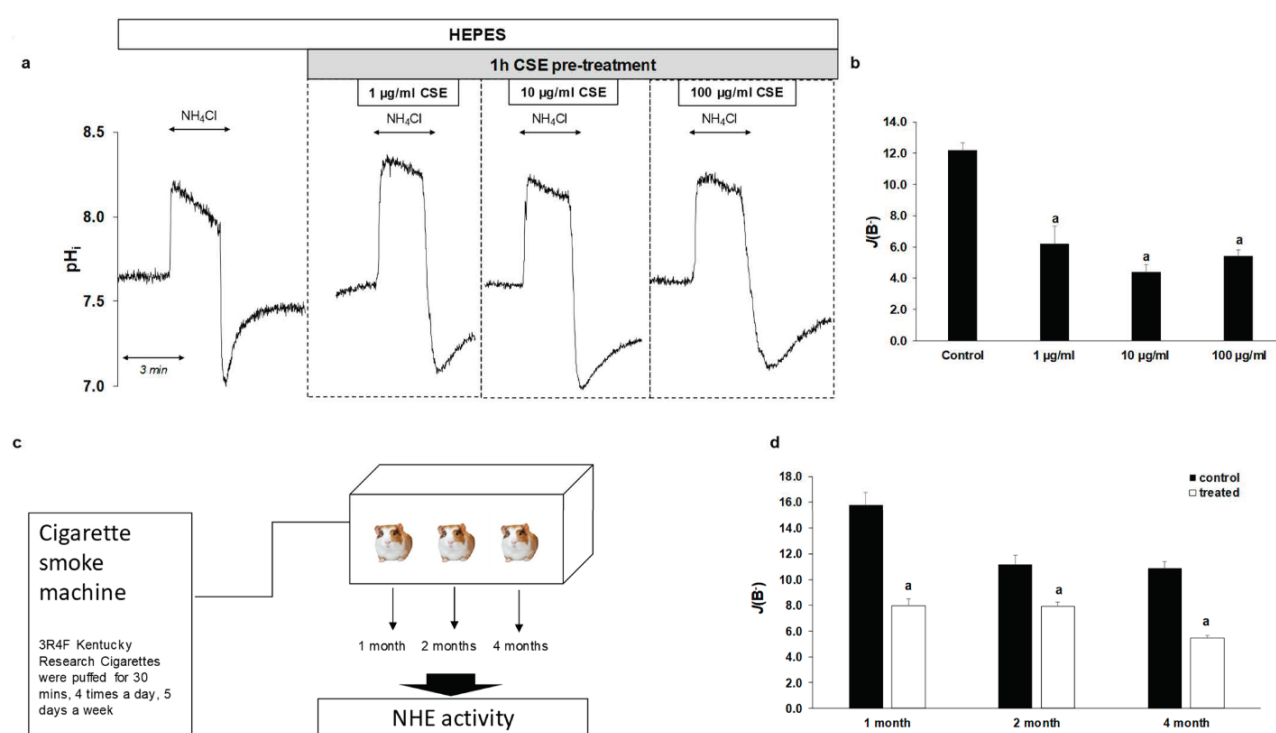


**Figure 5.** Effects of cigarette smoke extract (CSE) treatment and smoking on the activity of  $Na^+/H^+$  exchanger-1 (NHE-1) in guinea pig esophageal epithelial cells (EECs). (a) Normal guinea pig EECs were pretreated with different concentrations of CSE (1, 10 and 100  $\mu g/ml$ ) for 1 h and the activity of NHE-1 was measured. Representative intracellular pH ( $pH_i$ ) curves show the recovery from acidosis. (b) Summary data of the calculated activity of NHE-1 in guinea pig EECs. The rate of pH recovery ( $J(B^-)$ ) was calculated as described in Figure 2b. Data are presented as the mean  $\pm$  SEM; a:  $p \leq 0.05$  vs. control;  $n = 13$ –18 exp./86–99 ROIs. (c) Chronic effect of cigarette smoking was investigated, using smoking chamber. Guinea pigs were exposed to whole body cigarette smoke 4 times a day, 5 days a week, 30 min each time, using a TE2 closed-chamber manual smoking system. After 1, 2, or 4 months of smoking, the animals were sacrificed and NHE-1 activity was measured. (d) Summary data of the calculated activity of NHE-1 in guinea pig EECs. The rate of pH recovery ( $J(B^-)$ ) was calculated as described in Figure 2b. Data are presented as the mean  $\pm$  SEM; a:  $p \leq 0.05$  vs. control;  $n = 8$ –16 exp./81–210 ROIs.

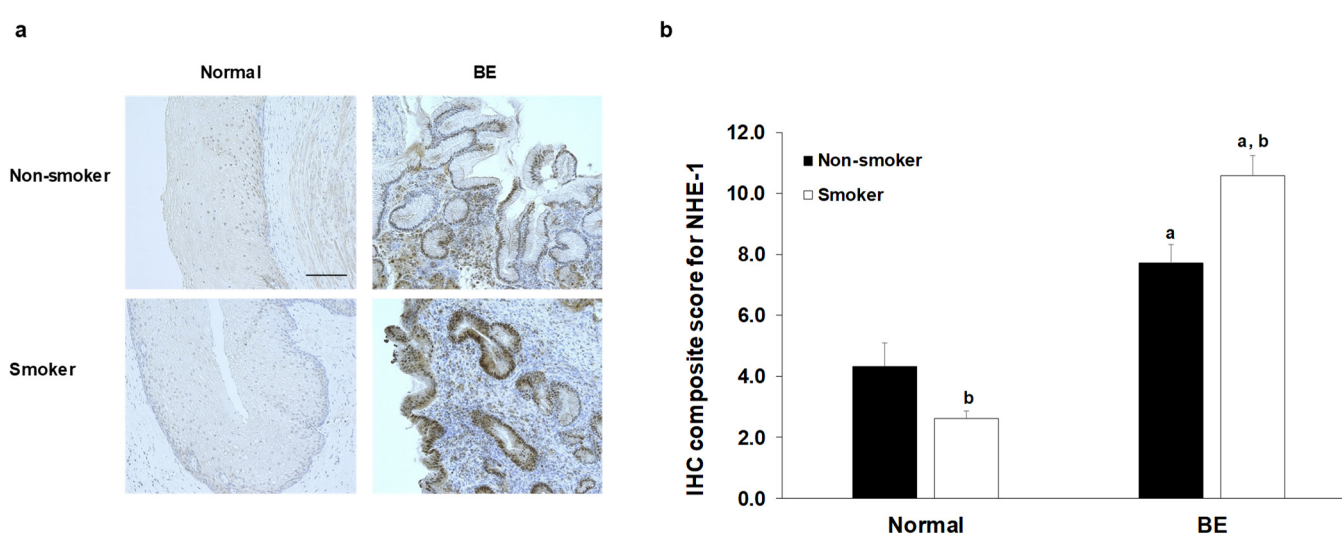


**Figure 6.** Expression of  $Na^+/H^+$  exchanger-1 (NHE-1) in human esophageal samples. (a) Representative immunohistochemical stainings show the presence of NHE-1 in human esophageal samples. Scale bar represents 100  $\mu m$ . (b) Quantification of DAB intensities were calculated, using a semi-quantitative scoring system. Data represent mean  $\pm$  SEM of 23–25 specimens/3–6 patients each group; a:  $p \leq 0.05$  vs. normal; b:  $p \leq 0.05$  vs. non-smoker. BE: Barrett's esophagus.

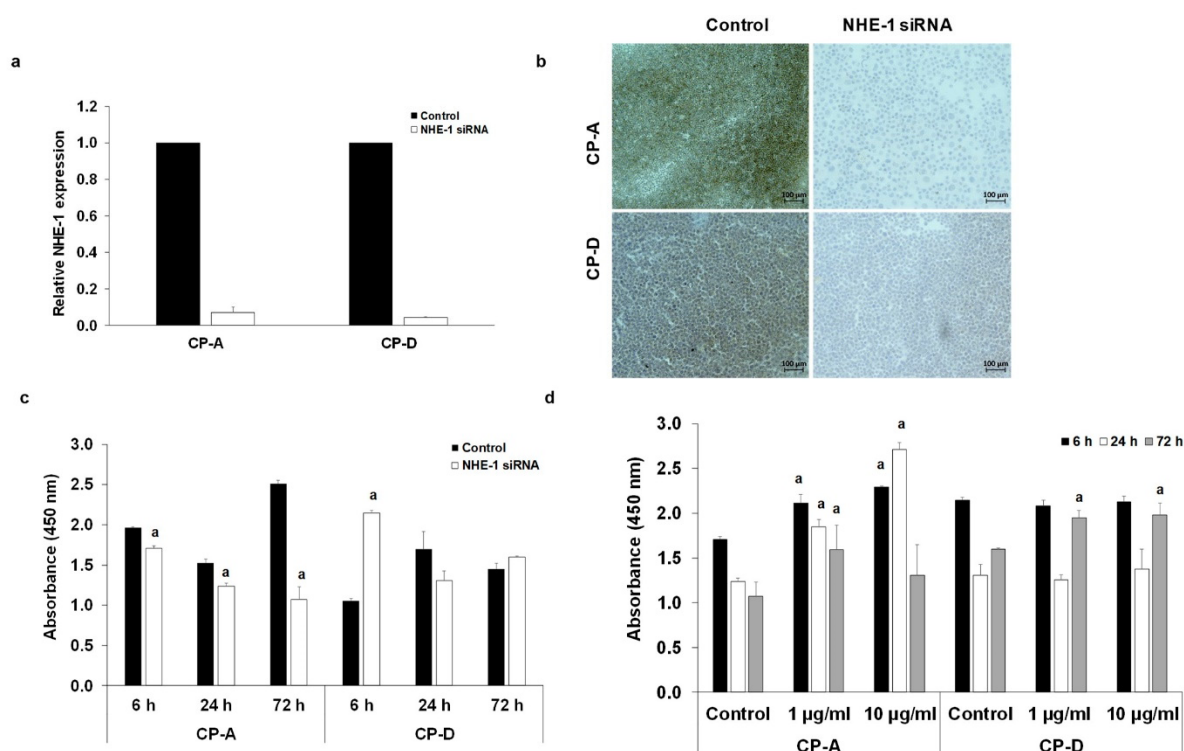


**Figure 7.** Knockdown of  $\text{Na}^+/\text{H}^+$  exchanger-1 (NHE-1) in human esophageal cell lines. The expression levels of NHE-1 were investigated by RT-PCR (a) and immunohistochemistry (b) in control cells and in cells treated with specific siRNA for *SLC9A1*. The rate of proliferation was determined in the non-treated (c) and cigarette smoke extract-treated (d) CP-A and CP-D cells. Data represent mean  $\pm$  SEM of three independent experiments;  $a = p \leq 0.05$  vs. control.

### 3. Discussion

Recent studies have described that altered expression or activity of ion transporters play an important role in the development or progression of different types of cancer [22–26]. For this reason, many ion transporters emerged as potential targets for cancer therapy [27,28]. Our study demonstrates, for the first time, that smoking affects cell proliferation in BE in which the ubiquitously expressed transmembrane transporter, NHE-1, plays a central role. In the presence of NHE-1, CSE decreased the proliferation of metaplastic cells, whereas, in the absence of the exchanger, cell proliferation increased due to the CSE treatment. This result may be significant from the point of view that NHE-1 plays a protective role in BE, and decreased NHE-1 expression may contribute to the neoplastic progression of BE in smoking patients.

An interesting observation of our study is that CSE treatment slightly reduced the proliferation of metaplastic cells, while it increased the proliferation of dysplastic cells. The decreased proliferation in the metaplastic cells is presumably due to the decreased cell viability at higher concentrations of CSE. In contrast, dysplastic cells were much more resistant to CSE, and despite the low degree of cell death, cell proliferation increased with treatment. In order to study the underlying mechanisms, we investigated the effect of smoking on ion transport processes. Esophageal ion transporters play an important protective role in EECs by preventing acidic or basic shift in  $\text{pH}_i$ . Therefore, disruption of pH regulatory processes leads to an upset of extra- and intracellular pH, which can result in changes in cellular function and also causes genetic instability. It is well-known that the pH of tumor is dysregulated and typically an acidic microenvironment develops within the tumor that promotes cell division and migration [29–32]. Among the ion transporters NHE-1 is an ubiquitously expressed plasma membrane protein that plays an essential role in maintaining physiological  $\text{pH}_i$ . Inadequate function of this transporter has been described in several cancer types, including esophageal cancer [13,16,33–37]; therefore,

NHE-1 emerged as a potential target in anti-cancer therapy [37,38]. We showed that, in the case of acute CSE exposure, higher concentrations of CSE increased NHE-1 activity in the metaplastic cells; this is presumably a defense mechanism by which the cells try to maintain the normal pH homeostasis. In contrast, decreased activity of NHE-1 in CP-D cells indicates damaged compensatory pH regulatory mechanisms. We have previously shown that bile, which is an important etiological factor in the development of GERD and BE, had the opposite effect that is decreased the activity of NHE-1 in the metaplastic cells and increased it in the dysplastic cells [8]. In order to get a more complete picture of the effect of CSE, we treated the cells with CSE for 6, 24 and 72 h and the mRNA, and the protein expressions of NHE-1 were investigated. In CP-A cells, CSE treatment induced an increase in mRNA expression, but this did not reach a significant level. However, a clear elevation was found at the protein level that is thought to be associated with the increased NHE-1 activity by CSE. Examination of human esophageal samples also showed that smoking increases NHE-1 expression in both intestinal and non-intestinal metaplasia, consistent with the results obtained on the CP-A cells. In the case of CP-D cells, no significant change in either mRNA or protein expressions was observed after long-term or higher-dose CSE administration, indicating that only the activity of the protein changes due to the CSE treatment. In order to investigate how smoking affects NHE activity under normal conditions, we examined the effect of acute and chronic tobacco exposure on guinea pig EECs. We chose guinea pigs because we have previously shown that ion-transport processes in the secretory gland of the guinea pig is similar to humans; in addition, more cells can be obtained from the esophagus of guinea pig than from the esophagus of mice or rat [39]. The duration of chronic *in vivo* smoking was determined based on the literature data [40–42]. Our results showed that both acute and chronic tobacco smoke exposures significantly reduce NHE-1 function. In the case of acute CSE exposure no dose-dependent effect was observed. This can be explained by the fact, that the composition of each CSE preparation may slightly differ from each other as it contains thousands of components, most of which are unstable molecules. Since the CSE extract was not analyzed and only the concentration of the whole extract was calculated minor or larger differences in the preparations may be responsible for the lack of a dose-response effect. In the case of chronic smoking, smoking did not cause as much a decrease in the 2-month-old guinea pigs as in the 1- and 4-month-old animals. One explanation for this is that the effects of smoking and/or the activity of NHE-1 differs in each age group. The effect of chronic smoking in humans was only studied at expression level because human EECs are not suitable for functional measurements due to the high sensitivity and low viability of the human primary cells. Consistent with the result obtained in guinea pig EECs, smoking reduced the expression of NHE-1 in humans. Although NHE-1 is expressed in a very low level in the normal human esophageal mucosa [8,13,15,16], the decreased expression of NHE-1 associates with cellular acidosis, which may increase the risk of cancer development, as a greater number of DNA damage and thus mutations develop in an acidic environment [15]. In order to clarify the role of NHE-1 in the CSE-induced proliferation, we downregulated NHE-1 by specific siRNA transfection. In the absence of NHE-1, the CSE-induced proliferation increased in the metaplastic cell line, suggesting that NHE-1, in addition to being essential in maintaining the normal pH of cells, also performs an important protective function and regulates cell proliferation against toxic agents. The protective role of NHE-1 against the carcinogenic processes has been also demonstrated in esophageal squamous cell carcinoma (ESCC), where suppression of NHE-1 increased the malignant potential and associated with poor prognosis in ESCC patients [13]. In contrast, Guan et al. have found that inhibition of NHE-1 suppressed esophageal cancer cell growth in EAC and ESCC cell lines and in nude mouse xenografts [16]. It has also been demonstrated in other cancer types that NHE-1 promotes tumor malignancy by providing appropriate pH conditions for tumor growth and invasion [11,43]. These data suggest that NHE-1 acts as a tumor oncogene rather than a suppressor in cancer. In BE, most studies agree that increased NHE activity and/or expression is more likely part of a defense or adaptive mechanism

which protects cells against toxic-agent-induced cellular acidification [8,14,15,18,44]. In the more advanced dysplastic state, inhibition of NHE-1 had no effect on the CSE-induced proliferation, indicating that, in dysplasia, the proliferative effect of CSE is independent from NHE-1.

Taken together, smoking affects NHE-1 function in normal, metaplastic and dysplastic cells differently. Under normal conditions, smoking reduces the activity and expression of NHE-1, resulting in the acidosis of  $\text{pH}_i$ . Disturbance of the pH homeostasis can lead to cell deaths or to the malignant transformation of the cells. In the metaplastic state, smoking increases the function of NHE-1, which is presumably a compensatory mechanism that prevents the onset of cancerous processes by keeping the intracellular pH in the normal range. As the expression of NHE-1 decreases, this protective mechanism disappears and the proliferative potential of the cells increases. In contrast to BE, decreased activity or expression of NHE-1 had no effect on smoking-induced proliferation in the dysplastic state indicating the involvement of other mechanisms.

We propose that upregulation of NHE-1 is the part of a protective mechanism against the harmful effects of smoking; however, further investigation would be needed to support this hypothesis. Direct increase in NHE-1 expression by using NHE-1 agonists or the use of transgenic mice models in which the *SLC9A1* gene is modified would give a more complete picture of the role of NHE-1. Nevertheless, the present results indicate that direct augmentation of NHE-1 function may provide new avenues for decreasing the damaging effect of smoking.

## 4. Materials and Methods

### 4.1. Chemicals and Solutions

All general laboratory chemicals and Trypan Blue solution (Catalogue No. T8154) were purchased from Sigma-Aldrich (Budapest, Hungary). We obtained 2,7-bis-(2-carboxyethyl)-5 (6)-carboxyfluorescein acetoxymethyl ester (BCECF-AM) from Invitrogen (Waltham, MA, USA), prepared (2  $\mu\text{mol/L}$ ) in dimethyl sulfoxide and stored at  $-20\text{ }^{\circ}\text{C}$ . Nigericin (10  $\mu\text{M}$ ) was dissolved in ethanol and stored at  $-20\text{ }^{\circ}\text{C}$ . High-Capacity Reverse Transcription Kit, TaqMan gene expression Master Mix, lipofectamine 2000 transfection reagent were purchased from Thermo Fisher Scientific (Waltham, MA, USA). Cell Counting Kit-8 was from Dojindo Molecular Technologies (Rockville, MD, USA). Citotoxicity detection kit (LDH) was obtained from Roche (Catalogue No. 11644793001, Roche). *SLC9A1* siRNAs (siRNA ID: 119643) was from Life Technologies. The standard  $\text{Na}^+$ -HEPES solution contained (in mM): 130 NaCl, 5 KCl, 1  $\text{CaCl}_2$ , 1  $\text{MgCl}_2$ , 10 D-glucose and 10 Na-HEPES.  $\text{NH}_4\text{Cl}$ -HEPES solution was supplemented with 20 mM  $\text{NH}_4\text{Cl}$ , while NaCl concentration was lowered to 110 mM. HEPES-buffered solutions were gassed with 100%  $\text{O}_2$ , and their pH was set to 7.5 with HCl.

### 4.2. Animals

Guinea pigs (4–12 weeks old, male) were kept in standard plastic cages on 12:12 h light–dark cycle at room temperature ( $23 \pm 1\text{ }^{\circ}\text{C}$ ) and had free access to standard laboratory chow and drinking solutions. Animal experiments were conducted in accordance with the *Guide for the Care and Use of Laboratory Animals* (United States, Department of Health and Human Services). In addition, the experimental protocol performed on non-smoking animals was approved by the local Ethical Board of the University of Szeged, Hungary.

### 4.3. Patients

Formalin-fixed paraffin-embedded esophageal tissue samples were retrieved from the archives of the Department of Pathology, University of Szeged (Szeged, Hungary), from January 2018 to May 2021. Retrospective data collection of patients was performed by the approval of the Ethics Committee of the University of Szeged (No. 4658), according to Helsinki Declaration and GDPR. We collected data based on diagnosis, histopathological features of the esophageal lesion, state of the disease and smoking history of the



patients from patient database used in Hungarian healthcare system (eMedSolution). Each esophageal biopsy and surgical resection sample was analyzed by pathologists earlier. Patients were basically classified into two groups: smoking group with a smoking history of more than 20 years and non-smoking group who had never smoked or had not smoked for at least a year. As a control, tumor-free resection margins and normal esophageal biopsy samples were used. The average age of BE patients was  $55.1 \pm 4.6$  years in the smoking group ( $n = 7$ ), and  $57.3 \pm 3.8$  years in the non-smoking group ( $n = 20$ ). The average age in the control group was  $38.5 \pm 11.5$  years in the smoking group ( $n = 3$ ), and  $59.7 \pm 3.8$  years in the non-smoking group ( $n = 7$ ).

#### 4.4. Cell Cultures

CP-A (human metaplastic esophageal epithelial cell line) and CP-D (human dysplastic esophageal epithelial cell line) cells were purchased from American Type Culture Collection (Manassas, VA, USA). The complete growth medium consists of MCDB-153 basal medium, 5% fetal bovine serum, 4 mM L-glutamine,  $1 \times$  ITS supplement (Sigma I1884; 5  $\mu$ g/mL Insulin, 5  $\mu$ g/mL Transferrin and 5 ng/mL Sodium Selenite), 140  $\mu$ g/mL Bovine Pituitary Extract (Sigma P1476), 20 mg/L adenine, 0.4  $\mu$ g/mL hydrocortisone, 8.4  $\mu$ g/L cholera toxin (Sigma C8052), 20 ng/mL recombinant human EGF (Epidermal Growth Factor) and 1% (*v/v*) penicillin/streptomycin. The cells were cultured at 37 °C and gassed with a mixture of 5% CO<sub>2</sub>–95% air. Cells were seeded at 100% confluency and were used between 3 and 19 passage numbers.

#### 4.5. Preparation of Cigarette-Smoke Extract

CSE was prepared at the Department of Pharmacognosy, University of Szeged. Briefly, mainstream smoke from 15 Kentucky Research Cigarettes (3R4F; 12 mg tar and 1.0 mg nicotine/cigarette), was continuously bubbled through 10 mL of distilled water. Dry weight was measured after evaporation of the crude extract with N<sub>2</sub>. CSE solution was then diluted to the appropriate concentration, using HEPES or culture media. CSE was freshly prepared for each experiments or used within 2 days of preparation.

#### 4.6. Cigarette-Smoke Exposure

The chronic effect of cigarette smoking was investigated by using a smoking chamber at the Department of Pharmacology and Pharmacotherapy, University of Pécs. Male guinea pigs were divided into three groups, according to the period of cigarette-smoke exposure (1-, 2- and 4-month exposure,  $n = 3$ /group). In order to avoid large age differences at the time of sacrifice, animals were selected for each group based on their age, so all animals were 5 months old at the time of sacrifice. Guinea pigs were maintained under 12:12 h light/dark cycle, with free access to food and water. Animals were exposed to whole body cigarette-smoke exposure 4 times a day, 5 days a week, for 30 min each time, using a TE2 whole body smoke exposure chamber (Teague Enterprises, Woodland, CA, USA). During the experiment, 3R4F Kentucky Research Cigarettes (Kentucky Tobacco Research and Development Center, Lexington, KY, USA) were smoked and ventilated inside the chamber. The animals were sacrificed 24–48 h after the last CSE exposure, and EECs were isolated. Intact age- and sex-matched animals served as controls. All experimental procedures were in accordance with the institutional guidelines under approved protocols (No. XII./2222/2018, University of Pécs).

#### 4.7. Isolation of Guinea Pig Esophageal Epithelial Cells

Animals were sacrificed by cervical dislocation, the esophagus was removed and EECs were isolated as described previously [45]. Briefly, the organ was cut longitudinally, rinsed in Hank's Balanced Salt Solution (HBSS, Sigma H9269) and digested in dispase solution (2 U/mL, Sigma D4818) for 40 min. After digestion, the inner, epithelial layer of the esophagus was detached from the submucosa and rinsed in HBSS. Then the epithelial layer was incubated in 0.5% Trypsin–EDTA solution supplemented with 1% (*v/v*) antimy-

coticum/antibioticum for  $2 \times 15$  min. The trypsin was inhibited by a filtered Soybean trypsin inhibitor (Gibco, 10684033) solution, and the whole lysate was centrifuged for 5 min, at 1000 rpm. The cell pellet was diluted in keratinocyte serum free media (KSFM, Gibco, Catalogue No. 17005042) supplemented with 1% (*v/v*) antimycoticum/antibioticum and seeded onto cover glasses and incubated until use. Viability of guinea pig EECs was investigated by using Trypan Blue reagent. After the incubation, bright field images were taken under  $40\times$  magnification, and stained cells were counted and considered not viable.

#### 4.8. Immunohistochemistry

Immunohistochemical analysis of NHE-1 expressions was performed on 4% buffered formalin-fixed sections of human esophageal samples embedded in paraffin. The 5  $\mu\text{m}$ -thick sections were stained in an automated system (Autostain, Dako, Glostrup, Denmark). Briefly, the slides were deparaffinized, and endogenous peroxidase activity was blocked by incubation with 3%  $\text{H}_2\text{O}_2$  (10 min). Antigenic sites were disclosed by applying citrate buffer in a pressure cooker (120 °C, 3 min). To minimize non-specific background staining, the sections were then pre-incubated with milk (30 min). Subsequently, the sections were incubated with a human anti-NHE-1 (1:100 dilution, 30 min, Alomone Laboratories) primary polyclonal antibody and exposed to LSAB2 labeling (Dako, Glostrup, Denmark) for  $2 \times 10$  min. The immunoreactivity was visualized with 3,3'-diaminobenzidine (10 min); then the sections were dehydrated, mounted and examined. NHE-1 expressing cells were identified by the presence of a dark red/brown chromogen. A semi-quantitative scoring system was used to evaluate the expression of NHE-1. The intensity of staining (0 = negative, 1 = weak, 2 = moderate and 3 = strong) and the percentage of positive cells (1–0–25% of the cells are positive, 2–25–50% of the cells are positive, 3–50–75% of the cells are positive and 75–100% of the cells are positive) were scored and then the composite score was obtained by multiplying the intensity of staining and the percentage of immunoreactive cells.

#### 4.9. Quantitative Real-Time PCR Analysis

Total mRNA was isolated by using an RNA isolation kit of Macherey-Nagel (Nucleospin RNA Plus kit, Macherey-Nagel, Germany) according to manufacturer's instructions. The concentration of RNA was determined by spectrophotometry (NanoDrop 3.1.0, Rockland, DE, USA). Two micrograms of total RNA were reverse-transcribed, using High-Capacity cDNA Archive Kit (Applied Biosystems) according to manufacturer's instructions. Quantitative real-time PCR was carried out on a Roche LightCycler 96 SW (Roche, Basel, Switzerland). TaqMan probe sets of *SLC9A1* were used to check gene expression. Target gene expression levels were normalized to a human housekeeping gene,  $\beta$ -actin (*ACTB*), and then, using the  $\Delta\Delta\text{C}_\text{T}$  method, relative gene expression was calculated. Fold changes were represented ( $2^{-\Delta\Delta\text{C}_\text{T}}$ ). Values below 0.5 and above 2.00 were considered significant.

#### 4.10. Western Blot

Cells were lysed in Cell Lysis Buffer (Catalogue No. 9803, Cell Signaling Technology, Danvers, MA, USA) supplemented with complete EDTA-free protease inhibitor (Roche, Catalogue No. 11873580001). Then samples were centrifuged at 2500 rpm for 20 min at 4 °C, and the supernatants were used. Protein concentration in the samples was determined by using a BCA assay (Pierce Chemical, Rockford, IL, USA) or Bradford reagent (Bio-Rad Laboratories, Hercules, CA, USA), and equal amounts of proteins (20 or 30  $\mu\text{g}$ ) were resolved on polyacrylamide gel and transferred onto Protran (GE Healthcare Amersham™) or PVDF (Invitrogen, Waltham, MA, USA) membranes. Membranes were incubated overnight with rabbit polyclonal anti-NHE-1 (Catalogue No. ANX-010, Alomone Labs, Jerusalem, Israel), mouse monoclonal anti-GAPDH (Catalogue No. MAB 374, Sigma Aldrich, Hungary) or mouse monoclonal anti- $\alpha$ -Tubulin antibody (Catalogue No. T9026, Merck, Darmstadt, Germany) followed by the incubation with the appropriate HRP-conjugated secondary antibody (Catalogue No. P0448 goat anti-rabbit and P0161 rabbit anti-mouse, DAKO, Glostrup,

Denmark or G-21040 goat anti-mouse, Invitrogen, Waltham, MA, USA). The peroxidase activity was visualized by using the enhanced chemi-luminescence assay (Advansta, Menlo Park, CA, USA) or with Clarity Chemiluminescence Substrate (Bio-Rad Laboratories, Hercules, CA, USA). Signal intensities were quantified by using the QuantityOne software (Bio-Rad, Hercules, CA, USA) or Image Lab Software, version 5.2 (Bio-Rad Laboratories, Hercules, CA, USA). The results from each membrane were normalized to the GAPDH or  $\alpha$ -Tubulin values and compared to the 6 h control.

#### 4.11. Measurement of Intracellular pH

Cells were seeded onto 24 mm cover glasses which were placed on the stage of an inverted microscope connected with an Xcellence imaging system (Olympus, Budapest, Hungary). Cells were incubated with a pH-sensitive fluorescence dye, BCECF-AM for 30–60 min according to cell type. Cells were perfused with solutions at 37 °C at a 5 to 6 mL/min perfusion rate. Average 5–12 regions of interest (ROIs) were marked in each measurement, and one image was taken per second. The cells were excited with 440 and 495 nm wavelength, and a 440/495 ratio was detected at 535 nm. One  $\text{pH}_i$  measurement was obtained per second. In situ calibration of the fluorescence signal was performed by using the high  $\text{K}^+$ -nigericin technique. Since CSE alone influences fluorescence signals, cells were pretreated with freshly prepared CSE (1, 10 and 100  $\mu\text{g/mL}$ ) for 1 h before microfluorometric measurements.

#### 4.12. Determination of Buffering Capacity

The total buffering capacity ( $\beta_{\text{total}}$ ) of cells was estimated according to the  $\text{NH}_4\text{Cl}$  pre-pulse technique, as previously described [46,47]. Briefly, EECs were exposed to various concentrations of  $\text{NH}_4\text{Cl}$  in  $\text{Na}^+$ - and  $\text{HCO}_3^-$ -free solutions. The total buffering capacity of the cells was calculated by using the following equation:  $\beta_{\text{total}} = \beta_i + \beta_{\text{HCO}_3^-} = \beta_i + 2.3 \times [\text{HCO}_3^-]_i$ , where  $\beta_i$  refers to the ability of intrinsic cellular components to buffer changes of  $\text{pH}_i$  and was estimated by the Henderson–Hasselbach equation. The measured rates of  $\text{pH}_i$  change ( $\Delta\text{pH}/\Delta t$ ) were converted to transmembrane base flux  $J(\text{B}^-)$ , using the following equation:  $J(\text{B}^-) = \Delta\text{pH}/\Delta t \times \beta_i$ . The  $\beta_i$  value at the start point  $\text{pH}_i$  was used for the calculation of  $J(\text{B}^-)$ .

#### 4.13. Measurement of $\text{Na}^+/\text{H}^+$ Exchanger Activity

For evaluating the activity of NHE-1,  $\text{NH}_4\text{Cl}$  pre-pulse technique was used. EECs were exposed to  $\text{NH}_4\text{Cl}$  (20 mM) for 3 min, which resulted in a sudden  $\text{pH}_i$  elevation through  $\text{NH}_3$  diffusion into the cells.  $\text{NH}_4\text{Cl}$  withdrawal caused a remarkable decrease in  $\text{pH}_i$  as the intracellular  $\text{NH}_4^+$  and  $\text{H}^+$  dissociating and basic  $\text{NH}_3$  exiting the cells. The regeneration from acidosis (the first 60 s) reflects the activity of NHEs in standard HEPES-buffered solutions. The following equation was used for estimating the transmembrane base flux:  $J(\text{B}^-) = \Delta\text{pH}/\Delta t \times \beta_i$ , where  $\Delta\text{pH}/\Delta t$  was calculated by linear regression analysis, whereas the intrinsic buffering capacity ( $\beta_i$ ) was determined by the Henderson–Hasselbach equation.

#### 4.14. SLC9A1 Gene Silencing

Cells were seeded on a 6-well plate in antibiotic-free complete growth medium and incubated overnight. *SLC9A1* gene silencing was performed at 40–50% confluency. Then 100 pmol *SLC9A1* siRNA was dissolved in 250  $\mu\text{L}$  Opti-MEM (Gibco, Catalogue No. 31985070) reduced serum medium. Then 5 or 7.5  $\mu\text{L}$  Lipofectamine 2000 was added to 250  $\mu\text{L}$  Opti-MEM and incubated for 5 min at room temperature. Then the prepared siRNA solution and Lipofectamine 2000 were mixed and incubated for 20 min to form complexes. The complexes were added to the wells, mixed gently by rocking the plate back and forth and then incubated for 72 h. After transfection, RT-qPCR and immunocytochemistry was performed to estimate mRNA and protein levels.

#### 4.15. Proliferation

Cells were seeded at  $10^3$  cells per well into a 96-well plate (100  $\mu$ L/well) in complete growth medium and allowed to attach for 24 h. Cells were then treated with CSE (1 and 10  $\mu$ g/mL) for 6, 24 and 72 h. After the treatments, 10  $\mu$ L of CCK8 solution was added to each well and the cells were incubated for further 3 h. Absorbance was detected at 450 nm, using a FLUOstar OPTIMA Spectrophotometer (BMG Labtech, Ortenberg, Germany).

#### 4.16. Cytotoxicity Assay

For cytotoxicity assay, 100  $\mu$ L of cell suspension was seeded into a 96-well plate ( $2.5 \times 10^4$  cells/well) and allowed to adhere overnight. On the following day, the cells were incubated with CSE (1, 10 and 100  $\mu$ g/mL) for 6, 24 and 72 h. Then 100  $\mu$ L of supernatant from each of the wells was carefully transferred into a new 96-well plate containing 100  $\mu$ L reaction mixture. We then measured lactate dehydrogenase (LDH) activity at 490 nm using a FLUOstar OPTIMA Spectrophotometer (BMG Labtech, Ortenberg, Germany). For background controls, we measured 200  $\mu$ L assay medium, without cells. For low controls, we used 100  $\mu$ L cell suspension and 100  $\mu$ L assay medium. In the case of high controls, the mixture of 100  $\mu$ L cell suspension and 100  $\mu$ L Triton-X 100 (0.1%) solution was measured. The LDH release induced by Triton-X 100 was assigned to 100%. The average absorbance values of each of the triplicates were calculated, and the average value of the background control (LDH activity contained in the assay medium) was subtracted from each of the samples to reduce background noises. We then calculated the percentage of cytotoxicity by using the following formula: Cytotoxicity (%) = (exp. value–low control/high control–low control)  $\times$  100. Low control determines the LDH activity released from the untreated normal cells (spontaneous LDH release), whereas high control determines the maximum releasable LDH activity in the cells (maximum LDH release).

#### 4.17. Statistical Analysis

Results were described as means  $\pm$  SE. For statistical analysis, one-way ANOVA and Student's *t*-test were used,  $p \leq 0.05$  were considered significant.

**Author Contributions:** Conceptualization, V.V.; data curation, E.B., M.M.K., E.G., Z.H. (Zsófia Hoyk), Z.M.K., A.H. and K.C.; formal analysis, E.B., E.G., L.T., Z.H. (Zsófia Hoyk), M.A.D., Z.M.K., A.K.-P., K.C., Z.H. (Zsuzsanna Helyes) and P.H.; funding acquisition, V.V.; investigation, E.B., M.M.K. and E.G.; methodology, E.B., M.M.K., E.G., M.A.D., A.K.-P., A.H., Z.H. (Zsuzsanna Helyes) and P.H.; supervision, V.V.; validation, L.T.; writing—original draft, V.V.; writing—review and editing, E.B., M.M.K., E.G., L.T., Z.H. (Zsófia Hoyk), M.A.D., Z.M.K., A.K.-P., A.H., K.C., Z.H. (Zsuzsanna Helyes), P.H. and V.V. All authors have read and agreed to the published version of the manuscript.

**Funding:** This study was supported by the National Research, Development and Innovation Office (FK123982) and by the Ministry of Human Capacities (EFOP 3.6.2-16-2017-00006).

**Institutional Review Board Statement:** Retrospective data collection of patients was performed by the approval of the Ethics Committee of the University of Szeged (No. 4658), according to Helsinki Declaration and GDPR. Smoking studies were in accordance with the institutional guidelines under approved protocols (No. XII./2222/2018, University of Pécs).

**Informed Consent Statement:** Patient consent was waived due to retrospective data collection.

**Conflicts of Interest:** The authors declare no conflict of interest.

## References

1. Cook, M.B.; Kamangar, F.; Whiteman, D.C.; Freedman, N.D.; Gammon, M.D.; Bernstein, L.; Brown, L.M.; Risch, H.A.; Ye, W.; Sharp, L.; et al. Cigarette smoking and adenocarcinomas of the esophagus and esophagogastric junction: A pooled analysis from the international BEACON consortium. *J. Natl. Cancer Inst.* **2010**, *102*, 1344–1353. [[CrossRef](#)] [[PubMed](#)]
2. Cook, M.B.; Shaheen, N.J.; Anderson, L.A.; Giffen, C.; Chow, W.H.; Vaughan, T.L.; Whiteman, D.C.; Corley, D.A. Cigarette smoking increases risk of Barrett's esophagus: An analysis of the Barrett's and Esophageal Adenocarcinoma Consortium. *Gastroenterology* **2012**, *142*, 744–753. [[CrossRef](#)] [[PubMed](#)]



3. Kuang, J.J.; Jiang, Z.M.; Chen, Y.X.; Ye, W.P.; Yang, Q.; Wang, H.Z.; Xie, D.R. Smoking Exposure and Survival of Patients with Esophagus Cancer: A Systematic Review and Meta-Analysis. *Gastroenterol. Res. Pract.* **2016**, *2016*, 7682387. [\[CrossRef\]](#) [\[PubMed\]](#)
4. Wang, Q.L.; Xie, S.H.; Li, W.T.; Lagergren, J. Smoking Cessation and Risk of Esophageal Cancer by Histological Type: Systematic Review and Meta-analysis. *J. Natl. Cancer Inst.* **2017**, *109*, djx115. [\[CrossRef\]](#) [\[PubMed\]](#)
5. Coleman, H.G.; Bhat, S.; Johnston, B.T.; McManus, D.; Gavin, A.T.; Murray, L.J. Tobacco smoking increases the risk of high-grade dysplasia and cancer among patients with Barrett's esophagus. *Gastroenterology* **2012**, *142*, 233–240. [\[CrossRef\]](#) [\[PubMed\]](#)
6. Orlando, R.C.; Bryson, J.C.; Powell, D.W. Effect of cigarette smoke on esophageal epithelium of the rabbit. *Gastroenterology* **1986**, *91*, 1536–1542. [\[CrossRef\]](#)
7. Becskehazi, E.; Korsos, M.M.; Eross, B.; Hegyi, P.; Venglovecz, V. OEsophageal Ion Transport Mechanisms and Significance Under Pathological Conditions. *Front. Physiol.* **2020**, *11*, 855. [\[CrossRef\]](#)
8. Laczko, D.; Rosztoczy, A.; Birkas, K.; Katona, M.; Rakonczay, Z., Jr.; Tiszlavicz, L.; Roka, R.; Wittmann, T.; Hegyi, P.; Venglovecz, V. Role of ion transporters in the bile acid-induced esophageal injury. *Am. J. Physiol. Gastrointest. Liver Physiol.* **2016**, *311*, G16–G31. [\[CrossRef\]](#)
9. Demaurex, N.; Grinstein, S. Na<sup>+</sup>/H<sup>+</sup> antiport: Modulation by ATP and role in cell volume regulation. *J. Exp. Biol.* **1994**, *196*, 389–404. [\[CrossRef\]](#)
10. Grinstein, S.; Rotin, D.; Mason, M.J. Na<sup>+</sup>/H<sup>+</sup> exchange and growth factor-induced cytosolic pH changes. Role in cellular proliferation. *Biochim. Biophys. Acta* **1989**, *988*, 73–97. [\[CrossRef\]](#)
11. Stock, C.; Schwab, A. Role of the Na/H exchanger NHE1 in cell migration. *Acta Physiol.* **2006**, *187*, 149–157. [\[CrossRef\]](#) [\[PubMed\]](#)
12. Shallat, S.; Schmidt, L.; Reaka, A.; Rao, D.; Chang, E.B.; Rao, M.C.; Ramaswamy, K.; Layden, T.J. NHE-1 isoform of the Na<sup>+</sup>/H<sup>+</sup> antiport is expressed in the rat and rabbit esophagus. *Gastroenterology* **1995**, *109*, 1421–1428. [\[CrossRef\]](#)
13. Ariyoshi, Y.; Shiozaki, A.; Ichikawa, D.; Shimizu, H.; Kosuga, T.; Konishi, H.; Komatsu, S.; Fujiwara, H.; Okamoto, K.; Kishimoto, M.; et al. Na<sup>+</sup>/H<sup>+</sup> exchanger 1 has tumor suppressive activity and prognostic value in esophageal squamous cell carcinoma. *Oncotarget* **2017**, *8*, 2209–2223. [\[CrossRef\]](#)
14. Fujiwara, Y.; Higuchi, K.; Tominaga, K.; Watanabe, T.; Oshitani, N.; Arakawa, T. Functional oesophageal epithelial defense against acid. *Inflammopharmacology* **2005**, *13*, 1–13. [\[CrossRef\]](#)
15. Goldman, A.; Shahidullah, M.; Goldman, D.; Khailova, L.; Watts, G.; Delamere, N.; Dvorak, K. A novel mechanism of acid and bile acid-induced DNA damage involving Na<sup>+</sup>/H<sup>+</sup> exchanger: Implication for Barrett's oesophagus. *Gut* **2010**, *59*, 1606–1616. [\[CrossRef\]](#)
16. Guan, B.; Hoque, A.; Xu, X. Amiloride and guggulsterone suppression of esophageal cancer cell growth in vitro and in nude mouse xenografts. *Front. Biol.* **2014**, *9*, 75–81. [\[CrossRef\]](#)
17. Tobey, N.A.; Koves, G.; Orlando, R.C. Human esophageal epithelial cells possess an Na<sup>+</sup>/H<sup>+</sup> exchanger for H<sup>+</sup> extrusion. *Am. J. Gastroenterol.* **1998**, *93*, 2075–2081. [\[CrossRef\]](#)
18. Goldman, A.; Chen, H.; Khan, M.R.; Roesly, H.; Hill, K.A.; Shahidullah, M.; Mandal, A.; Delamere, N.A.; Dvorak, K. The Na<sup>+</sup>/H<sup>+</sup> exchanger controls deoxycholic acid-induced apoptosis by a H<sup>+</sup>-activated, Na<sup>+</sup>-dependent ionic shift in esophageal cells. *PLoS ONE* **2011**, *6*, e23835. [\[CrossRef\]](#)
19. Liu, Y.; Wang, B.; Liu, X.; Lu, L.; Luo, F.; Lu, X.; Shi, L.; Xu, W.; Liu, Q. Epigenetic silencing of p21 by long non-coding RNA HOTAIR is involved in the cell cycle disorder induced by cigarette smoke extract. *Toxicol. Lett.* **2016**, *240*, 60–67. [\[CrossRef\]](#) [\[PubMed\]](#)
20. Zhao, Y.; Xu, Y.; Li, Y.; Xu, W.; Luo, F.; Wang, B.; Pang, Y.; Xiang, Q.; Zhou, J.; Wang, X.; et al. NF-kappaB-mediated inflammation leading to EMT via miR-200c is involved in cell transformation induced by cigarette smoke extract. *Toxicol. Sci.* **2013**, *135*, 265–276. [\[CrossRef\]](#) [\[PubMed\]](#)
21. Kong, J.; Nakagawa, H.; Isariyawongse, B.K.; Funakoshi, S.; Silberg, D.G.; Rustgi, A.K.; Lynch, J.P. Induction of intestinalization in human esophageal keratinocytes is a multistep process. *Carcinogenesis* **2009**, *30*, 122–130. [\[CrossRef\]](#)
22. Boedtker, E. Ion Channels, Transporters, and Sensors Interact with the Acidic Tumor Microenvironment to Modify Cancer Progression. *Rev. Physiol. Biochem. Pharmacol.* **2021**, 1–46. [\[CrossRef\]](#)
23. Chen, J.; Zhang, M.; Ma, Z.; Yuan, D.; Zhu, J.; Tuo, B.; Li, T.; Liu, X. Alteration and dysfunction of ion channels/transporters in a hypoxic microenvironment results in the development and progression of gastric cancer. *Cell Oncol.* **2021**, *44*, 739–749. [\[CrossRef\]](#)
24. Lu, C.; Ma, Z.; Cheng, X.; Wu, H.; Tuo, B.; Liu, X.; Li, T. Pathological role of ion channels and transporters in the development and progression of triple-negative breast cancer. *Cancer Cell Int.* **2020**, *20*, 377. [\[CrossRef\]](#)
25. Stock, C. How Dysregulated Ion Channels and Transporters Take a Hand in Esophageal, Liver, and Colorectal Cancer. *Rev. Physiol. Biochem. Pharmacol.* **2020**. [\[CrossRef\]](#)
26. Zhang, M.; Li, T.; Zhu, J.; Tuo, B.; Liu, X. Physiological and pathophysiological role of ion channels and transporters in the colorectum and colorectal cancer. *J. Cell Mol. Med.* **2020**, *24*, 9486–9494. [\[CrossRef\]](#) [\[PubMed\]](#)
27. Arcangeli, A.; Becchetti, A. New Trends in Cancer Therapy: Targeting Ion Channels and Transporters. *Pharmaceuticals* **2010**, *3*, 1202–1224. [\[CrossRef\]](#) [\[PubMed\]](#)
28. Ramirez, A.; Garcia-Quiroz, J.; Aguilar-Eslava, L.; Sanchez-Perez, Y.; Camacho, J. Novel Therapeutic Approaches of Ion Channels and Transporters in Cancer. *Rev. Physiol. Biochem. Pharmacol.* **2020**, 1–57. [\[CrossRef\]](#)
29. Corbet, C.; Feron, O. Tumour acidosis: From the passenger to the driver's seat. *Nat. Rev. Cancer* **2017**, *17*, 577–593. [\[CrossRef\]](#) [\[PubMed\]](#)

30. Estrella, V.; Chen, T.; Lloyd, M.; Wojtkowiak, J.; Cornnell, H.H.; Ibrahim-Hashim, A.; Bailey, K.; Balagurunathan, Y.; Rothberg, J.M.; Sloane, B.F.; et al. Acidity generated by the tumor microenvironment drives local invasion. *Cancer Res.* **2013**, *73*, 1524–1535. [[CrossRef](#)]
31. Kato, Y.; Ozawa, S.; Miyamoto, C.; Maehata, Y.; Suzuki, A.; Maeda, T.; Baba, Y. Acidic extracellular microenvironment and cancer. *Cancer Cell Int.* **2013**, *13*, 89. [[CrossRef](#)] [[PubMed](#)]
32. Swietach, P.; Vaughan-Jones, R.D.; Harris, A.L.; Hulikova, A. The chemistry, physiology and pathology of pH in cancer. *Philos Trans. R Soc. Lond B Biol. Sci.* **2014**, *369*, 20130099. [[CrossRef](#)] [[PubMed](#)]
33. Brisson, L.; Driffort, V.; Benoist, L.; Poet, M.; Counillon, L.; Antelmi, E.; Rubino, R.; Besson, P.; Labbal, F.; Chevalier, S.; et al. NaV1.5 Na(+) channels allosterically regulate the NHE-1 exchanger and promote the activity of breast cancer cell invadopodia. *J. Cell Sci.* **2013**, *126*, 4835–4842. [[CrossRef](#)]
34. Li, S.; Bao, P.; Li, Z.; Ouyang, H.; Wu, C.; Qian, G. Inhibition of proliferation and apoptosis induced by a Na<sup>+</sup>/H<sup>+</sup> exchanger-1 (NHE-1) antisense gene on drug-resistant human small cell lung cancer cells. *Oncol. Rep.* **2009**, *21*, 1243–1249. [[CrossRef](#)]
35. Serafino, A.; Moroni, N.; Psaila, R.; Zonfrillo, M.; Andreola, F.; Wannenes, F.; Mercuri, L.; Rasi, G.; Pierimarchi, P. Anti-proliferative effect of atrial natriuretic peptide on colorectal cancer cells: Evidence for an Akt-mediated cross-talk between NHE-1 activity and Wnt/beta-catenin signaling. *Biochim. Biophys. Acta* **2012**, *1822*, 1004–1018. [[CrossRef](#)]
36. Vaish, V.; Sanyal, S.N. Role of Sulindac and Celecoxib in chemoprevention of colorectal cancer via intrinsic pathway of apoptosis: Exploring NHE-1, intracellular calcium homeostasis and Calpain 9. *Biomed. Pharm.* **2012**, *66*, 116–130. [[CrossRef](#)]
37. Reshkin, S.J.; Cardone, R.A.; Harguindey, S. Na<sup>+</sup>-H<sup>+</sup> exchanger, pH regulation and cancer. *Recent Pat. Anticancer Drug Discov.* **2013**, *8*, 85–99. [[CrossRef](#)]
38. Loo, S.Y.; Chang, M.K.; Chua, C.S.; Kumar, A.P.; Pervaiz, S.; Clement, M.V. NHE-1: A promising target for novel anti-cancer therapeutics. *Curr. Pharm. Des.* **2012**, *18*, 1372–1382. [[CrossRef](#)]
39. Venglovecz, V.; Rakonczay, Z., Jr.; Ozsvari, B.; Takacs, T.; Lonovics, J.; Varro, A.; Gray, M.A.; Argent, B.E.; Hegyi, P. Effects of bile acids on pancreatic ductal bicarbonate secretion in guinea pig. *Gut* **2008**, *57*, 1102–1112. [[CrossRef](#)] [[PubMed](#)]
40. Bracke, K.R.; D'Hulst, A.I.; Maes, T.; Demedts, I.K.; Moerlose, K.B.; Kuziel, W.A.; Joos, G.F.; Brusselle, G.G. Cigarette smoke-induced pulmonary inflammation, but not airway remodelling, is attenuated in chemokine receptor 5-deficient mice. *Clin. Exp. Allergy* **2007**, *37*, 1467–1479. [[CrossRef](#)] [[PubMed](#)]
41. D'Hulst, A.I.; Vermaelen, K.Y.; Brusselle, G.G.; Joos, G.F.; Pauwels, R.A. Time course of cigarette smoke-induced pulmonary inflammation in mice. *Eur. Respir. J.* **2005**, *26*, 204–213. [[CrossRef](#)]
42. Stevenson, C.S.; Docx, C.; Webster, R.; Battram, C.; Hynx, D.; Giddings, J.; Cooper, P.R.; Chakravarty, P.; Rahman, I.; Marwick, J.A.; et al. Comprehensive gene expression profiling of rat lung reveals distinct acute and chronic responses to cigarette smoke inhalation. *Am. J. Physiol. Lung Cell Mol. Physiol.* **2007**, *293*, L1183–L1193. [[CrossRef](#)]
43. Stock, C.; Pedersen, S.F. Roles of pH and the Na(+)/H(+) exchanger NHE1 in cancer: From cell biology and animal models to an emerging translational perspective? *Semin. Cancer Biol.* **2017**, *43*, 5–16. [[CrossRef](#)] [[PubMed](#)]
44. Fujiwara, Y.; Higuchi, K.; Takashima, T.; Hamaguchi, M.; Hayakawa, T.; Tominaga, K.; Watanabe, T.; Oshitani, N.; Shimada, Y.; Arakawa, T. Roles of epidermal growth factor and Na<sup>+</sup>/H<sup>+</sup> exchanger-1 in esophageal epithelial defense against acid-induced injury. *Am. J. Physiol. Gastrointest Liver Physiol.* **2006**, *290*, G665–G673. [[CrossRef](#)] [[PubMed](#)]
45. Kalabis, J.; Wong, G.S.; Vega, M.E.; Natsuzaka, M.; Robertson, E.S.; Herlyn, M.; Nakagawa, H.; Rustgi, A.K. Isolation and characterization of mouse and human esophageal epithelial cells in 3D organotypic culture. *Nat. Protoc.* **2012**, *7*, 235–246. [[CrossRef](#)] [[PubMed](#)]
46. Hegyi, P.; Gray, M.A.; Argent, B.E. Substance P inhibits bicarbonate secretion from guinea pig pancreatic ducts by modulating an anion exchanger. *Am. J. Physiol. Cell Physiol.* **2003**, *285*, C268–C276. [[CrossRef](#)]
47. Weintraub, W.H.; Machen, T.E. pH regulation in hepatoma cells: Roles for Na-H exchange, Cl-HCO<sub>3</sub> exchange, and Na-HCO<sub>3</sub> cotransport. *Am. J. Physiol.* **1989**, *257*, G317–G327. [[CrossRef](#)]

II.



OPEN

## Bile accelerates carcinogenic processes in pancreatic ductal adenocarcinoma cells through the overexpression of MUC4

Eleonóra Gál<sup>1</sup>, Zoltán Veréb<sup>2,3</sup>, Lajos Kemény<sup>2,3</sup>, Dávid Rakk<sup>4</sup>, András Szekeres<sup>4</sup>, Eszter Becskeházi<sup>1</sup>, László Tiszlavicz<sup>5</sup>, Tamás Takács<sup>6</sup>, László Czakó<sup>6</sup>, Péter Hegyi<sup>6,7,8</sup> & Viktória Venglovecz<sup>1</sup>✉

Pancreatic cancer (PC) is one of the leading causes of mortality rate globally and is usually associated with obstructive jaundice (OJ). Up to date, there is no clear consensus on whether biliary decompression should be performed prior to surgery and how high levels of serum bile affects the outcome of PC. Therefore, our study aims were to characterise the effect of bile acids (BAs) on carcinogenic processes using pancreatic ductal adenocarcinoma (PDAC) cell lines and to investigate the underlying mechanisms. Liquid chromatography-mass spectrometry was used to determine the serum concentrations of BAs. The effects of BAs on tumour progression were investigated using different assays. Mucin expressions were studied in normal and PDAC cell lines and in human samples at gene and protein levels and results were validated with gene silencing. The levels of BAs were significantly higher in the PDAC + OJ group compared to the healthy control. Treating PDAC cells with different BAs or with human serum obtained from PDAC + OJ patients enhanced the rate of proliferation, migration, adhesion, colony forming, and the expression of MUC4. In PDAC + OJ patients, MUC4 expression was higher and the 4-year survival rate was lower compare to PDAC patients. Silencing of MUC4 decreased BAs-induced carcinogenic processes in PDAC cells. Our results show that BAs promote carcinogenic process in PDAC cells, in which the increased expression of MUC4 plays an important role. Based on these results, we assume that in PC patients, where the disease is associated with OJ, the early treatment of biliary obstruction improves life expectancy.

### Abbreviations

BAs	Bile acids
BAC	Bile acid cocktail
GCA	Glycocholic acid
GCDCA	Glycochenodeoxycholic acid
GDCA	Glycodeoxycholic acid
LDH	Lactate dehydrogenase
MTT	3-(4,5-Dimethylthianol-2-yl)-2,5-diphenyltetrazolium bromide
NE	Neuroendocrine tumor
OJ	Obstructive jaundice

<sup>1</sup>Department of Pharmacology and Pharmacotherapy, University of Szeged, 6720 Szeged, Hungary. <sup>2</sup>Regenerative Medicine and Cellular Pharmacology Research Laboratory, Department of Dermatology and Allergology, University of Szeged, Szeged, Hungary. <sup>3</sup>HCEMM SZTE Skin Research Group, University of Szeged, Szeged, Hungary. <sup>4</sup>Department of Microbiology, University of Szeged, Szeged, Hungary. <sup>5</sup>Department of Pathology, University of Szeged, Szeged, Hungary. <sup>6</sup>First Department of Medicine, University of Szeged, Szeged, Hungary. <sup>7</sup>Institute for Translational Medicine, Medical School, Szentágotthai Research Centre, University of Pécs, Pécs, Hungary. <sup>8</sup>Division of Gastroenterology, First Department of Medicine, Medical School, University of Pécs, Pécs, Hungary. ✉email: venglovecz.viktoria@med.u-szeged.hu

PC	Pancreatic cancer
PDAC	Pancreatic ductal adenocarcinoma
TCA	Taurocholic acid
TCDCa	Taurochenodeoxycholic acid
TDCA	Taurodeoxycholic acid
TSBA	Total serum bile acid

Pancreatic cancer (PC) is associated with extremely poor survival and high mortality rate. Currently, PC is the seventh leading cause of cancer-related deaths worldwide<sup>1</sup>. One of the most common reasons for the poor clinical outcome is the lack of specific symptoms; as a result, approximately 80% of patients are diagnosed at an advanced stage, when most of them are inoperable<sup>2–5</sup>. The most common form of PC is pancreatic ductal adenocarcinoma (PDAC), which is responsible for approximately 90% of cases<sup>6</sup>. Most of the PDAC arises from ductal cells in the head of the pancreas. As tumour grows, it prevents the flow of bile and, as a result, obstructive jaundice (OJ) develops. Elevated serum levels of bile acids (BAs) influence the function of several organs; they have also proved to have tumorigenic potential in both gastrointestinal and breast cancer<sup>7</sup>. Although surgical intervention is widely regarded as the most effective way for the treatment of PC<sup>3,8</sup>, the use of preoperative biliary stenting is often the basis for debate and it usually takes time to make a decision<sup>9–11</sup>. Moreover, there is no consensus regarding the role of BAs in the initiation and progression of PC<sup>12</sup>. Some studies indicate that BAs inhibit the proliferation of PC cells due to their cytotoxic properties<sup>13,14</sup>, while others found that BAs promote tumour development and progression by increasing the expression of COX-2 or mucins<sup>15–17</sup>.

In recent years, considerable attention has been paid to the diagnostic use of mucins in PC. Twenty-one mucin genes have been identified in humans and, among them, MUC1, -4 and -5AC proved to be potential biomarkers to assess the progression of PC. These genes are mainly overexpressed in PC, play role in tumour cell growth and associate with a poor outcome for PC patients<sup>16,18–20</sup>. Several studies indicate that BAs play an extensive role in tumour progression by altering the expression of mucins<sup>17,21–25</sup>. In the oesophagus, BAs upregulate mucin expression, in which phosphatidylinositol 3-kinase and nuclear factor- $\kappa$ B (NK- $\kappa$ B) signalling pathways play a role<sup>17,23,24</sup>. The role of NK- $\kappa$ B in bile-induced mucin expression has also been implicated in gastric epithelial cells<sup>25</sup>. In contrast, there has not been in-depth study pertaining to the pancreas; thus, this study aims (i) to investigate how BAs treatment affect the behaviour of PDCA cells and ii) to identify the mechanisms that mediate the effects of BAs.

We have shown that BAs increase the tumorigenic potential of PDAC cells, through the overexpression of MUC4. In addition, we investigated the expression of MUC4 in human PC samples and identified a relation between the presence of OJ and increased expression of MUC4. Moreover, we have found that the 4-year overall survival rate of the PDAC + OJ patients was significantly poorer than that of the PDAC patients. Taken together our results show that bile accelerates carcinogenic processes, which can be of great importance in the therapy of PC.

## Materials and methods

**Ethical aspects.** The clinical part of the study was carried out with the approval of the Ethics Committee of the University of Szeged (No.: 4714), followed by the EU Member States' Directive 2004/23/EC on presumed consent practice for tissue collection, the guidelines of the Helsinki Declaration and GDPR. Written informed consent was obtained from all patients and healthy volunteers for sample and data collection.

**Pathological characterisation of the patients.** Serum levels of BAs were investigated in PDAC patients with OJ (average age:  $72.6 \pm 9.8$ ; male/female ratio: 5/5) or without OJ (average age:  $80 \pm 2.5$ ; male/female ratio: 2/3) and in healthy volunteers (average age:  $40.9 \pm 18.77$ ; male/female ratio: 6/8). In all groups, BAs were identified in fasting serum samples. See Table 1 for the details of patients.

We performed immunohistochemistry on pancreatic samples obtained from 65 patients. These patients have been classified into the following groups: (1) PDAC (average age:  $65.6 \pm 1.4$ ; male/female ratio: 17/8), (2) PDAC + OJ (average age:  $66.4 \pm 1.7$ ; male/female ratio: 13/12), (3) neuroendocrine tumour (NE) (average age:  $68.1 \pm 2.25$ ; male/female ratio: 8/3) and (4) control group (average age:  $62.75 \pm 3.3$ ; male/female ratio: 1/3). All the samples were obtained from surgical resection or biopsy. Pathological characterisation of the PDAC tumours, including PDAC + OJ tumours, confirmed that most of them were moderately differentiated (grade 2,  $n = 30$ ); 14 tumours were poorly differentiated (grade 3), whereas 6 tumours were well-differentiated (grade 1). The majority of PDAC developed in the head. Among the PDAC patients, 22 were in stage IV, 22 in stage III and 6 in stage II. Metastasis was present in 25 cases. We followed up on all patients for 48 months, during which time all PDAC and PDAC + OJ patients died. See Table 2 for the details of patients.

**Chemicals and solutions.** TaqMan gene expression assays, MTT 3-(4,5-dimethylthianol-2-yl)-2,5-diphenyltetrazolium bromide (MTT), siRNAs for MUC4 (Cat.No.:AM 16708), and the oligofectamine transfection kit were obtained from Thermo Fisher Scientific (Watham, MA, USA). Mouse MUC4 monoclonal IgG1 antibody was ordered from Santa Cruz Biotechnology (Cat.No.:sc-33654; Dallas, TX, USA). Guinea pig vimentin polyclonal antibody was ordered from Fitzgerald Industries International (Cat.No.:20R-VP044, Acton, MA, USA). Texas Red-AffiniPure Goat anti Guinea Pig IgG secondary antibody was from Jackson ImmunoResearch Laboratories, Inc. (Cat.No.:106-075-003; Cambridgeshire, UK). Technical Manual Cell Counting Kit-8 (CCK) was obtained from Dojindo Molecular Technologies (Rockville, MD, USA). Glycodeoxycholic acid (GDCA) was from Cayman Chemical Company (Michigan, MI, USA). BAs (glycocholic acid (GCA); taurocholic acid (TCA); taurodeoxycholic acid (TDCA); glycochenodeoxycholic acid (GCDCA); taurochenodeoxycholic acid

Variable	PDAC + OJ (n = 10)		PDAC (n = 5)			NORMAL (n = 14)		
	n	(%)	n	(%)	p value	n	(%)	p value
<b>Gender</b>								
Male	5	(50.0)	2	(40.0)		6	(42.9)	
Female	5	(50.0)	3	(60.0)	0.7376	8	(57.1)	0.9930
<b>Age</b>								
<65	2	(20.0)	0	(0.0)		10	(71.0)	
≥ 65	8	(80.0)	5	(100.0)	0.5877	4	(29.0)	0.7125
<b>Location of primary tumor</b>								
Papilla of Vater	3	(30.0)	0	(0.0)				
Head	4	(40.0)	5	(100.0)				
Head/Body	2	(20.0)	0	(0.0)				
Body	1	(10.0)	0	(0.0)				
Tail	0	(0.0)	0	(0.0)	0.4369			
<b>Hystological type</b>								
Well differentiated	0	(0.0)	0	(0.0)				
Moderately differentiated	7	(70.0)	5	(100.0)				
Poorly differentiated	3	(30.0)	0	(0.0)	0.5599			
<b>Stage of the cancer</b>								
II	0	(0.0)	0	(0.0)				
III	4	(40.0)	4	(80.0)				
IV	6	(60.0)	1	(20.0)	0.4456			
<b>Lymphatic invasion</b>								
Negative	7	(70.0)	5	(100.0)				
Positive	3	(30.0)	0	(0.0)	0.5166			
<b>Metastasis</b>								
Lung	0	(0.0)	0	(0.0)				
Liver	4	(40.0)	3	(60.0)				
Colon	1	(10.0)	2	(30.0)				
Gall bladder	0	(0.0)	0	(0.0)	0.6540			
<b>Bile acids in human serum (ng/ml)</b>								
GCA	9890.5 ± 3267.1	(27.43)	41.46 ± 53.45	(5.65)		27.35 ± 26.66	(6.82)	
GDCA	217.22 ± 193.27	(0.62)	67.83 ± 93.28	(9.25)		70.01 ± 86.59	(17.44)	
GCDCa	4770.8 ± 2375.1	(13.23)	339.93 ± 376.6	(46.31)		186.77 ± 108.37	(46.54)	
TCA	13,299 ± 2827.1	(36.88)	98.96 ± 57.09	(13.49)		0.0 ±	(0.0)	
TDCA	0.0 ±	(0.0)	47.6 ± 27.4847.6 ± 27.48	(6.48)		61.32 ± 53.02	(15.28)	
TCDCa	7878.1 ± 1644.3	(21.84)	138.07 ± 126.27	(18.81)		55.85 ± 31.55	(13.92)	
Total serum bile acids	36,055.7 ± 2182.2		733.85 ± 118.7		0.0275	401.3 ± 35.38		0.0228

**Table 1.** Clinicopathological characteristics of pancreatic cancer patients selected for serum bile acid measurements.

(TCDCa)) and all other laboratory chemicals were ordered from Sigma-Aldrich Kft. (Budapest, Hungary). For more details on gene expression assays see Suppl. Table S1.

**Cell lines and culture conditions.** The human PDAC cell lines, Capan-1, Miapaca-2, Panc-1 and BxPC-3 were obtained from American Type Culture Collection (Manassas, VA, USA). Capan-1 and BxPC-3 cells were cultured in RPMI-1640 media supplemented with 15% (v/v) fetal bovine serum (FBS); 1% (v/v) L-glutamine and 2% (v/v) antimycoticum/antibioticum. Miapaca-2 and Panc-1 were maintained in Dulbecco's Modified Eagle's Medium high glucose medium supplemented with 10% (v/v) FBS, 1% (v/v) L-glutamine, 2.5% (v/v) horse serum, and 1% (v/v) penicillin/streptomycin. HPDEC, human pancreatic ductal epithelial cell line was ordered from Hölzel Diagnostika Handels GMBH (Köln, Germany) and the cells were cultured in keratinocyte serum-free media supplied with prequalified human recombinant Epidermal Growth Factor and Bovine Pituitary Extract. The cells were cultured under standard conditions (37 °C and 5% CO<sub>2</sub>) the medium was replaced in every alternate day and the cells were cultured at 100% confluence. Capan-1 cells were used between 30 and 35, BxPC-3 cells between 2 and 5, Panc-1 and Miapaca-2 cells between 20 and 25 and HPDEC cells between 9 and 11 passage numbers.



Variable	PDAC + OJ (n = 25)		PDAC (n = 25)		NE (n = 11)		NORMAL (n = 4)	
	n	(%)	n	(%)	n	(%)	n	(%)
<b>Gender</b>								
Male	13	(52.0)	17	(68.0)	8	(72.7)	1	(25.0)
Female	12	(48.0)	8	(32.0)	3	(27.3)	3	(75.0)
<b>Age</b>								
< 65	6	(24.0)	10	(40.0)	4	(36.36)	4	(100.0)
≥ 65	19	(76.0)	15	(60.0)	7	(63.64)	0	(0.0)
<b>Location of primary tumor</b>								
Papilla of Vater	3	(12.0)	0	(0.0)	0	(0.0)		
Head	22	(88.0)	18	(72.0)	6	(54.54)		
Head/Body	0	(0.0)	5	(20.0)	0	(0.0)		
Body	0	(0.0)	1	(4.0)	1	(9.1)		
Tail	0	(0.0)	1	(4.0)	4	(36.36)		
<b>Hystological type</b>								
Well differentiated	3	(12.0)	3	(12.0)	4	(36.37)		
Moderately differentiated	12	(48.0)	18	(72.0)	7	(63.63)		
Poorly differentiated	10	(40.0)	4	(16.0)	0	(0.0)		
<b>Stage of the cancer</b>								
II	2	(8.0)	4	(16.0)	8	(72.73)		
III	10	(40.0)	12	(48.0)	3	(27.27)		
IV	13	(52.0)	9	36.0)				
<b>Lymphatic invasion</b>								
Negative	17	(68.0)	20	(80.0)	11	(100.0)		
Positive	8	(32.0)	5	(20.0)	0	(0.0)		
<b>Metastasis</b>								
Lung	2	(8.0)	4	(16.0)	0	(0.0)		
Liver	6	(24.0)	10	(40.0)	2	(18.18)		
Colon	0	(0.0)	2	(8.0)	0	(0.0)		
Gall bladder	1	(4.0)	0	(0.0)	0	(0.0)		

**Table 2.** Clinicopathological characteristics of pancreatic cancer patients selected for MUC4 staining.

**Bile acid treatment.** The cells were seeded into 25 cm<sup>2</sup> tissue culture flasks or 96-well tissue plates, two days before the BAs treatment. The treatment was performed with six different types of BAs (GCA, TCA, GDCA, TDCA, GCDCA, TCDCA) in two different concentrations (100 and 500 µM), for 24, 48 and 72 h. Bile acid cocktail (BAC) contained all BAs in equal concentrations, with a final concentration of 500 µM.

**Cell adhesion assay.** We coated 96-well tissue plates with 40 µg/ml type 1 collagen from rat-tail in PBS at 4 °C. Next, we added 100 µl of cell suspension (10<sup>5</sup> cells/ml) to each of the coated wells and incubated the cells at 37 °C for 20 min to allow them to adhere to the surface. After washing, the cells were incubated with BAs and 10 µl of MTT substrate was added to each well. MTT-treated cells were then lysed in DMSO and absorbance was measured using a FLUOstar OPTIMA Spectrophotometer (BMG Labtech, Ortenberg, Germany) at 560 nm with background subtraction at 620 nm.

**Proliferation.** For proliferation, 100 µl of cell suspension was seeded into a 96-well plate (5 × 10<sup>3</sup> cells/well), then the cells were incubated with BAs. After the treatments, 10 µl of CCK8 solution was added to each well and the cells were incubated for further 3 h. We measured absorbance at 450 nm using a FLUOstar OPTIMA Spectrophotometer (BMG Labtech, Ortenberg, Germany).

**Cytotoxicity assay.** For cytotoxicity assay, 100 µl of cell suspension was seeded into a 96-well plate (2 × 10<sup>4</sup> cells/well) and allowed to adhere overnight. On the following day, the cells were incubated with BAs then 100 µl supernatant from each of the wells was carefully transferred into a new 96-well plate containing 100 µl reaction mixture. We then measured lactate dehydrogenase (LDH) activity at 490 nm using a FLUOstar OPTIMA Spectrophotometer (BMG Labtech, Ortenberg, Germany). For background controls, we measured 200 µl assay medium, without cells. For low controls, we used 100 µl cell suspension and 100 µl assay medium. In the case of high controls, the mixture of 100 µl cell suspension and 100 µl Triton-X 100 (0.1%) solution was measured. The LDH release induced by Triton-X 100 was assigned to 100%. The average absorbance values of each of the triplicates were calculated and the average value of the background control (LDH activity contained in the assay medium) was subtracted from each of the samples to reduce background noises. We then calculated the per-

centage of cytotoxicity using the following formula: Cytotoxicity (%) = (exp. value–low control/high control–low control)\*100. Low control determines the LDH activity released from the untreated normal cells (spontaneous LDH release), whereas high control determines the maximum releasable LDH activity in the cells (maximum LDH release).

**Wound healing assay.** Cells were seeded onto 24-well cell culture plates in a  $2.5 \times 10^5$  cell density and allowed to adhere overnight. On the following day, the confluent monolayer was gently scratched using P2 tips. Only the wells containing even-sided and sharp-edged wounds were used for experiments. After gentle washing with the complete medium, we added BAs to the wells. We carried out automated time lapse imaging using an Olympus IX83 inverted microscope with Olympus ScanR screening platform (Olympus, Japan) upgraded with OKOLAB incubator system (with gas, temperature, and humidity controller; Pozzuoli, NA, Italy). Digital images were analysed by Image J.

**Clonogenic assay.** Capan-1 and BxPC-3 cells ( $10^3$  cells/well) were seeded onto 6-well cell culture plates and allowed to adhere overnight. On the following day, the cells were treated with BAs then the normal media was given back. The cells were allowed to grow until day 9 after which the media was removed, and the cells were washed with PBS, fixed with methanol-ethanol solutions (3:1 dilution) and then stained with Giemsa. Olympus IX83 microscope-based screening platform was used for image acquisition and the Olympus Cellsense Dimension software was used for automated object detection, classification and measurement to enumerate colonies organised by the treated and untreated cells.

**Invasion assay.** For the invasion assay Matrigel-coated transwell inserts were used. 200  $\mu$ l cells ( $\sim 2.5 \times 10^5$ /ml in serum-free medium) were added into the inserts whereas the lower chambers contained 750  $\mu$ l complete medium with or without BAs. Cells were then incubated at 37 °C for 24–72 h in 5% CO<sub>2</sub> in a humidified incubator. Cells that migrated to the bottom surface were fixed in formaldehyde (3.7% in PBS) for 5 min, permeabilized with 100% methanol and stained with Giemsa dye for 30 min. The non-invading cells on the upper surface of the membrane were gently scraped off using a cotton swab. Invasion was quantified by counting the average number of invaded cells in five different microscopic fields in each treatment. Percent invasion was calculated from the mean of the average number of invaded cells obtained from 3 independent experiments.

**siRNA silencing.** MUC4 expression was silenced transiently, using MUC4-targeted siRNA oligonucleotides. Transfection was performed with Oligofectamine™ Transfection Reagent following the manufacturer's instructions. We then plated  $2 \times 10^5$  cells per well onto 6-well plates a day before the transfection. At 50–60% confluency, the MUC4-targeted siRNAs were transfected and the cells were incubated for 72 h. MUC4 mRNA and protein levels were assessed by RT-PCR and immunocytochemistry, respectively.

**RT-PCR.** The total RNA was isolated from the cells using the NucleoSpin RNA Kit (Macherey–Nagel, Düren, Germany). Two micrograms of RNA were reverse-transcribed using the High-Capacity cDNA Reverse Transcription Kit (Applied Biosystems, Foster City, USA). Real-time PCR reactions of samples were performed with TaqMan RT-PCR assays (Supplementary Table S1) from Thermo Fisher Scientific (Darmstadt, Germany). Reactions were carried out with ABI PRISM 7000 Sequence Detection System (Applied Biosystems, Foster City, CA, USA) platform with the following conditions: 10 min initial denaturation at 95 °C, followed by 40 steps cycles: 15 s at 95 °C and 1 min at 60 °C. Fluorescein dye (FAM) intensity was detected after each cycle. All the samples were run in triplicates and non-template control sample was used for each PCR run to check the primer-dimer formation. The expression level of the gene of interest was normalised to the human  $\beta$ -actin (*Actb*) housekeeping gene ( $\Delta$ CT), and then relative gene expression ratios were calculated using the  $\Delta\Delta$ C<sub>T</sub> method as previously described<sup>26,27</sup>. The results were expressed as fold changes ( $2^{-\Delta\Delta$ CT). Genes with expression values less than or equal to 0.5 were considered to be down-regulated, whereas the values higher than or equal to 2 were considered to be upregulated. Values ranging from 0.51 to 1.99 were not considered to be significant.

**Immunostainings.** Immunocytochemistry (ICC) was performed using cytospin preparation during which 100  $\mu$ l ( $2 \times 10^6$  cells/ml) of cell suspension was added to 100  $\mu$ l of neutral formalin buffer and incubated for 5 min. After the incubation, 100  $\mu$ l from this mixture were spin (Shandon Cytospin3, Marshall Scientific, Cambridge, MA, US) to an Ultra Plus Microscope Slide (Thermo Fisher Scientific, Darmstadt, Germany). Pre-treatment was carried out with heat-induced epitope retrieval procedure using PT Link (Autostainer Link 48, Agilent, Dako, Santa Clara, CA, US) with EnVision™ Flex Target Retrieval Solution for 20 min at 92 °C in low pH (pH 6.1; citrate buffer). Slides were then washed with EnVision™ Wash Buffer (20  $\times$ ) for 5 min. The endogenous peroxidase blocking was carried out with EnVision™ Flex Peroxidase Blocking Reagent. For staining procedure, the slides were incubated with MUC4 (1:100 dilutions) primary antibodies for 30 min. After incubation, the slides were washed and incubated with secondary antibody (EnVision™ Flex/HRP anti-mouse/rabbit) for 30 min. For visualisation, the Ultra View Universal diaminobenzidine (DAB) Detection Kit (EnVision™ Flex DAB) was applied and nuclear staining was carried out with EnVision™ Flex Hematoxylin. After the staining procedure, the slides were mounted with Xylene Substitute mount (Shandon, Marshall Scientific, Cambridge, MA, US). All specimens were scanned by the Olympus IX83-based system and the pictures were further analysed by ImageJ, whereas the intensities of the pixels of the DAB staining were quantified. In the case of vimentin staining, Capan-1 cells (20,000/chamber) were seeded on chamber slides, fixed with 3.6% paraformaldehyde and permeabilized with 0.2% Triton X-100 and 0.3% protease-free bovine serum albumin. Cells were then incubated with 10% donkey



serum to reduce non-specific binding than anti-vimentin primary antibody (1:100 dilution) was added to the chambers and slides were incubated overnight in moist atmosphere at 4 °C. Chamber slides were then washed with PBS and incubated with TexasRed-conjugated anti-mouse secondary antibody (1:400 dilution) for 60 min at RT. Nuclei were counterstained with Hoechst 33342. Slides were then mounted and observed by a Fluoview 10i-W confocal microscopy (Olympus, Budapest, Hungary). In the human pancreatic samples, MUC4 expression was analysed using formalin-fixed, and paraffin-embedded tissue specimens were obtained from patients. Control tissues (n = 4) were collected from the tumour-free region of the pancreas of patients with NE tumour. Briefly, 3 to 4 µm thick sections of section specimens were deparaffinised in xylene and rehydrated in graded ethanol. The diagnosis was assessed by a pathologist after staining the sections with haematoxylin–eosin–safran. Immunohistochemistry (IHC) was performed as described above, but the slides were incubated with the primary MUC4 antibody for 60 min. Quantification of MUC4 expression was evaluated using the method described by Rachagani et al.<sup>28</sup>.

**LC–MS measurement of the serum samples.** The measurement of BAs was based on the work of Ghafarzadegan et al. with slight modifications<sup>29</sup>. The stock solution contained 1 mg/ml of each BA in methanol was used to form a seven-point calibration curve ranging from 5–1000 ng/ml determining the concentration of BA in serum samples. In the calibration solutions the concentration of internal standard (IS) were set to 700 ng/ml and 210 ng/ml for GCDA-D4 (used for TCA, GCA, GCDA and GDCA) and DCA-D4 (used for TDCA and TCDCA), respectively. The frozen serum samples were allowed to thaw at 25 °C, then 50 µl of each was spiked with 175 µl methanol, containing IS in 400 ng/ml (GCDA-D4) and 120 ng/ml (DCA-D4). Samples were vortexed (LSE W, Corning, USA) for 1 min then incubated for 30 min in -20 °C. The incubated samples were centrifuged (Heraus Fresco 17, Thermo Scientific, USA) at 13,000 rpm for 15 min in 10 °C. The supernatant was transferred to microcentrifuge tubes and evaporated with vacuum concentrator (Savant SC250EXP, Thermo Scientific, USA) at 40 °C and 1 mbar for 60 min. The residue was dissolved in 100 µl water and 5 µl was subjected to a Nexera XR UHPLC system (Shimadzu, Japan) coupled with a TSQ Quantum Access mass spectrometer (Thermo Scientific, USA). The separations were performed on a Purospher Star RP-18 Hibar HR 100 × 2.1 mm, 2 µm reversed phase column (Merck KGaA, Germany) tempered at 50 °C. The solvent A was 0.1% formic acid in water and the solvent B was 0.1% formic acid in methanol:acetonitrile 1:1. The flow rate was 300 µl/min and the following gradient elution was applied: 0–0.5 min, 30% B; at 1.5 min, 50% B; at 9 min, 58% B; at 9.5 min 85% B; at 12 min, 95% B; at 15 min, 95% B; at 15.5 min, 30% B; at 20 min, 30% B. The mass spectrometer operated in negative ionization mode using HESI ion source where the spray voltage was 3500 V, the vaporizer temperature was 350 °C, the ion-transfer capillary temperature was 275 °C, the sheath gas pressure was 30 in arbitrary units and the aux gas pressure was 20 in arbitrary units. The BAs were detected in SRM mode using two mass transitions for each analyte at the following retention times: TCA (5.3 min,  $m/z$  514.3 → 124.7/60.0), GCA (6.7 min,  $m/z$  464.3 → 402.3/75.60), TCDCA (7.2 min,  $m/z$  498.0 → 125.2/108.3), TDCA (7.9 min,  $m/z$  497.9 → 125.2/108.3), GCDA (8.8 min,  $m/z$  448.2 → 75.6/330.5), GDCA (9.6 min,  $m/z$  448.3 → 402.3/75.6), DCA-D4 (11.9 min,  $m/z$  395.4 → 349.8/330.5) and GCDA-D4 (8.8 min,  $m/z$  452.3 → 390.4/387.6). For the instrument control and the data evaluations, the TraceFinder 4.1 software (Thermo Scientific, USA) was applied.

**Statistical analysis.** Quantitative variables were described as means ± SE. Significant differences between groups were performed by ANOVA,  $p \leq 0.05$  were accepted as significant. Survival curves were prepared using the method of Kaplan and Meier, and differences in survival were studied by the Log-rank test.

## Results

**Serum levels of bile acids in PDAC patients.** The total serum bile acid (TSBA) concentration in healthy controls was  $401.3 \pm 35.38$  ng/ml, whereas in PDAC + OJ patients it increased tremendously ( $36,055.7 \pm 2182.2$  ng/ml; Fig. 1A). Analysis of individual BAs has shown higher concentrations of GCA, TCA, GCDA and TCDCA in the serum of PDAC + OJ patients. Interestingly, TCA was completely absent in healthy control, but increased dramatically in PDAC + OJ. Serum levels of TDCA were low in controls and could not be detected in PDAC + OJ patients (Fig. 1A). In PDAC patients without OJ, the TSBA concentration was  $733.9 \pm 118.7$  ng/ml. Table 1 shows the clinicopathological characteristics and the level of BAs in human serum.

**Bile acids play a key role in the progression of PC.** In the next step, we treated Capan-1 cells for 24, 48 and 72 h with serum obtained from PDAC patients (with or without OJ) and healthy volunteers (normal). Treatment with human serum induced a changed morphology and growth characteristic of the cells, therefore, we examined whether this altered morphology is associated with epithelial-mesenchymal transition (EMT). Vimentin is a structural protein that is expressed in mesenchymal cells but not in epithelial cells. In the case of PDAC + OJ a strong positive staining for vimentin was detected (Fig. 1B). In the PDAC group, only a slight staining was observed, whereas the control and the normal groups were completely negative for vimentin. These data indicate that BAs have a prominent role in the progression of cancer. To confirm this hypothesis, we supplemented PDAC serum with 0.5 mM BAs cocktail (BAC). The concentration and composition of BAC were selected on the basis of serum BAs measurements. Supplementation of PDAC serum with BAC resulted in similarly strong vimentin staining as observed for PDAC + OJ. As a positive control gastric myofibroblast were used. Moreover, we investigated proliferation, viability, and adhesion capability of the cells. As expected, serum from PDAC patients increased the rate of proliferation, adhesion and survival of Capan-1 cells compared to the normal serum (Fig. 1C–E.) Importantly, there was also a significant difference between the effect of serum from PDAC patients and that of PDAC + OJ patients, suggesting a specific role of BAs in PC pathogenesis.

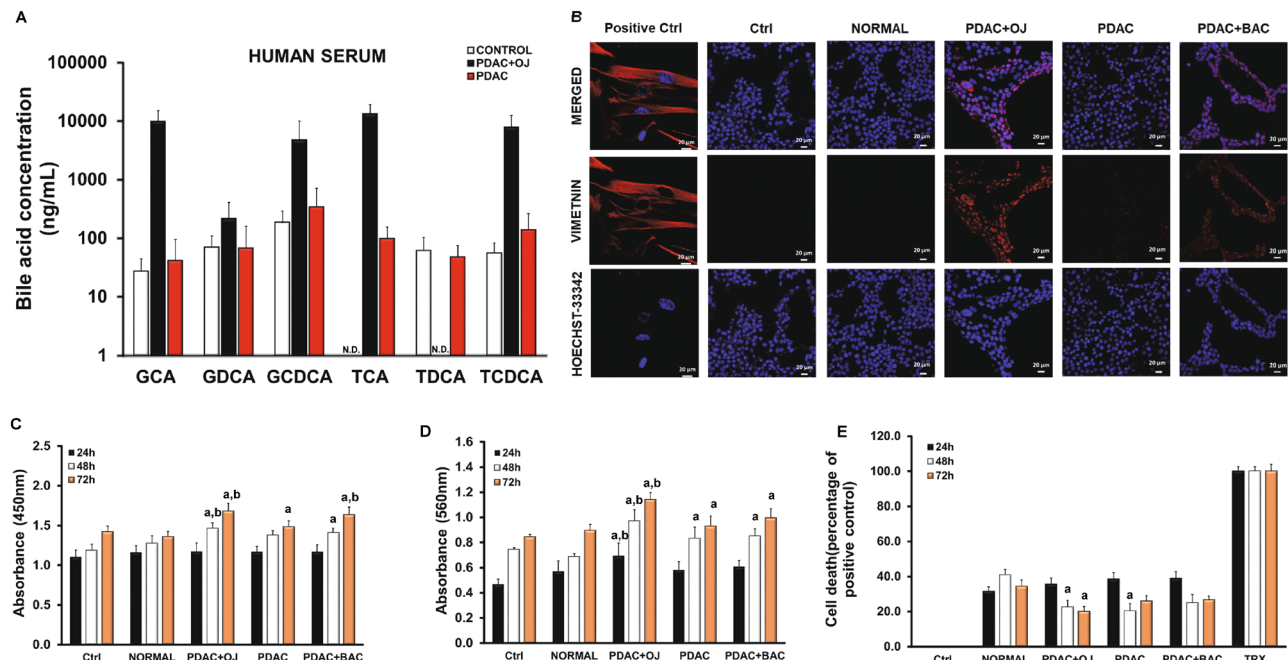


**Figure 1.** Serum levels of bile acids in pancreatic cancer patients and the effect of serum on Capan-1 cells. (A) Serum levels of bile acids (BAs) in healthy volunteers and pancreatic ductal adenocarcinoma patients (PDAC) with or without obstructive jaundice (OJ) were measured by LC–MS. GCA glycocholic acid, TCA taurocholic acid, GDCA glycodeoxycholic acid, TDCA taurodeoxycholic acid, GCDCA glycochenodeoxycholic acid, TCDCA taurochenodeoxycholic acid. N.D. not detected. (B) Capan-1 cells were treated with human serum obtained from healthy volunteers and PDAC patients and the expression of vimentin was investigated by immunocytochemistry. Control (Ctrl) samples were treated with culture medium only. As a positive control gastric myofibroblasts were used. The rate of proliferation (C), adhesion (D) and viability (E) was measured in Capan-1 cells. a =  $p \leq 0.05$  vs. Control, b =  $p \leq 0.05$  vs. PDAC. BAC bile acid cocktail, TRX Triton-X-100.

**Bile acids promote proliferation, adhesion, invasion, migration and colony forming of pancreatic ductal adenocarcinoma cells.** The role of individual BAs in cancer progression was investigated in two PDAC cell lines. Capan-1 and BxPC-3 cells were treated with different BAs and the proliferation and metastatic potential of the cells were investigated using different cell-based assays. Interestingly, most of the BAs decreased cell viability largely in normal pancreatic cell line (HPDEC) (Fig. 2A). The average cell deaths induced by 100  $\mu$ M BAs were  $28.35 \pm 5.78\%$  at 24 h,  $51.03 \pm 4.69\%$  at 48 h and  $40.91 \pm 6.2\%$  at 72 h, whereas the effects of 500  $\mu$ M BAs were more pronounced ( $44.32 \pm 5.54\%$  at 24 h,  $62.47 \pm 5.32\%$  at 48 h and  $48.86 \pm 5.3\%$  at 72 h). Low concentration (100  $\mu$ M) of BAs were only slightly toxic to the Capan-1 cells; they induced cell death in approximately 16–20% of the cells. (Fig. 2A) The average cell death induced by 100  $\mu$ M BAs was  $16.98 \pm 3.05\%$  at 24 h,  $18.82 \pm 3.27\%$  at 48 h and  $20.20 \pm 2.88\%$  at 72 h. As the concentration of BAs increased (500  $\mu$ M), the rate of cell death elevated depending on time. The average cell death induced by 500  $\mu$ M BAs was  $37.01 \pm 5.91\%$  at 24 h,  $29.67 \pm 5.79\%$  at 48 h and  $31.41 \pm 1.19\%$  at 72 h. Similar results were obtained with the BxPC-3 cell line.

Incubation of Capan-1 and BxPC-3 cells with BAs, increased the rate of proliferation almost in all treated groups (Fig. 2B). Among BAs, the effect of TDCA was dose-dependent especially at 24 h; it suppressed proliferation of the cells ( $0.83 \pm 0.06$ ) at a low concentration (100  $\mu$ M), and increased it ( $1.64 \pm 0.02$ ) at a high concentration (500  $\mu$ M), depending on time. Binding of cells to extracellular matrix plays an important role in survival of cells and determines the progression and outcome of PC. Subsequently, we have investigated the effect of BAs treatment on the adhesion of Capan-1 and BxPC-3 cells to collagen 1. As shown in Fig. 2C, adhesion of cells increased with the incubation time, mainly at high doses of TCDCA-treated group. BAs treatment also promoted the invasion of Capan-1 and BxPC-3 cells, as demonstrated on Fig. 2D,E. We have also investigated the metastatic potential of cancer cells using the wound healing assay. Treatment with BAs, especially high concentration of TCDCA (500  $\mu$ M), significantly increased the migration rate of both Capan-1 and BxPC-3 cells (Fig. 2F). Next, we have investigated the ability of Capan-1 and BxPC-3 cells to form colonies using the clonogenic assay. Figure 3A shows a representative picture regarding the effect of TCDCA at high (500  $\mu$ M) concentration. These pictures and the summary bar chart (Fig. 3B) clearly show that high concentration of BAs increase the colony forming ability of the cells especially at 72 h. We have also investigated the size of the colony in differently treated groups (Fig. 3C–E). Furthermore, we have distinguished the colonies according to the following criteria: small: 1000–10,000  $\mu$ m<sup>2</sup>, medium: 10,000–20,000  $\mu$ m<sup>2</sup>, large: 20,000–30,000  $\mu$ m<sup>2</sup> and extra-large: 30,000–100,000  $\mu$ m<sup>2</sup>. In the case of small colonies, a number of colonies were significantly higher in the non-treated, control group, compared to the BA-treated groups. Medium-sized colonies did not show any difference between the BA-treated and control groups. In contrast, BA treatment significantly increased the number of colonies in the large and

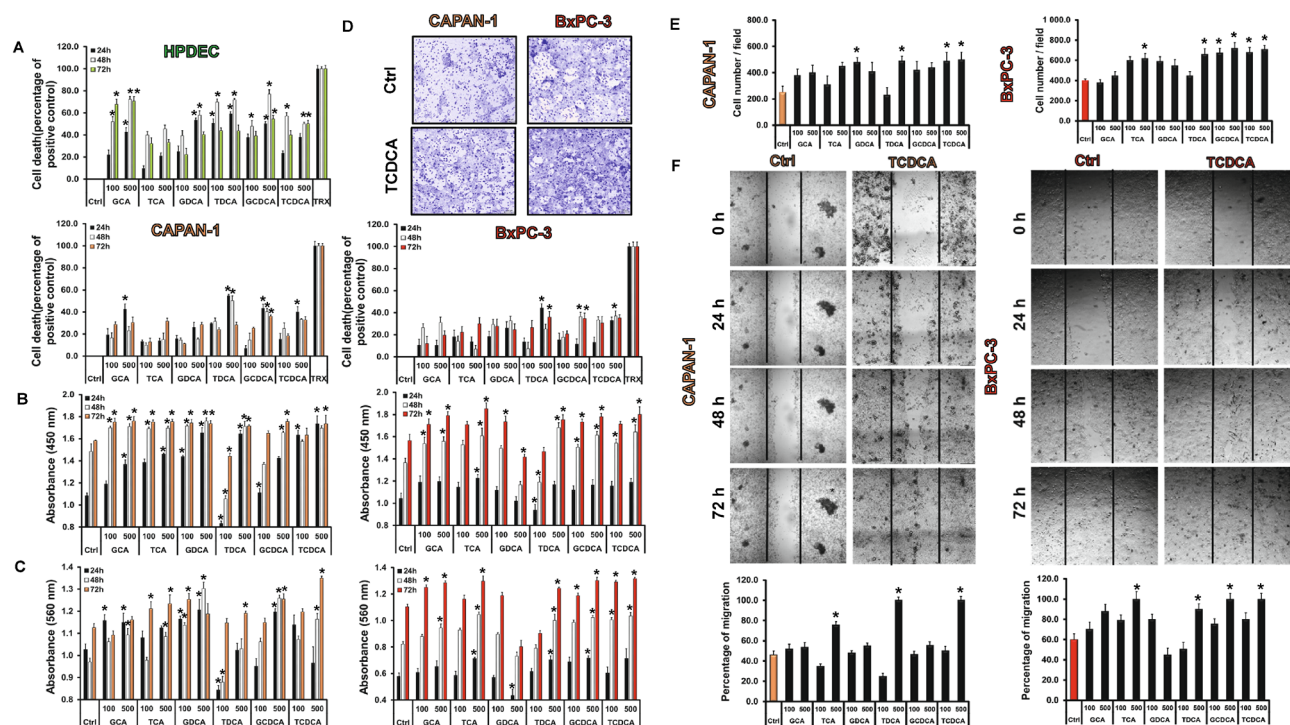


**Figure 2.** Effects of bile acid treatment on cell viability, proliferation, adhesion, invasion and migration. Capan-1 and BxPC3 cells were exposed to different concentration of bile acids (BAs) for 24, 48 and 72 h and the effects on cellular viability (A), proliferation (B), adhesion (D,E) and migration (F) were studied using different assays, as described in Materials and Methods. In the case of viability assay, as a positive control, 0.1% Triton-X-100 (TRX) was used. The rate of migration was investigated by the wound healing assay. Photography was taken at 0, 24, 48 and 72 h after TCDCA (500  $\mu$ M) treatment using Olympus IX83 inverted microscope (Olympus cellSense Dimension software version 2.3, <https://www.olympus-lifescience.com/en/software/cellsens/>) and the rate of wound closure was expressed as % of migration at 72 h. Data represent mean  $\pm$  SEM of three, independent experiments. \* =  $p \leq 0.05$  vs. Control. GCA glycocholic acid, TCA taurocholic acid, GDCA glycodeoxycholic acid, TCDCA taurodeoxycholic acid, GCDCA glycochenodeoxycholic acid, TCDCA taurochenodeoxycholic acid. Orange indicates Capan-1 whereas red BxPC-3 cells.

extra-large groups, indicating that BAs induce the formation of large and extra-large colonies both in the Capan-1 (Fig. 3D) and BxPC-3 (Fig. 3E) cells, an action that promotes larger tumour tissue development.

**Expression of mucin genes in pancreatic ductal cell lines.** Our results clearly demonstrate that BAs accelerate tumour processes; thus, we aimed to identify the mechanism that mediates the effects of BAs. Mucins are glycoproteins whose significance has been identified in many cancer types. To examine whether BAs are acting through the altered mucin expression, we investigated the effect of BAs on mucin expression. First, we studied the mRNA expression of mucin genes in HPDEC, Capan-1 and BxPC-3 cells using RT-PCR and TaqMan primer-probe sets, specific for mucin genes (Suppl. Table S1). We have investigated those genes (MUC1, -2, -4, -5AC, -5B, -12, -13, -15, -17, -19 and -20), which are proved to play a central role in gastrointestinal tumours, and TaqMan probe sets were available for them. In the normal cell line, the presence of MUC1, -2, -17 and -20 was shown (Table 3). In the case of Capan-1, expressions of MUC1, -4, -5AC, -5B, -13, -17 and -20 were observed, whereas in the BxPC-3 cells the presence of MUC1, -2, -4, -5AC, -5B and -13 was detected. Mucin expressions were also tested in two other PDAC cell lines, PANC-1 and MIAPaCa-2. Interestingly, much less mucin genes were detected in these cell lines (Table 3). The mucin genes used as a biomarker in PC, such as MUC4, -5AC and -5B, are expressed only in Capan-1 and BxPC-3 cells. The expression of mucin genes is summarised in Table 3.

**Effect of bile acids on mucin expression.** In the next step, we pre-treated the cells with various BAs (100 and 500  $\mu$ M) for 24, 48 and 72 h and the mRNA expression of mucin genes was investigated by RT-PCR. In the normal cell line, long time incubation with the BAs decreased the expression of MUC1 and -2 in most of the treated groups (Suppl. Fig. S1A). In contrast, all of the investigated BAs dose-dependently increased the expression of MUC20 (Suppl. Fig. S1A). Treatment with BAs did not affect the expression of the other genes (data not shown). In the Capan-1 cell line, BAs treatment dose- and time-dependently upregulated the expression of MUC4 (Fig. 4A). Among the BAs, the highest effect has the conjugated forms of DC and CDC acids. In contrast, GCA and TCA induced significant increase only at higher concentrations. Interestingly, TCDCA induced a robust increase (approx. fivefold compared to the control) in the expression of MUC17 at a high concentration (500  $\mu$ M), at all three incubation times (Suppl. Fig. S1B). The expression of the other genes did not change



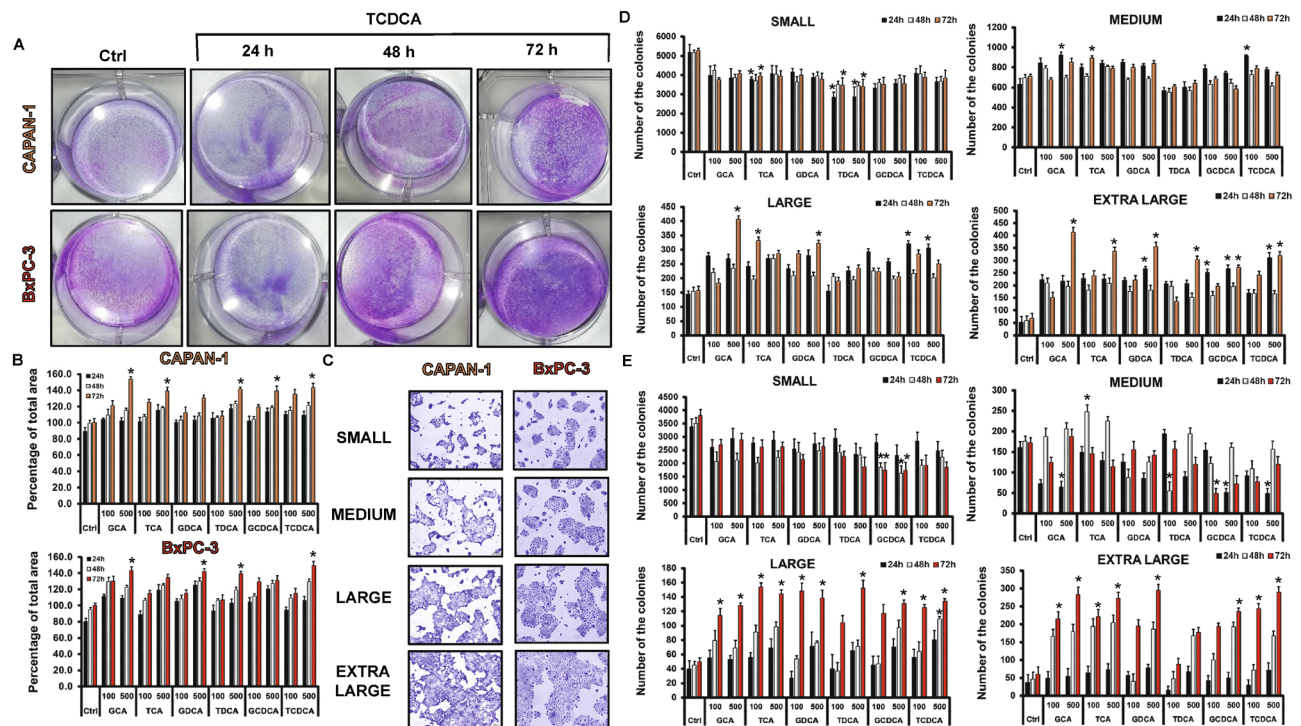


**Figure 3.** Effects of bile acid treatment on the colony forming of Capan-1 and BxPC-3 cells. Cells were exposed to different concentration of bile acids (BAs) and the colony forming ability of the cells was investigated by the clonogenic assay. (A) Representative pictures show the effect of taurochenodeoxycholic acid (TCDCA; 500  $\mu$ M) at 24, 48 and 72 h. (B) Quantification of the colonies was performed using an Olympus IX83 microscope-based screening platform (Olympus cellSense Dimension software version 2.3, <https://www.olympus-lifescience.com/en/software/cellsense/>). (C–E) For the classification and counting of the colonies an automatic Olympus Cellsense Dimension software was used. (C) Representative images showing colonies for each cell line. Summary diagrams for Capan-1 (D) and BxPC-3 (E) cells. Data represent mean  $\pm$  SEM of three, independent experiments. \* =  $p \leq 0.05$  vs. Control. GCA glycocholic acid, TCA taurocholic acid, GDCA glycodeoxycholic acid, TDCA: taurodeoxycholic acid, GCDCA glycochenodeoxycholic acid, TCDCA taurochenodeoxycholic acid.

Isoforms	Capan-1	BxPC-3	MiaPaca-2	Panc-1	HPDEC
MUC1	✓	✓	✓	✓	✓
MUC2	–	✓	–	✓	✓
MUC4	✓	✓	–	–	–
MUC5AC	✓	✓	–	–	–
MUC5B	✓	✓	–	–	–
MUC12	–	–	✓	✓	–
MUC13	✓	✓	–	–	–
MUC15	–	–	–	–	–
MUC17	✓	–	–	–	✓
MUC19	–	–	–	–	–
MUC20	✓	–	✓	–	✓

**Table 3.** mRNA expression of mucin genes in the different pancreatic ductal cell lines.

significantly in most of the groups (Supp. Fig. S1B). Similarly to the Capan-1 cells, BAs treatment increased the expression of MUC4 in the BxPC-3 cell line (Fig. 4A), however it did not or hardly affect the expression of the other genes (Suppl. Fig. S1C). MUC4 has been shown to be aberrantly expressed in PC; it promotes metastasis, and it is used as a prognostic factor; thus, we investigated the expression of this gene also at a protein level. Using immunostaining, we have shown that, similar to the RT-PCR data, pre-treatment with BAs time- and dose-dependently increased the protein expression of MUC4 in both PDAC cell lines (Fig. 4B,C).

Hierarchical clustering of genes showed that TDCA, TCDCA, GCDCA and GCA (in high concentration) initiated similar MUC gene expression level changes in both cell lines and formed a separated cluster from the other BAs. The expression pattern of MUC2, -4 and -17 has changed more pronouncedly than the other genes

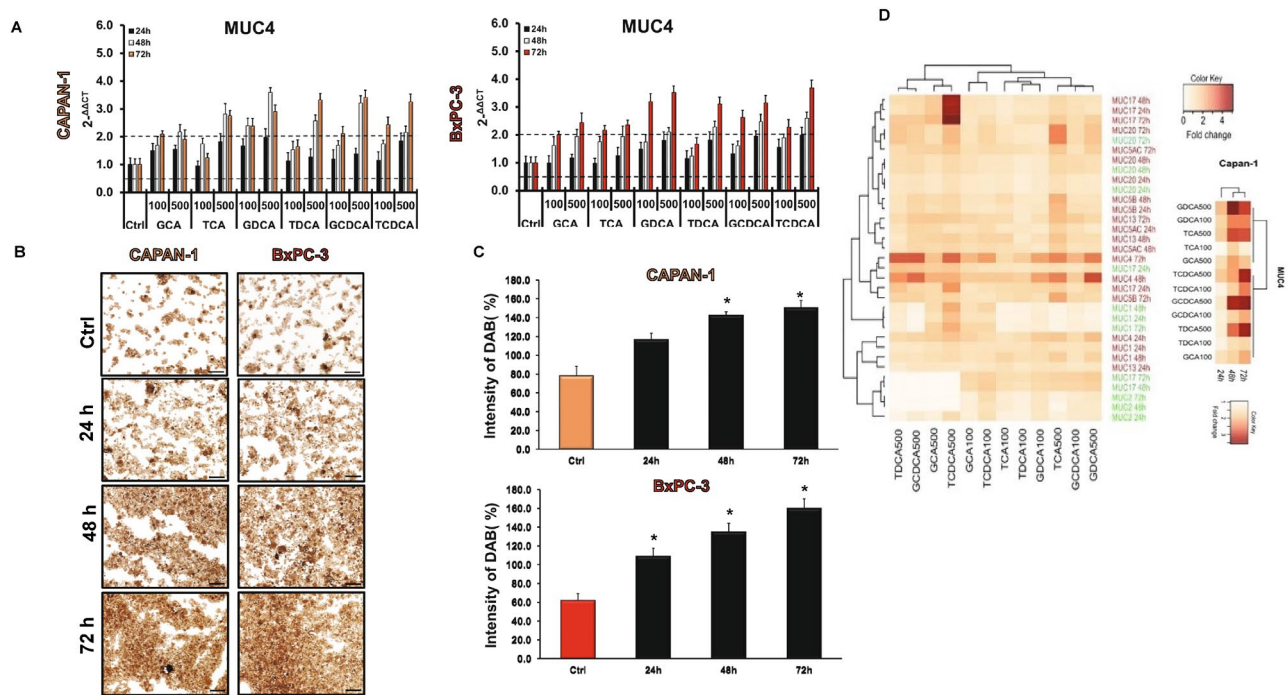


**Figure 4.** Effects of bile acid treatment on the mRNA and protein expression of mucins in pancreatic ductal cells. **(A)** Capan-1 and BxPC-3 cells were treated with different bile acids (BAs) for 24, 48 and 72 h and the relative gene expressions of MUC4 gene was investigated by real-time PCR. **(B)** Representative immunofluorescence staining of Capan-1 and BxPC-3 cells shows the expression of MUC4 after the treatment with taurochenodeoxycholic acid (TCDCA; 500  $\mu$ M) for 24, 48 and 72 h. **(C)** Quantification of MUC4 protein expression. Specimens were scanned using Olympus IX83 based system (Olympus cellSense Dimension software version 2.3, <https://www.olympus-lifescience.com/en/software/cellsens/>) and DAB staining intensities were analysed by ImageJ software. Data represent mean  $\pm$  SEM of three, independent experiments. \* =  $p \leq 0.05$  vs. Control. Scale bar represents 100  $\mu$ m. **(D)** The cluster analysis and dendrogram show the difference between the effect of BAs treatment at different concentrations and time points. Red and white colours indicate high and low expression, respectively. (Values represent the fold change in the gene expression level of MUC genes). Data represent mean  $\pm$  SEM of three, independent experiments. GCA glycocholic acid, TCA taurocholic acid, GDCA glycodeoxycholic acid, TDCA taurodeoxycholic acid, GCDCA glycochenodeoxycholic acid, TCDCA taurochenodeoxycholic acid.

upon BAs treatments, which suggest that these genes are more sensitive to BAs. Deeper analysis focusing on just the Capan-1 cell line showed that MUC4 pattern changed only after 48 h of the BAs treatment (Fig. 4D).

**Expression of MUC4 in human pancreatic samples.** The presence of MUC4 has also been investigated in human pancreatic samples by IHC. In the normal pancreas and in NE, there was no detectable staining for MUC4 (Fig. 5A). In contrast, in the case of PDAC (with or without OJ), we observed a strong expression of MUC4 in the intra- and interlobular ducts. Interestingly, in those patients where PDAC was diagnosed without OJ, the expression of MUC4 was significantly low compared to the PDAC + OJ group. (Fig. 5B) There was no significant difference in gender, age, location of primary tumour, histological type, stage, lymphatic invasion or metastasis between the PDAC and PDAC + OJ groups (Table 2). In addition, in the PDAC + OJ group the expression of MUC4 increased with the progression of the disease, whereas in the PDAC group, there was no difference in the expression of MUC4 between the early and advanced stages. Quantification of the staining has been shown in Fig. 5B. We also examined how high serum levels of bile affects the outcome of PC. The 4-year overall survival rate of the PDAC + OJ group was significantly lower than that of the PDAC group ( $p = 0.0191$ ) (Fig. 6).

**Knockdown of MUC4 decreases the carcinogenic effect of BAs.** Next, we have investigated the effect of MUC4 knockdown on the proliferation of Capan-1 and BxPC-3 cells. MUC4 was silenced by MUC4-specific siRNA. The efficiency of MUC4 knockdown was confirmed by RT-PCR (Fig. 7A) and ICC (Fig. 7B). We found that knockdown of MUC4 significantly increased cell death and decreased the rate of proliferation, adhesion, migration and colony forming in a time-dependent manner. (Fig. 7C-G) These results indicate that MUC4 is key mucoprotein in the growth of PDAC cells. In the next step we tested the effect of BAs on the MUC4-silenced cells. Among BAs, the effect of TCDCA was investigated, as this BA showed the greatest effect on both Capan-1 and BxPC-3 cells. When TCDCA was added in the absence of MUC4, an increase in the above-mentioned parameters has been observed, although it was still significantly lower than in the presence of MUC4, indicating that the effect of BAs is mediated by MUC4, although other factors also play a role in it (Fig. 7C-G and Suppl. Fig. S2.).

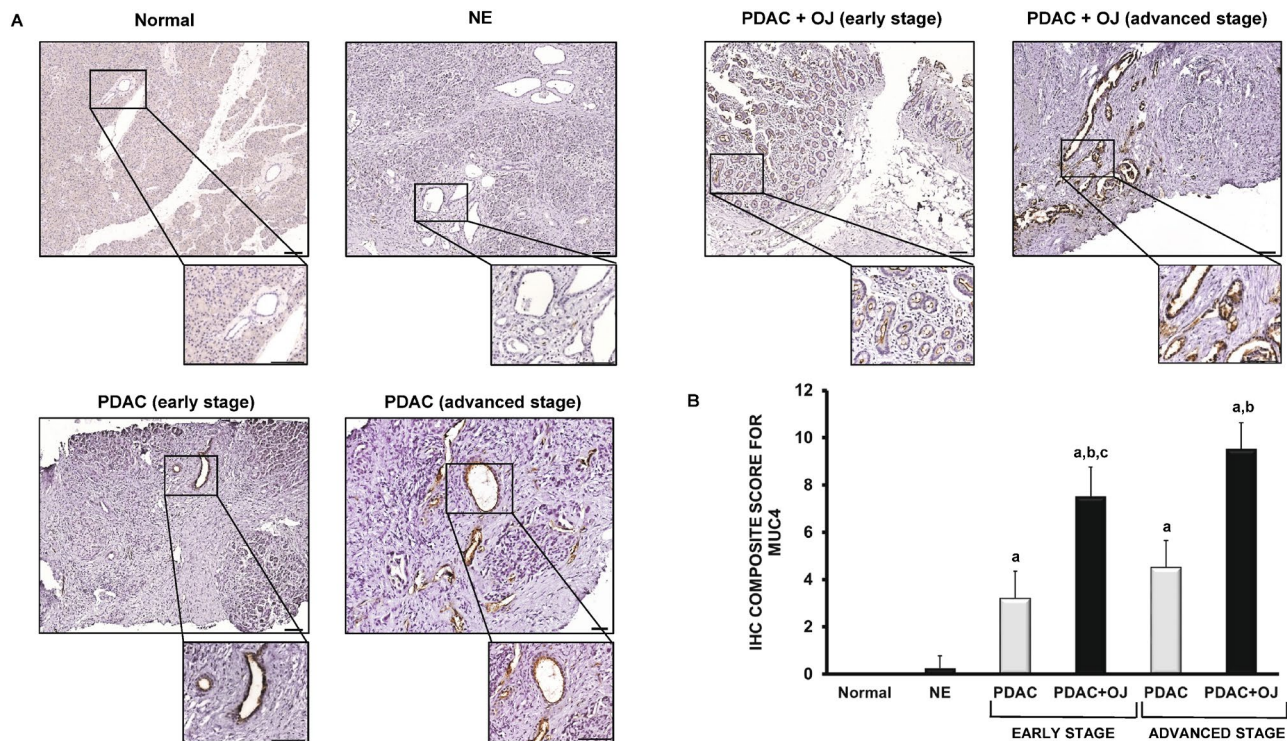


**Figure 5.** Expression of MUC4 in human pancreatic samples. **(A)** Representative immunohistochemical stainings show the presence of MUC4 in human pancreatic samples. **(B)** Composite scores of human pancreatic samples stained with anti-MUC4 antibody. Data represent mean  $\pm$  SEM of 23–25 specimens/4–25 patients each group. a =  $p \leq 0.05$  vs. normal, b =  $p \leq 0.05$  vs. PDAC, c =  $p \leq 0.05$  vs. advanced stage. Scale bar represents 100  $\mu$ m. PDAC pancreatic ductal adenocarcinoma; OJ obstructive jaundice; NE neuroendocrine tumour.

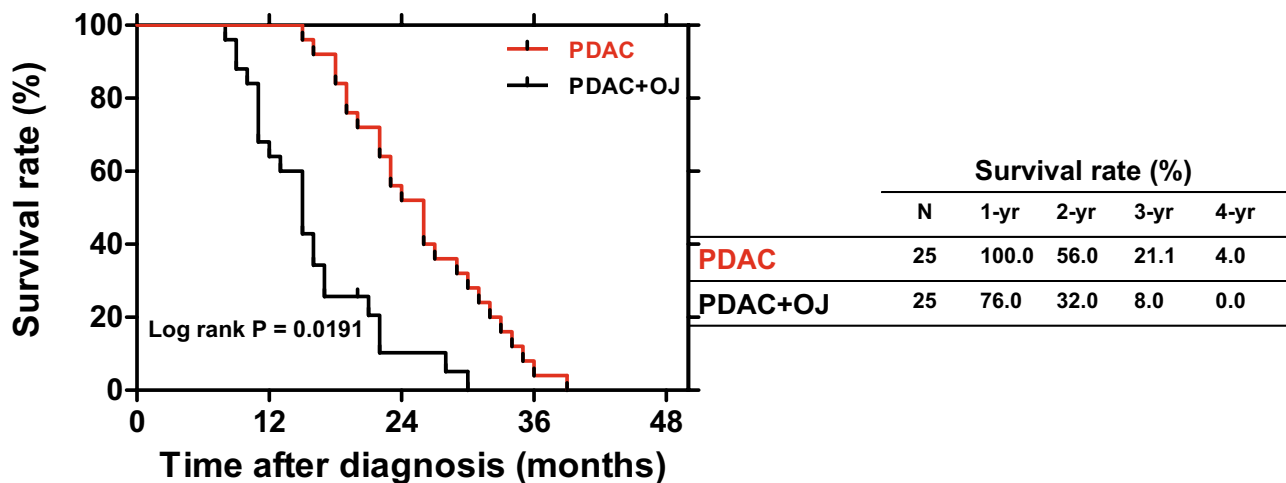


**Figure 6.** Survival curves of PDAC patients. The 4-year overall survival rate was significantly poorer in the PDAC + OJ group than in the PDAC group (log rank  $p = 0.0191$ ). PDAC pancreatic ductal adenocarcinoma, OJ obstructive jaundice.

### Discussion

Since most of the PCs develop in the head of the pancreas, PDAC is frequently associated with increased levels of BAs in the serum; however, the effect of bile on PC progression has not been evaluated yet. In this study, we used two PDAC cell lines to show that BAs promote carcinogenic processes in which expression of MUC4 plays a huge role.

We have shown that the serum levels of BAs extremely increase in PDAC + OJ patients and the most abundant BAs are GCA, TCA, GCDCA and TCDCA. In order to investigate how elevated serum bile influences carcinogenic processes, a PDAC cell line, Capan-1 was treated with serum obtained from PDAC patients. Capan-1 is



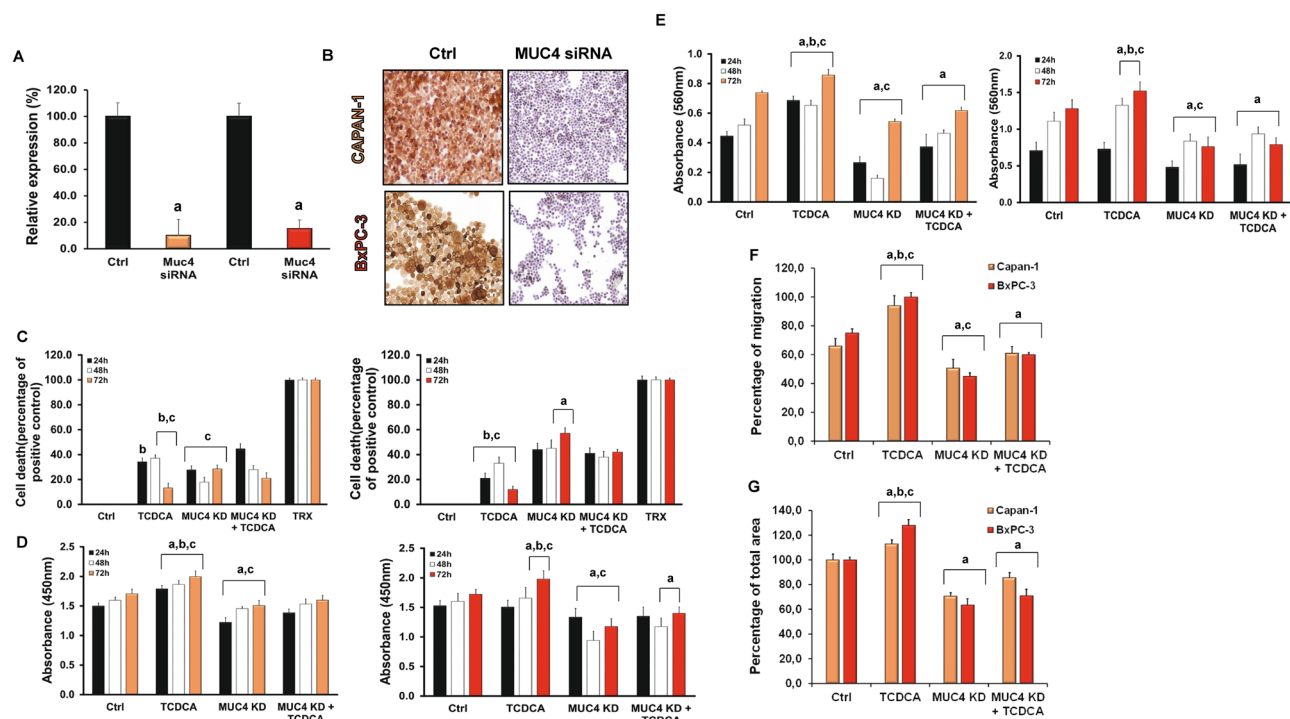


**Figure 7.** Knockdown of MUC4 in Capan-1 cells. The expression levels of MUC4 was investigated by RT-PCR (A) and immunohistochemistry (B) in control cells and in cells treated with specific siRNA for MUC4. Orange indicates Capan-1 whereas red BxPC-3 cells. The rate of viability (C), proliferation (D) and adhesion (E) was determined at 24, 48 and 72 h, whereas migration (F) and colony forming (G) at 72 h. Data represent mean  $\pm$  SEM of three, independent experiments. a =  $p \leq 0.05$  vs. Control, b =  $p \leq 0.05$  vs. MUC4 KD, c =  $p \leq 0.05$  vs. MUC4 KD + TCDCA. TCDCA: taurochenodeoxycholic acid, KD: knock down.

one of the most aggressive commercially available cell line; therefore, it proved to be a good model for the characterisation of PC progression<sup>30</sup>. High concentration of bile in the serum enhanced the tumorigenic potential of Capan-1 cells and also promoted EMT, indicating that BAs play a prominent role in the pathomechanism of PC. Previous studies indicated that the structure (number of -OH groups or the conjugation with glycine or taurine) of individual BAs determines their carcinogenic effect<sup>31</sup>. Moreover, the studies show that hydrophobic bile acids are mostly toxic to cells, by generating oxidative stress and DNA damage, while hydrophilic bile acids play a protective role<sup>32</sup>. In this study, we focused on those BAs that we detected in the serum of PDAC patients and literature data also confirm their altered concentrations in both the serum and pancreatic juice of PC patients<sup>12,15,16</sup>. In terms of cell survival, the normal and PC cells reacted differently to BAs. In normal cells, the higher rate of cell death was observed, especially after 48 h of BAs treatment, which indicates that, under normal conditions, the ductal cells respond by cell death to this noxious agent. Similar results have been shown on isolated, guinea pig pancreatic ducts, where the treatment of ducts with high dose (1 mM) of CDCA damaged the mitochondria and induced apoptosis in the ductal cells<sup>32</sup>. The apoptotic effect of BAs on normal epithelial cells has also been demonstrated in hepatocytes and in oesophageal and nasopharyngeal epithelial cells<sup>33–35</sup>. We hypothesised that the bile-induced cell death in the normal cells is an anti-cancer defence, by which the malignant transformation of the cells can be avoided. In contrast, cancer cells were more resistant to BAs treatment. Long-term incubation of Capan-1 and BxPC-3 cells with BAs increased their survival, which was consistent with the increased proliferation rate of these cells. The different response of normal and PDAC cells to BAs treatment can be explained by the fact that BAs are more likely to induce DNA damage than apoptosis in cancerous cells. Since gene mutations are more frequent in the damaged DNA, this favours the tumour progression<sup>36</sup>. In contrast, some studies have found that BAs treatment inhibit the proliferation of pancreatic cancer cell lines (PANC-1 and MIAPaCa-2) due to the cytotoxic effects of BAs<sup>13,14</sup>. In these studies, relatively low concentrations (< 50  $\mu$ M) of BAs were used and that might cause the difference. This is also proved by the fact that, among the BAs we investigated, the effect of TDCA was dose-dependent. High concentration of this BA promoted proliferation, and low concentration strongly inhibited it. The dose-dependent effect of the unconjugated form of TDCA has also been shown on colonocytes<sup>37</sup> and in gastric and oesophageal carcinoma<sup>38,39</sup>; however, the exact explanation is unknown. In addition, we have found that the adhesion, invasion, migration and colony forming ability of Capan-1 and BxPC-3 cells increased due to the BAs treatment, indicating that BAs enhance both the migratory and cell growth potential of PDAC cells. In the following, we wanted to identify the mechanism by which BAs exert their effects. Mucins can be found throughout the whole body, where they provide the hydration and lubrication of the mucosal surfaces and their pivotal role in different cancer types is generally known<sup>40</sup>. Depending on the tissue type, some of the genes act as a tumour suppressor and some of them promote tumour development

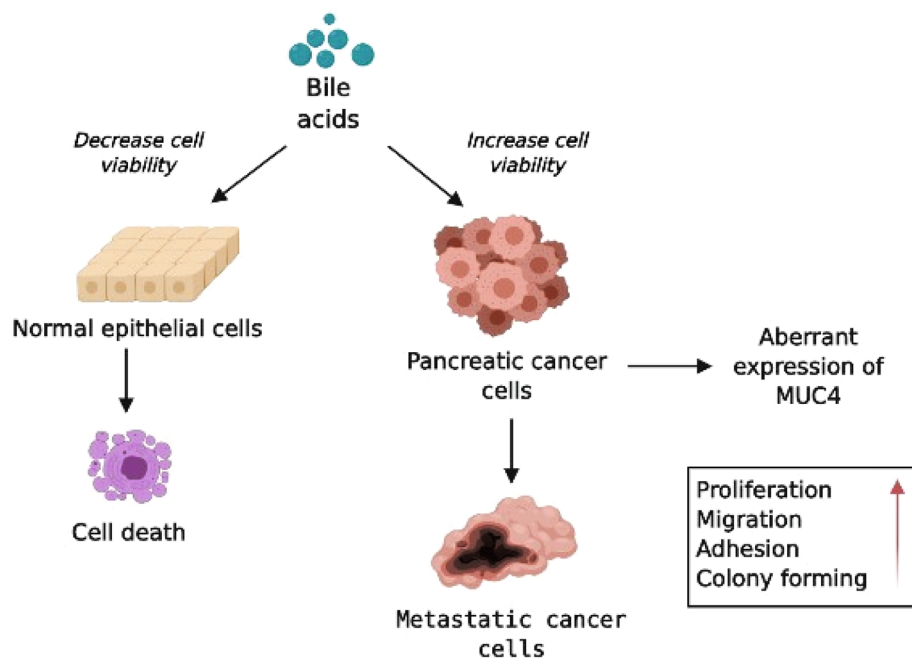


**Figure 8.** Schematic diagram of the effect of bile acids. Bile acids (BAs) decrease the cell viability of normal pancreatic ductal cells and induce cell death in order to avoid malignant transformation. In the case of pancreatic ductal adenocarcinoma (PDAC) bile promotes the tumorigenic potential of the cancer cells in which the increased expression of MUC4 plays essential role.

or growth<sup>16,18–20,41</sup>. MUC4 is a transmembrane mucin, which has an outstanding role in PC. The expression of this gene dramatically increases in PC and the overexpression of MUC4 is associated with poor prognosis<sup>18,41,42</sup>. We used RT-PCR to show the presence of MUC4 in Capan-1 and BxPC-3 cells, but not in the normal cell line or in the other two PDAC cell lines. Besides MUC4, expression of MUC1, -5AC, -5B, -13, -17 and -20 have been shown in Capan-1 and the expression of MUC1, -2, -17 and -20 in the normal cells. The different expression pattern of mucins in normal and PDAC probably plays important role in cancer development. A tumour suppressor role of MUC2 has been shown in pancreatic neoplasia<sup>43</sup>, whereas overexpression of MUC1 and -20 correlated with poor survival in PDAC patients<sup>43,44</sup>. MUC5AC, -5B and -13 are absent in normal pancreas, but can be detected in pancreatic intraepithelial neoplasia and PDAC<sup>45</sup>. The role of MUC17 is controversial. Some data indicate that MUC17 decreases the tumorigenic potential of PDAC cells<sup>46</sup>, whereas others have found that this gene is aberrantly expressed in PC<sup>47,48</sup>.

In the normal cell line, BAs treatment decreased the expression of MUC2, and upregulated MUC20. Since MUC2 is a tumour suppressor, whereas overexpression of MUC20 favours tumour progression, these data indicate that BAs facilitate tumour development under normal conditions, by altering the expression of these mucins. In contrast, the expression of other, oncogenic mucins, such as MUC4, did not change due to the BAs treatment. In the Capan-1 and BxPC3 cell lines, BAs induced changes in the expression of MUC4 and at least two days of BAs treatment were needed to detect changes in its expression pattern. The expression of MUC17 was only affected by high concentration of TCDCA in the Capan-1 cells and it could be detected 24 h after the treatment. Using human pancreatic samples, we showed that MUC4 was completely abolished from the normal pancreatic tissue and also in NE. In contrast, strong expression was detected in PDAC, which further increased in PDAC + OJ. To exclude that elevated MUC4 levels can be explained by the more advanced stages of PDAC + OJ patients, we compared MUC4 expressions both at the early and late stages of PC. Expression of MUC4 increased with the disease progression in the PDAC + OJ group, but not in the PDAC group, indicating that the elevated level of MUC4 is due to the specific action of BAs. We also found that the presence of biliary obstruction was related to poor survival of the PDAC + OJ patients. Several studies have revealed that overexpression of MUC4 is associated with a poor clinical outcome and this gene has been reported to be an independent prognostic factor in PC<sup>49–52</sup>. In order to clarify the role of MUC4 in the bile-induced cancer progression, we down-regulated MUC4 by siRNA transfection and found that MUC4 act as an oncogenic mucin. The oncogenic potential of MUC4 is not surprising since silencing of MUC4 decreases the proliferation of many cancer cells. Li et al. have shown that 96 h after the transfection with shRNA, lentivector for MUC4 decreased the cell growth of BxPC-3 cells, both under in vitro and in vivo conditions<sup>42</sup>. Similar results have been found in other pancreatic cancer cell lines<sup>18,41,53,54</sup>. We have also demonstrated that inhibition of MUC4 expression significantly decreased the effect of TCDCA, one of the most effective BAs, indicating that the tumorigenic effect of bile is mediated by MUC4.

Figure 8 shows a hypothetical schematic figure regarding the role of BAs in PC progression. BAs induce cell death in normal pancreatic ductal cells; that are probably an anti-cancer, defensive mechanism. In contrast, elevated serum BAs levels increase MUC4 expression in PC, that presumably accelerates tumour progression.



Based on these results, we believe that in PC patients with OJ, treatment of biliary obstruction needs to be done as early as possible to decrease the tumorigenic potential of PC cells and improve the life expectancy.

Received: 28 April 2020; Accepted: 4 December 2020

Published online: 16 December 2020

## References

1. Saad, A. M., Turk, T., Al-Husseini, M. J. & Abdel-Rahman, O. Trends in pancreatic adenocarcinoma incidence and mortality in the United States in the last four decades; a SEER-based study. *BMC Cancer* **18**, 688. <https://doi.org/10.1186/s12885-018-4610-4> (2018).
2. Cao, H., Le, D. & Yang, L. X. Current status in chemotherapy for advanced pancreatic adenocarcinoma. *Anticancer Res.* **33**, 1785–1791 (2013).
3. Ozawa, F. *et al.* Treatment of pancreatic cancer: the role of surgery. *Dig. Dis.* **19**, 47–56. <https://doi.org/10.1159/000050653> (2001).
4. Boeck, S. & Heinemann, V. Improving post-surgical management of resected pancreatic cancer. *Lancet* **390**, 847–848. [https://doi.org/10.1016/S0140-6736\(17\)31806-8](https://doi.org/10.1016/S0140-6736(17)31806-8) (2017).
5. Jeune, F. *et al.* Pancreatic cancer surgical management. *Presse Med.* **48**, e147–e158. <https://doi.org/10.1016/j.lpm.2019.02.027> (2019).
6. Adamska, A., Domenichini, A. & Falasca, M. Pancreatic ductal adenocarcinoma: Current and evolving therapies. *Int. J. Mol. Sci.* <https://doi.org/10.3390/ijms18071338> (2017).
7. Di Ciaula, A. *et al.* Bile acids and cancer: direct and environmental-dependent effects. *Ann. Hepatol.* **16**, s87–s105. <https://doi.org/10.5604/01.3001.0010.5501> (2017).
8. Wagner, M. *et al.* Curative resection is the single most important factor determining outcome in patients with pancreatic adenocarcinoma. *Br. J. Surg.* **91**, 586–594. <https://doi.org/10.1002/bjs.4484> (2004).
9. Bonin, E. A. & Baron, T. H. Preoperative biliary stents in pancreatic cancer. *J. Hepatobiliary Pancreat. Sci.* **18**, 621–629. <https://doi.org/10.1007/s00534-011-0403-8> (2011).
10. Jinkins, L. J. *et al.* Current trends in preoperative biliary stenting in patients with pancreatic cancer. *Surgery* **154**, 179–189. <https://doi.org/10.1016/j.surg.2013.03.016> (2013).
11. Scheufele, F. *et al.* Preoperative biliary stenting versus operation first in jaundiced patients due to malignant lesions in the pancreatic head: A meta-analysis of current literature. *Surgery* **161**, 939–950. <https://doi.org/10.1016/j.surg.2016.11.001> (2017).
12. Feng, H. Y. & Chen, Y. C. Role of bile acids in carcinogenesis of pancreatic cancer: An old topic with new perspective. *World J. Gastroenterol.* **22**, 7463–7477. <https://doi.org/10.3748/wjg.v22.i33.7463> (2016).
13. Lu, Y. *et al.* The cytotoxic effects of bile acids in crude bile on human pancreatic cancer cell lines. *Surg. Today* **30**, 903–909. <https://doi.org/10.1007/s005950070042> (2000).
14. Wu, Z., Lu, Y., Wang, B., Liu, C. & Wang, Z. R. Effects of bile acids on proliferation and ultrastructural alteration of pancreatic cancer cell lines. *World J. Gastroenterol.* **9**, 2759–2763 (2003).
15. Tucker, O. N., Dannenberg, A. J., Yang, E. K. & Fahey, T. J. 3rd. Bile acids induce cyclooxygenase-2 expression in human pancreatic cancer cell lines. *Carcinogenesis* **25**, 419–423. <https://doi.org/10.1093/carcin/bgh010> (2004).
16. Joshi, S. *et al.* Bile acids-mediated overexpression of MUC4 via FAK-dependent c-Jun activation in pancreatic cancer. *Mol. Oncol.* **10**, 1063–1077. <https://doi.org/10.1016/j.molonc.2016.04.007> (2016).
17. Mariette, C. *et al.* Transcriptional regulation of human mucin MUC4 by bile acids in oesophageal cancer cells is promoter-dependent and involves activation of the phosphatidylinositol 3-kinase signalling pathway. *Biochem. J.* **377**, 701–708. <https://doi.org/10.1042/BJ20031132> (2004).
18. Chaturvedi, P. *et al.* MUC4 mucin potentiates pancreatic tumor cell proliferation, survival, and invasive properties and interferes with its interaction to extracellular matrix proteins. *Mol. Cancer Res.* **5**, 309–320. <https://doi.org/10.1158/1541-7786.MCR-06-0353> (2007).
19. Nagata, K. *et al.* Mucin expression profile in pancreatic cancer and the precursor lesions. *J. Hepatobiliary Pancreat. Surg.* **14**, 243–254. <https://doi.org/10.1007/s00534-006-1169-2> (2007).
20. Nath, S., Roy, L. D., Grover, P., Rao, S. & Mukherjee, P. Mucin 1 regulates Cox-2 gene in pancreatic cancer. *Pancreas* **44**, 909–917. <https://doi.org/10.1097/MPA.0000000000000371> (2015).
21. Pyo, J. S. *et al.* Bile acid induces MUC2 expression and inhibits tumor invasion in gastric carcinomas. *J. Cancer Res. Clin. Oncol.* **141**, 1181–1188. <https://doi.org/10.1007/s00432-014-1890-1> (2015).
22. Shekels, L. L., Lyftogt, C. T. & Ho, S. B. Bile acid-induced alterations of mucin production in differentiated human colon cancer cell lines. *Int. J. Biochem. Cell Biol.* **28**, 193–201 (1996).
23. Song, S. *et al.* Induction of MUC5AC mucin by conjugated bile acids in the esophagus involves the phosphatidylinositol 3-kinase/protein kinase C/activator protein-1 pathway. *Cancer* **117**, 2386–2397. <https://doi.org/10.1002/cncr.25796> (2011).
24. Wu, J., Gong, J., Geng, J. & Song, Y. Deoxycholic acid induces the overexpression of intestinal mucin, MUC2, via NF- $\kappa$ B signaling pathway in human esophageal adenocarcinoma cells. *BMC Cancer* **8**, 333. <https://doi.org/10.1186/1471-2407-8-333> (2008).
25. Yu, J. H. *et al.* Bile acids promote gastric intestinal metaplasia by upregulating CDX2 and MUC2 expression via the FXR/NF- $\kappa$ B signalling pathway. *Int. J. Oncol.* **54**, 879–892. <https://doi.org/10.3892/ijo.2019.4692> (2019).
26. Laczko, D. *et al.* Role of ion transporters in the bile acid-induced esophageal injury. *Am. J. Physiol. Gastrointest. Liver Physiol.* **311**, G16–31. <https://doi.org/10.1152/ajpgi.00159.2015> (2016).
27. Venglovecz, V. *et al.* The importance of aquaporin 1 in pancreatitis and its relation to the CFTR Cl<sup>-</sup> channel. *Front. Physiol.* **9**, 854. <https://doi.org/10.3389/fphys.2018.00854> (2018).
28. Rachagani, S. *et al.* Mucin (Muc) expression during pancreatic cancer progression in spontaneous mouse model: potential implications for diagnosis and therapy. *J. Hematol. Oncol.* **5**, 68. <https://doi.org/10.1186/1756-8722-5-68> (2012).
29. Ghaffarzadegan, T. *et al.* Determination of free and conjugated bile acids in serum of Apoe(-/-) mice fed different lingonberry fractions by UHPLC-MS. *Sci. Rep.* **9**, 3800. <https://doi.org/10.1038/s41598-019-40272-8> (2019).
30. Deer, E. L. *et al.* Phenotype and genotype of pancreatic cancer cell lines. *Pancreas* **39**, 425–435. <https://doi.org/10.1097/MPA.0b013e3181c15963> (2010).
31. Rees, D. O. *et al.* Comparison of the composition of bile acids in bile of patients with adenocarcinoma of the pancreas and benign disease. *J. Steroid Biochem. Mol. Biol.* **174**, 290–295. <https://doi.org/10.1016/j.jsmb.2017.10.011> (2017).
32. Katona, M. *et al.* A novel, protective role of ursodeoxycholate in bile-induced pancreatic ductal injury. *Am. J. Physiol. Gastrointest. Liver Physiol.* **310**, G193–204. <https://doi.org/10.1152/ajpgi.00317.2015> (2016).
33. Rust, C. *et al.* Bile acid-induced apoptosis in hepatocytes is caspase-6-dependent. *J. Biol. Chem.* **284**, 2908–2916. <https://doi.org/10.1074/jbc.M804585200> (2009).
34. Tan, S. N. & Sim, S. P. Bile acids at neutral and acidic pH induce apoptosis and gene cleavages in nasopharyngeal epithelial cells: implications in chromosome rearrangement. *BMC Cancer* **18**, 409. <https://doi.org/10.1186/s12885-018-4327-4> (2018).

35. Zhang, R., Gong, J., Wang, H. & Wang, L. Bile salts inhibit growth and induce apoptosis of culture human normal esophageal mucosal epithelial cells. *World J. Gastroenterol.* **11**, 6466–6471 (2005).
36. Bernstein, H., Bernstein, C., Payne, C. M., Dvorakova, K. & Garewal, H. Bile acids as carcinogens in human gastrointestinal cancers. *Mutat. Res.* **589**, 47–65. <https://doi.org/10.1016/j.mrrrev.2004.08.001> (2005).
37. Peiffer, L. P., Peters, D. J. & McGarrity, T. J. Differential effects of deoxycholic acid on proliferation of neoplastic and differentiated colonocytes in vitro. *Dig. Dis. Sci.* **42**, 2234–2240 (1997).
38. Cronin, J. *et al.* The role of secondary bile acids in neoplastic development in the oesophagus. *Biochem. Soc. Trans.* **38**, 337–342. <https://doi.org/10.1042/BST0380337> (2010).
39. Redlak, M. J. & Miller, T. A. Targeting PI3K/Akt/HSP90 signaling sensitizes gastric cancer cells to deoxycholate-induced apoptosis. *Dig. Dis. Sci.* **56**, 323–329. <https://doi.org/10.1007/s10620-010-1294-2> (2011).
40. Kufe, D. W. Mucins in cancer: function, prognosis and therapy. *Nat. Rev. Cancer* **9**, 874–885. <https://doi.org/10.1038/nrc2761> (2009).
41. Singh, A. P., Moniaux, N., Chauhan, S. C., Meza, J. L. & Batra, S. K. Inhibition of MUC4 expression suppresses pancreatic tumor cell growth and metastasis. *Cancer Res.* **64**, 622–630 (2004).
42. Li, Y. *et al.* Effects of RNAi-mediated MUC4 gene silencing on the proliferation and migration of human pancreatic carcinoma BxPC-3 cells. *Oncol. Rep.* **36**, 3449–3455. <https://doi.org/10.3892/or.2016.5152> (2016).
43. Levi, E., Klimstra, D. S., Andea, A., Basturk, O. & Adsay, N. V. MUC1 and MUC2 in pancreatic neoplasia. *J. Clin. Pathol.* **57**, 456–462 (2004).
44. Chen, S. T. *et al.* Silencing of MUC20 suppresses the malignant character of pancreatic ductal adenocarcinoma cells through inhibition of the HGF/MET pathway. *Oncogene* **37**, 6041–6053. <https://doi.org/10.1038/s41388-018-0403-0> (2018).
45. Kaur, S., Kumar, S., Momi, N., Sasson, A. R. & Batra, S. K. Mucins in pancreatic cancer and its microenvironment. *Nat. Rev. Gastroenterol. Hepatol.* **10**, 607–620. <https://doi.org/10.1038/nrgastro.2013.120> (2013).
46. Junker, W. & Batra, S. In *AACR Annual Meeting* Vol. 68 (San Diego, CA, 2008).
47. Hirono, S. *et al.* Molecular markers associated with lymph node metastasis in pancreatic ductal adenocarcinoma by genome-wide expression profiling. *Cancer Sci.* **101**, 259–266. <https://doi.org/10.1111/j.1349-7006.2009.01359.x> (2010).
48. Moniaux, N., Junker, W. M., Singh, A. P., Jones, A. M. & Batra, S. K. Characterization of human mucin MUC17. Complete coding sequence and organization. *J. Biol. Chem.* **281**, 23676–23685. <https://doi.org/10.1074/jbc.M600302200> (2006).
49. Andrianifahanana, M. *et al.* Mucin (MUC) gene expression in human pancreatic adenocarcinoma and chronic pancreatitis: A potential role of MUC4 as a tumor marker of diagnostic significance. *Clin. Cancer Res.* **7**, 4033–4040 (2001).
50. Huang, X. *et al.* Clinicopathological and prognostic significance of MUC4 expression in cancers: Evidence from meta-analysis. *Int. J. Clin. Exp. Med.* **8**, 10274–10283 (2015).
51. Saitou, M. *et al.* MUC4 expression is a novel prognostic factor in patients with invasive ductal carcinoma of the pancreas. *J. Clin. Pathol.* **58**, 845–852. <https://doi.org/10.1136/jcp.2004.023572> (2005).
52. Swartz, M. J. *et al.* MUC4 expression increases progressively in pancreatic intraepithelial neoplasia. *Am. J. Clin. Pathol.* **117**, 791–796. <https://doi.org/10.1309/7Y7N-M1WM-R0YK-M2VA> (2002).
53. Rachagani, S. *et al.* MUC4 potentiates invasion and metastasis of pancreatic cancer cells through stabilization of fibroblast growth factor receptor 1. *Carcinogenesis* **33**, 1953–1964. <https://doi.org/10.1093/carcin/bgs225> (2012).
54. Jonckheere, N. *et al.* The mucin MUC4 and its membrane partner ErbB2 regulate biological properties of human CAPAN-2 pancreatic cancer cells via different signalling pathways. *PLoS ONE* **7**, e32232. <https://doi.org/10.1371/journal.pone.0032232> (2012).

## Acknowledgements

This study was supported by Bolyai Postdoctoral Fellowship of the Hungarian Academy of Sciences (HAS) to VV (00509/16), by the National Research, Development and Innovation Office (FK123982), the Economic Development and Innovation Operative Programme Grants (GINOP-2.3.2-15-2016-00015), by the HAS-USZ Momentum Grant (LP2014-10/2017) and UNKP-18-4 New National Excellence Program Of The Ministry of Human Capacities. The work of Zoltán Veréb has been supported by the EU-funded Hungarian grant EFOP-3.6.1-16-2016-00008 and the Regenerative Medicine and Cellular Pharmacology Research Laboratory was established through the GINOP-2.3.3-15-2016-00012 project (co-financed by the European Union and the European Regional Development Fund).

## Author contributions

E.G. performed all experiments and analysed the data. Z.V. was involved in wound healing, adhesion and clonogenic assays, in the siRNA silencing and quantified fluorescence intensity. A.S.Z. and D.R. performed the HPLC–MS measurements. EB participated in the culturing and treatment of the cells, in the proliferation and cytotoxicity assays. L.T. evaluated the human pancreas slices and assisted in the immunostainings. Human serum samples were provided by T.T. and L.C. L.K. and P.H. were involved in interpreting data and they edited the manuscript. V.V. supervised the project and drafted the manuscript. All authors approved the final version of the manuscript.

## Competing interests

The authors declare no competing interests.

## Additional information

**Supplementary Information** The online version contains supplementary material available at <https://doi.org/10.1038/s41598-020-79181-6>.

**Correspondence** and requests for materials should be addressed to V.V.

**Reprints and permissions information** is available at [www.nature.com/reprints](http://www.nature.com/reprints).

**Publisher's note** Springer Nature remains neutral with regard to jurisdictional claims in published maps and institutional affiliations.



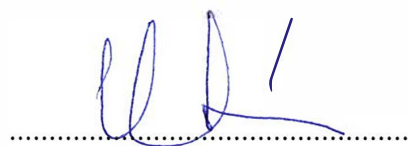
**Open Access** This article is licensed under a Creative Commons Attribution 4.0 International License, which permits use, sharing, adaptation, distribution and reproduction in any medium or format, as long as you give appropriate credit to the original author(s) and the source, provide a link to the Creative Commons licence, and indicate if changes were made. The images or other third party material in this article are included in the article's Creative Commons licence, unless indicated otherwise in a credit line to the material. If material is not included in the article's Creative Commons licence and your intended use is not permitted by statutory regulation or exceeds the permitted use, you will need to obtain permission directly from the copyright holder. To view a copy of this licence, visit <http://creativecommons.org/licenses/by/4.0/>.

© The Author(s) 2020

## Co-author certification

I, myself as a corresponding author of the following publication declare that the authors have no conflict of interest, and Eszter Becskeházi M.D. Ph.D. candidate had significant contribution to the jointly published research. The results discussed in her thesis were not used and not intended to be used in any other qualification process for obtaining a PhD degree.

Szeged, 2023-08-22



Viktória Venglovecz PhD. DSc

corresponding author

The publication(s) relevant to the applicant's thesis:

Gál, E., Veréb, Z., Kemény, L., Rakk, D., Szekeres, A., **Becskeházi, E.**, Tizslavicz, L., Takács, T., Czakó, L., Hegyi, P., & Venglovecz, V. (2020). Bile accelerates carcinogenic processes in pancreatic ductal adenocarcinoma cells through the overexpression of MUC4. *Scientific reports*, 10(1), 22088. <https://doi.org/10.1038/s41598-020-79181-6>